EUROPEAN COMMISSION

Community Research

EURATOM

ARCHER

Collaborative Project

Co-funded by the European Commission under the
Euratom Research and Training Programme on Nuclear Energy
within the Seventh Framework Programme

Grant Agreement Number: 269892
Start date: 01/02/2011Duration: 48 Months
www.archer-project.eu

Archer
Advanced Reactor
for Cogeneration of
Heat & Electricity-R&D

Deliverable D41.14: Microstructure analysis on irradiated graphite

M Heijna (NRG)

BIO-PROTECT – Contract Number: 269892
Advanced High-Temperature Reactors for Cogeneration of Heat and Electricity R&D

Document title	Deliverable D41.14: Microstructure analysis on irradiated graphite
Author(s)	M Heijna (NRG)
Number of pages	110
Document type	Deliverable
Work Package	WP41
Document number	D-41-14:
Issued by.	D Buckthorpe (AMEC)
Date of completion	11/2012
Dissemination level	Confidential, only for consortium members (including the Commission Services)

Summary

The irradiation behaviour of modern graphite grades have been investigated at two irradiation temperatures, 750°C and 950°C within the European graphite irradiation programme (HTR-M1 (5FP) and RAPHAEL-IP (6FP)). Full Post-Irradiation Examination (PIE) of selected grades from the high fluence experiments have been completed in the ARCHER project and samples have been prepared for additional PIE using optical microscopy and scanning electron microscopy (SEM). This report describes the microstructural analysis of 20 selected samples covering 7 graphite grades, with and against grain orientations and two locations in the block. The samples have been taken from the INNOGRAPH-1A and INNOGRAPH 1-B irradiation experiments performed at 750°C. All 20 samples were examined using optical microscopy and 9 of these were additonally scanned using the SEM. Bright field and polarisation micoscopy images are presented at x5,x10 and x20 magnifications for the different samples and for selected areas. Magnifications of up to x10,000 are presented using SEM. The results form a catalogue of images to be used in later investigations as part of the microstructure and modelling developments.

Approval

Rev.	Date	First author	SP leader	Project Coordinator
0	month/year	M Heijna (NRG)	D Buckthorpe; AMEC	S de Groot, NRG
	11/12		D Buckthorpe	

Distribution list

Name	Organisation	Comments
All beneficiaries	ARCHER	Through internet workspace
WP4 Participants	ARCHER	Through internet workspace

D41.14: Microstructure analysis on irradiated graphite

Optical microscopy and SEM

Under the contract of Euratom

grant agreement 269892

rev. no.	date	description
A	27-11-2012	1st version

author(s):	M.C.R. Heijna	reviewed:	T.O. van Staveren
name:	D41.14 Archer.docx	approved:	R.P.C. Schram
referencenr.:	22906/12.117312		
110 pages	27/11/2012		

Contents

Summary

In the European graphite irradiation programme, part of the HTR-M1-IP and RAPHAEL-IP, the irradiation behaviour of modern graphite grades is investigated at two irradiation temperatures, 750°C and 950°C. With the full Post-Irradiation Examination (PIE) of the high fluence experiments completed in the ARCHER project, samples are now available for additional PIE such as microscopy. This report describes the microstructural analysis using optical microscopy and scanning electron microscopy on samples from the INNOGRAPH-1A and INNOGRAPH-1B irradiation experiments at 750°C.

The work described was performed with financial support from the European Union and the Dutch Ministry of Economic Affairs, Agriculture, and Innovation. The views expressed in this report are those of the authors and do not necessarily represent those of the European Union, nor those of the Dutch government.

1 Introduction

Graphite is a suitable material to be used as a neutron moderator and reflector in nuclear reactors. Graphite has been used in Advanced Gas-Cooled Reactors, Magnox reactors, RBMK's (a Russian acronym meaning "reactor cooled by water and moderated by graphite"), Research Reactors, Materials Test Reactors and High Temperature Reactors (HTR's). Recently, there has been a renewed interest in HTR's. Two prototypes, one in Japan (HTTR) and one in China (HTR-10) are in operation. The Next Generation Nuclear Plant NGNP in the US is in development. The European Commission is supporting research projects for the development of HTR technology with the aim to determine the technological requirements for designing and constructing an HTR in Europe.

Much research has been done on the behaviour of graphite grades in a nuclear reactor environment, because graphite is already being used in reactors for decades. However, many of the historical graphite grades are no longer commercially available since the raw materials no longer exist. In addition, most historical data are from low temperature irradiation experiments (<550°C), whereas for HTR's the graphite temperatures will generally be higher than 550°C. In order to be able to design a European HTR, it is decided by the European commission to create a database that contains data of the materials behaviour of available graphite grades under neutron irradiation at temperatures relevant for the HTR's. This will allow the 'best' graphite(s) to be chosen, and provide the necessary data to allow the core design to be carried out.

Within the RAPHAEL-IP framework, graphite irradiation experiments were performed at 750°C and 950°C in the High Flux Reactor (HFR) in Petten. These were named INNOGRAPH-1B (750°C, high dose), INNOGRAPH-2A (950°C, medium dose) and INNOGRAPH-2B (950°C, high dose). In every experiment a selection of samples were also irradiated at lower temperatures of 650°C (in the 1B) and 850°C (in the 2A and 2B). Figure 1.1 shows schematically the expected volume change of graphite with neutron fluence at the two main irradiation temperatures. The boxes on the curves indicate the four different irradiation experiments. Box 1A indicates the low dose irradiation at 750°C named INNOGRAPH-1A. This has been performed within HTR-M1 in the 5th Framework Programme and had a target dose of 8 dpa [1]. Box 1B indicates INNOGRAPH-1B, the high dose (up to ~25 dpa) experiment at the same temperature. Boxes 2A and 2B indicate the medium and high dose experiments at 950°C, INNOGRAPH-2A and INNOGRAPH-2B respectively. In order to reach the target dose in as short a time as possible, the high dose experiments (INNOGRAPH-1B/2B) partly contain specimens that have been irradiated in the low dose experiments. These two high dose experiments had to be built in a hot-cell because of the radioactivity of the samples. The capability to do this delicate work with manipulators is essential to carry out this irradiation programme [2, 3].

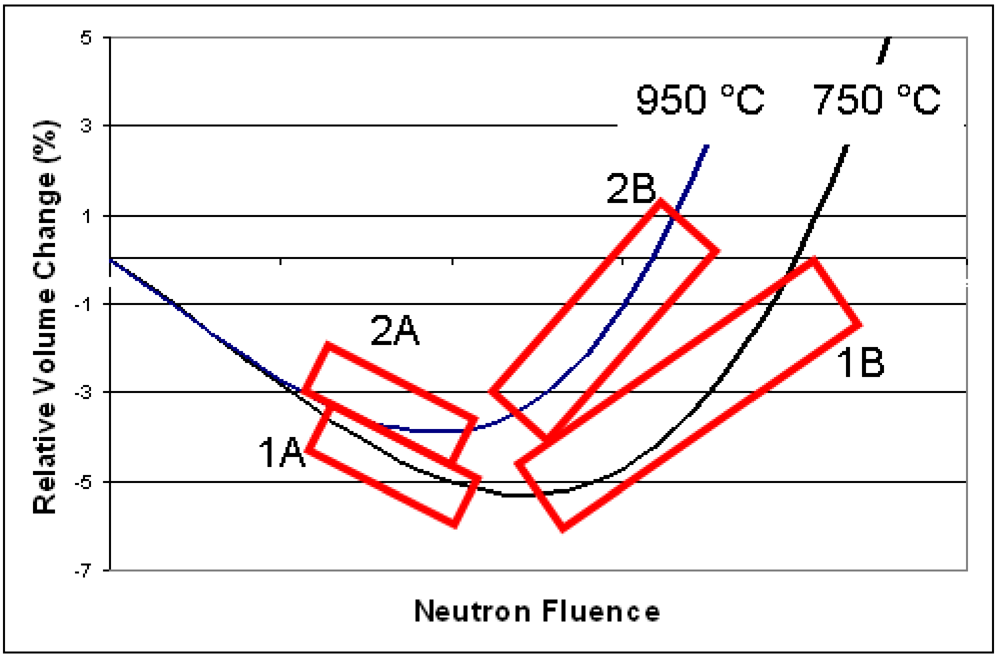

Figure 1-1 Schematic overview of the four INNOGRAPH irradiation experiments

Four graphite grades have been selected as major grades by the project partners in the 5th and 6th Framework projects; two produced by SGL Carbon and two by Graftech. In addition, minor graphite grades are included in the experiments with fewer samples. These also include graphite grades produced by Toyo Tanso.

The following properties were measured and compared before and after irradiation: specimen dimensions, mass, dynamic Young's modulus, coefficient of thermal expansion and thermal diffusivity. Density and thermal conductivity were calculated from the measurements. Full PIE programs have been performed on the INNOGRAPH-1A and -2A in the HTR-M1 and RAPHAEL projects [4, 5]. Full PIE programs on the INNOGRAPH-1B and -2B experiments have been performed in the ARCHER project [6].

This report presents the results of the microstructural analysis on irradiated graphite specimens out of the INNOGRAPH-1A and INNOGRAPH-1B experiments. With this report, ARCHER deliverable D41.13 is fulfilled.

2 Experiments and measurement techniques

2.1 Irradiation experiments

2.1.1 Graphite grades

The selection of graphite grades for the INNOGRAPH irradiations is based on several HTR design requirements such as thermal and mechanical properties, impurity levels, and availability [2]. The major grades, produced by Graftech and SGL Carbon, are chosen in such a way that the graphites cover a variety of microstructures. This is achieved by selecting grades based on different raw materials, i.e. coal tar pitch coke or petroleum coke, and different manufacturing methods, i.e. extrusion, isostatic moulding, or vibro –moulding.

The minor grades include graphites from three different manufacturers, SGL Carbon, Graftech, and Toyo Tanso. The minor grades include graphites based on needle coke.

The graphite grades used in the INNOGRAPH-1A and -1B experiments are listed in Table 2-1. Some grades were absent in the INNOGRAPH-1A experiment. For others, new insights and availability of new grades, the “major/minor” status for the INNOGRAPH-1B experiment was changed with respect to the INNOGRAPH-1A experiment.

Table 2-1 Selected grades for the INNOGRAPH-1A and -1B irradiation experiments

Grade	Manufacturer	Coke	Process	Status 1A	Status 1B
IG-110	Toyo Tanso	Petroleum	Iso-moulding	Major	Minor
IG-430	Toyo Tanso	Pitch	Iso-moulding	Minor	Minor
LPEB/BAN	GrafTech	Needle	Extrusion	n/a	Minor
LPIB	GrafTech	Needle	Iso-moulding	n/a	Minor
NBG-10	SGL	Pitch	Extrusion	Major	Major
NBG-17	SGL	Pitch	Vibro-moulding	n/a	Minor
NBG-18	SGL	Pitch	Vibro-moulding	n/a	Major
NBG-20	SGL	Petroleum	Extrusion	Minor	Minor
NBG-25	SGL	Petroleum	Iso-moulding	Major	Minor
PCEA	GrafTech	Petroleum	Extrusion	Major	Major
PCIB	GrafTech	Petroleum	Iso-moulding	Major	Minor
PPEA	GrafTech	Pitch	Extrusion	Minor	Major

2.1.2 Specimen types

All specimens are cylindrical. The diameter of all specimens is 8 mm and the length is either 6 mm or 12 mm; the majority of samples is 6 mm in length. Specimens of these sizes are small enough to allow a sufficient number of specimens in the irradiation rig, and large enough to perform reasonably accurate measurements. Specimens with a length of 6 mm are suitable for all type of standard PIE measurements (dimensional change, dynamic Young's modulus, coefficient of thermal expansion and thermal diffusivity). The 12 mm samples are included to obtain data points with higher measurement accuracy for dimensional change measurements.

Machining of the samples from the graphite blocks is described in a separate report [7]. The cylindrically shaped specimens are flattened by milling a plane with a width of 3 mm along the length. Figure 2-1 schematically shows the flattening. Producing a plane with a width of 3 mm reduces the volume of the cylinders by 1% only. The benefits of this plane are threefold. The first benefit is the possibility to indicate the z-direction from the original graphite blocks in the specimen. The plane is milled perpendicular to the *z*-direction if the axial direction of the cylinder is parallel to the *xy*-direction, and therefore the *z*-direction in the specimen is known after fabrication. The plane is milled on an arbitrary position if the axial direction of the cylinders is parallel to the *z*-direction, because in that case the *z*-direction is already indicated by the axial direction. The grain orientations quoted for samples in this report (e.g. in Table 2-2) are parallel to the *xy*-direction in Figure 2-1.

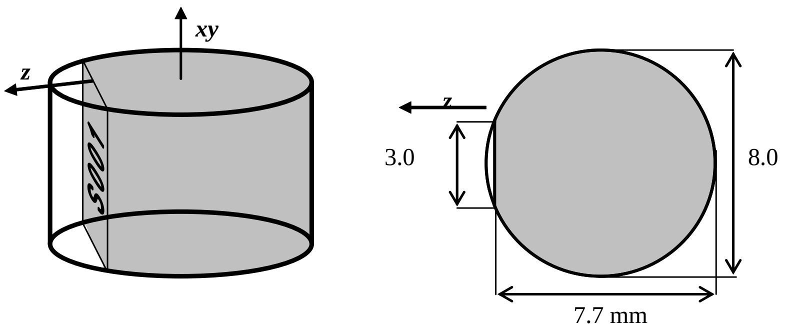

Figure 2-1 Flattening of the specimens. The figure on the left-hand side exaggeratedly shows the flatting of the cylinder. The figure on the right-hand side is a top-view of the specimen

The second benefit of the plane is that it gives an area to engrave the specimen with a unique code. This code is necessary to easily identify a specimen. The code consists of four characters. The first character is a letter that indicates the graphite manufacturer (S= SGL, U= UCAR (Graftech) and T= Toyo Tanso). The last three characters are numbers. A third benefit is that the milled plane can act as a marking that defines the measuring positions during the dimensional measurements before and after irradiation.

2.1.3 INNOGRAPH irradiation experiments at 750°C

The irradiation experiments were performed in the High Flux Reactor (HFR) Petten. The HFR is a tank-in-pool multi-purpose test reactor with a thermal power of 45 MW. Its core arrangement of 9 x 9 positions contains 33 fuel elements, six control rods and 22 beryllium reflector elements, and provides effective 20 in-core positions.

An INNOGRAPH capsule consists of a stack of eight metal drums (Figure 2-2). Each drum has either three or four channels, depending on the experiment, for sample stacks. The capsules are instrumented with 24 thermocouples, placed at different axial and radial positions, to monitor the irradiation temperature. The temperature can be controlled by changing the He/Ne gas mixture in the second containment and by vertical displacement of the capsule in the core.

For purposes of neutron metrology nine activation monitor sets were prepared. Five monitor sets were placed in the central channel of the specimen holder at various vertical levels. The remaining monitor sets were placed in the northern (2), eastern (1) and southern (1) channels, useful for an indication of the radial gradients and the orientation of the experiment. The neutron fluence is measured at the end of the experiment, after the monitoring sets have been removed.

It is important to keep the level of radioactivity of the graphite samples as low as reasonably possible, to make handling of the samples more practical after the irradiation experiment (for post irradiation examinations and reloading in next irradiation experiment) of the samples. Aside from extra purification steps that were made by the manufacturers, some measures are taken in the design. Contact between the metal drum and graphite samples is avoided by placing a graphite foil between them. Contamination of the graphite samples by the drum material is therefore not possible. For the same reason the inner containment is purged with high purity Helium. The design of the INNOGRAPH capsules is kept as simple as possible to allow loading and assembling in a lead shielded hot cell.

INNOGRAPH-1A consists of eight molybdenum drums (Ti-Zr-Mb:TZM alloy) all having a height of 60 mm. There are four stacks of samples in each drum. The irradiation temperature in the lower six drums was 750ºC, the irradiation temperature in the upper two drums was 650ºC.

The second irradiation capsule at 750ºC (INNOGRAPH-1B) contained samples that are irradiated to fluences above cross-over, i.e. the diameter of the samples might be larger than the original 8 mm. To make space for this potential swelling, the diameter of the sample stacks in the drums is larger in this capsule. Therefore, there is only space for three columns of samples in INNOGRAPH-1B. This capsule consists of seven drums (six drums of 60 mm and one drum with a height of 30 mm) that were irradiated at 750ºC. An extra drum at the top, having a height of 60 mm was irradiated at a temperature of 650ºC. The high vertical position of this upper drum makes it not feasible to reach 750ºC, because of the low gamma heating at this position. The extra drum is separated from the other drums by a thermal barrier.

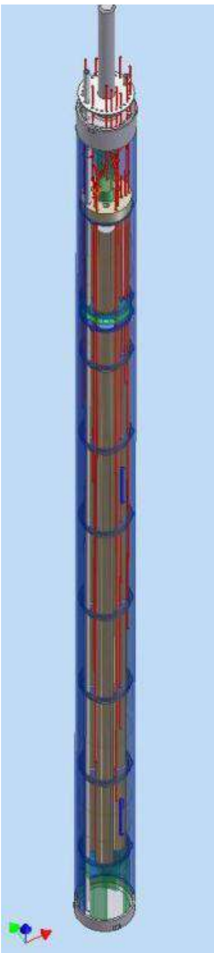

Figure 2-2 Schematic drawing of the INNOGRAPH-1B experiment, showing the eight drums that contain the graphite samples

2.2 Microstructural analysis

2.2.1 Test matrix

The microstructural analysis consists of optical microscopy (OM) and scanning electron microscopy (SEM). For both techniques, the same specimens are used. In total, twenty irradiated graphite specimens are selected. These samples are all samples that were irradiated at 750°C in the INNOGRAPH-1A or INNOGRAPH-1B experiment or both.

The decision to select samples only from experiments at 750°C was made for two reasons. First of all, the project allows for only a limited number of specimens to be investigated by microscopy. Rather than having only one specimen per dpa per grade per irradiation temperature, we decided to investigate per grade specimens at least at two different dpa levels but only one irradiation temperature. Secondly, the availability of specimens of the 950°C INNOGRAPH-2B experiment is limited. Due to activity levels and the amount of swelling only a limited amount of INNOGRAPH-2B samples have their physical property measurements completed [6]. Only samples that have their standard PIE completed can be selected for microscopy, because microscopy is a destructive test method due to the required sample preparation.

Figure 2-3 shows a schematic representation of the volume change versus neutron fluence (dpa) curve typical for nuclear graphites. Indicated are the typical states graphite undergoes due to irradiation. After an initial shrinkage (1), at turn-around fluence (2) graphite starts to swell again (3). At a certain fluence the sample reaches its original size again (cross-over, 4), after which the sample continues to swell beyond the original sample volume (5). Samples for microstructural analysis are selected to have as good a spread over the different states of graphite as sample availability allows. Sample availability is limited by re-irradiation of the INNGRAPH-1A samples and destructive diametric compression experiments on INNOGRAPH-1A and -1B samples in the framework of the ARCHER project. Table 2-2 and Table 2-3 show the specimens selected for optical microscopy and SEM respectively, ordered by graphite grade and increasing neutron fluence.

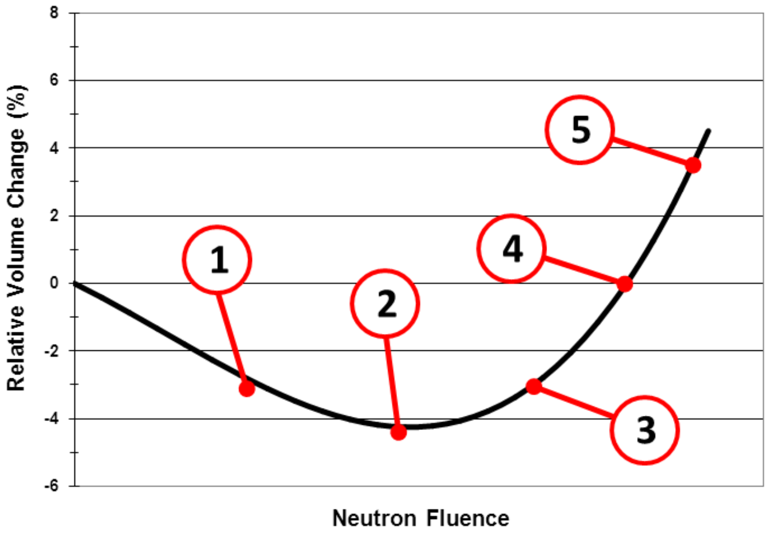

Figure 2-3 Schematic volume change versus neutron fluence curve, with indicated characteristic regions in these type of curves: 1) Shrinking. 2) Turn-around. 3) Swelling. 4) Cross-over. 5) Swollen.

Table 2-2 Test matrix for optical microscopy on irradiated graphite samples from the INNOGRAPH-1A and -1B experiments.

Specimen code	Grade	Location	Orientation	dpa	state
S040	NBG-10	heart	AG	7	Shrinking
S078	NBG-10	edge	AG	11.2	Turn-around
S074	NBG-10	edge	AG	19	Cross-over
S041	NBG-10	edge	AG	21.1	Swollen
S626	NBG-17	heart	WG	9.4	Shrinking
S579	NBG-17	edge	WG	13.2	Cross-over
S476	NBG-18	edge	AG	10	Shrinking
S468	NBG-18	edge	WG	13.1	Swelling
S114	NBG-25	heart	WG	6.3	Shrinking
S141	NBG-25	edge	WG	7.8	Shrinking
S107	NBG-25	heart	WG	11	Turn-around
S111	NBG-25	heart	WG	15.2	Cross-over
U021	PCEA	heart	AG	17	Swelling
U070	PCEA	edge	WG	20.6	Swollen
U163	PCIB	heart	AG	6.4	Shrinking
U113	PCIB	heart	AG	9.1	Turn-around
U329	PPEA	edge	WG	12.2	Turn-around
U277	PPEA	heart	WG	18.7	Cross-over
T024	IG-110	heart	WG	7.1	Shrinking
T040	IG-110	edge	AG	11.4	Turn-around

Table 2-3 Test matrix for SEM on irradiated graphite samples from the INNOGRAPH-1A and -1B experiments

Specimen code	Grade	Location	Orientation	dpa	state
S078	NBG-10	edge	AG	11.2	Turn-around
S041	NBG-10	edge	AG	21.1	Swollen
S579	NBG-17	edge	WG	13.2	Cross-over
S468	NBG-18	edge	WG	13.1	Swelling
U021	PCEA	heart	AG	17	Swelling
U113	PCIB	heart	AG	9.1	Turn-around
U329	PPEA	edge	WG	12.2	Turn-around
U277	PPEA	heart	WG	18.7	Cross-over
T040	IG-110	edge	AG	11.4	Turn-around

2.2.2 Sample preparation

All samples used in the microstructural analysis are 6 mm in length (see §2.1.2). Samples are placed in a sample holder that can be used in both the optical microscope and the SEM. The samples are fixed in the sample holder using an two-component resin with fluorescent dye. The samples are mounted such that they protrude 0.5 mm from the holder. After curing of the resin, the sample is grinded down to the level of the sample holder using silicon carbide paper. Next, the sample surface is polished using increasingly fine oil based diamond paste down to 1 µm grain size. Because of sample activity, all preparation is performed in gloveboxes.

The sample orientation in the test matrix (Table 2-2) indicates the direction of the sample with respect to the grain direction in the graphite source material. The length of the cylindrical sample is parallel to the indicated direction. Thus, the optical and scanning electron micrographs will show a plane orthogonal to the direction indicated in Table 2-2.

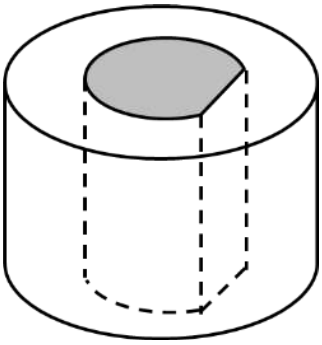

Figure 2-4 Schematic representation of a sample prepared for both optical microscopy and SEM. The grey area indicates the cross-section of the sample that is investigated by microscopy.

2.2.3 Optical microscopy

Optical microscopy is performed on an Olympus BX51 optical microscope. The microscope is placed in a glovebox to allow for radioactive samples to be investigated. Sample positioning is performed using a computer-controlled *xy*-stage. Bright field, polarised light, and fluorescence microscopy can be performed on the BX51. For bright field and polarised light microscopy, a 120W metal halide lamp is present. For fluorescence microscopy, a100W Halogen X-cite 120Q lamp with appropriate fluorescence filters is available. Objectives available on the Olympus BX51 are 5x, 10x, 20x, 50x, and 100x magnification long working distance objectives. Micrographs are obtained using a 5 megapixel, 14 bit CCD camera and "*Stream motion*" software by Olympus. The full image resolution is 2576 by 1932 pixels.

For the microstructure analysis, first bright field and polarised light micrographs of the whole sample cross-section are made. These micrographs are composed of approximately 35 micrographs at 5x magnification. Next, micrographs are made on 5x up to 100x magnification on 5 different locations on the sample. These 5 locations are chosen randomly once and used for all samples to have a comparable spread of locations over the sample cross-section. For 5x, 10x, and 20x magnification, next to bright field also polarised light micrographs are acquired.

2.2.4 SEM

At NRG, a JEOL JSM 6490 scanning electron microscope, equipped with several detectors (EDS, WDS and EBSD), is available. The SEM is placed in alpha tight hot-cell to allow analysing radioactive samples emitting α, γ and β radiation, therefore both nuclear structural materials and nuclear fuels can be analysed. Irradiation sensitive parts of the SEM are removed or protected and changes have been made to the SEM to allow remote handling and to allow maintenance of the important parts.

The SEM has a Tungsten filament and an acceleration voltage between 0.3- 30 keV. It can be operated in both low and high vacuum mode. Low vacuum mode is useful for bad conducting samples, the resolution of 3.0 nm is reached in the high vacuum mode at 30 keV. As graphite is conductive, high vacuum mode can be used. The resin used for sample fixation can be charged somewhat by the electron beam, although in this did not reduce the quality significantly for the investigated samples.

3 Results

3.1 Optical microscopy

All twenty samples were successfully prepared for microscopy. In section 3.1.1, bright field overview micrographs arranged by graphite grade and increasing dpa are presented. This allows for quick comparison of the microscopy results as function of dpa. In paragraphs 3.1.2 to 3.1.9 detailed micrographs of the irradiated graphite samples are presented for the various graphite grades.

3.1.1 Bright field overview micrographs

Figure 3-1 to Figure 3-8 show the bright field overview micrographs for all irradiated graphite samples, grouped per graphite grade. At first glance, the micrographs do not show any clear effect of the irradiation. The main visible effect is the expansion of the samples as at high dpa the samples barely fit in the field of view of the overview micrographs.

The fine-grain graphites show apparent stained areas (IG-110, Figure 3-1, and PCIB, Figure 3-7). In these areas, the resin has not penetrated the pores of the samples. Multiple non-filled pores together appear as black stains.

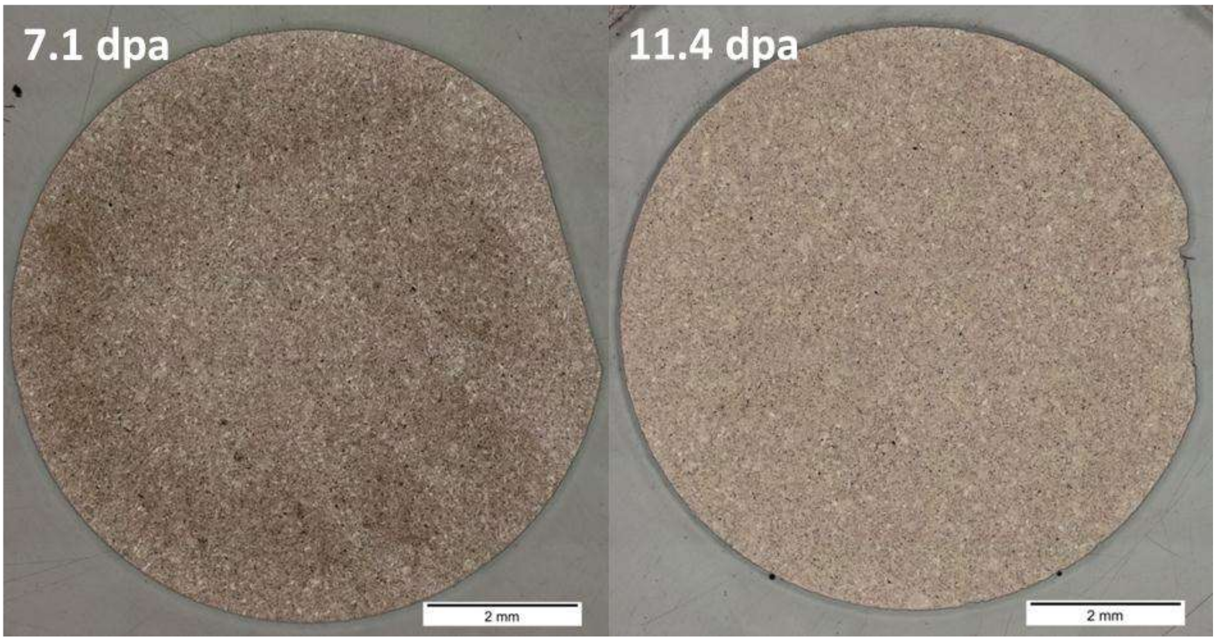

Figure 3-1 Bright field overview optical micrographs of irradiated IG-110 samples

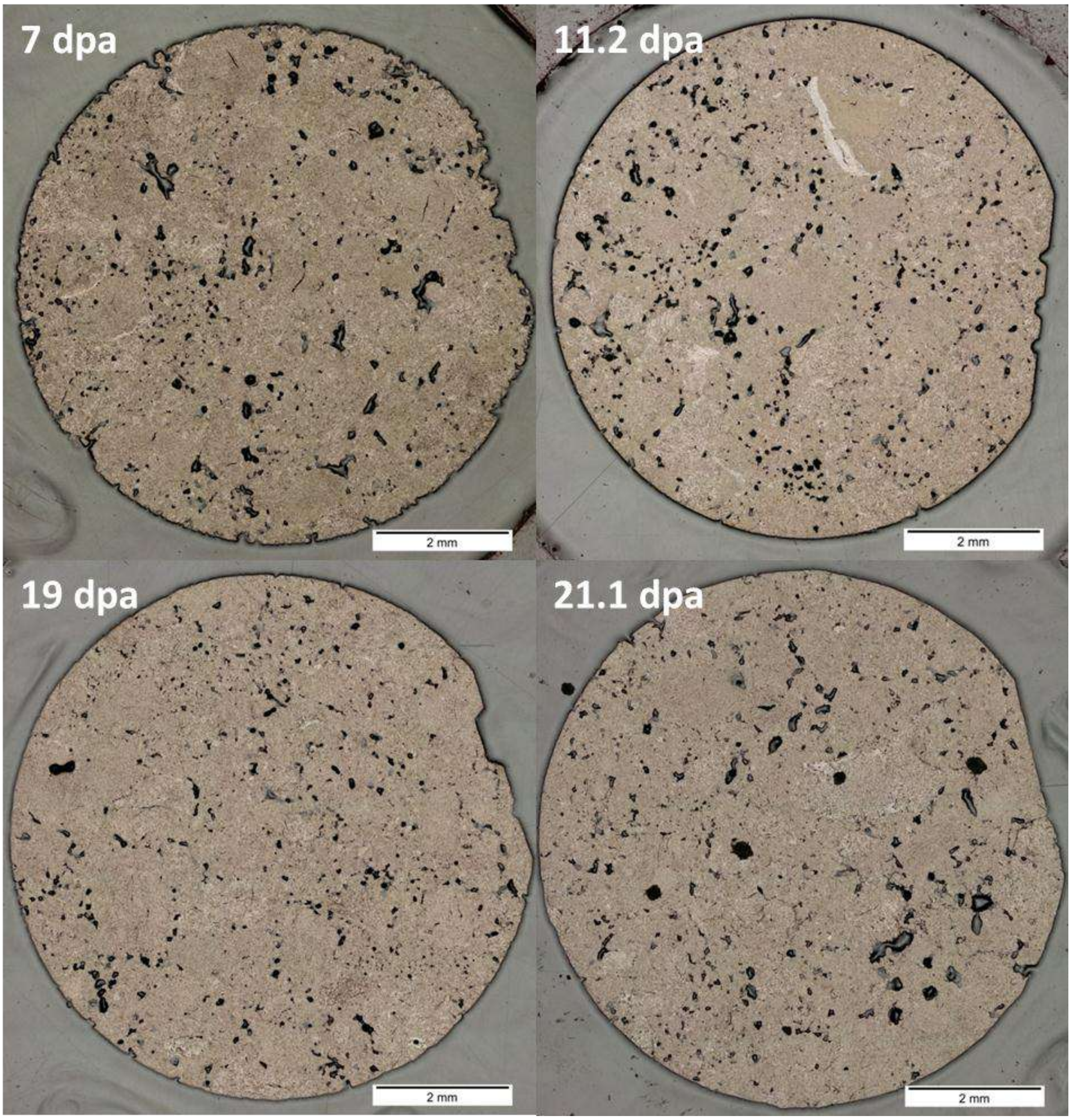

Figure 3-2 Bright field overview optical micrographs of irradiated NBG-10 samples

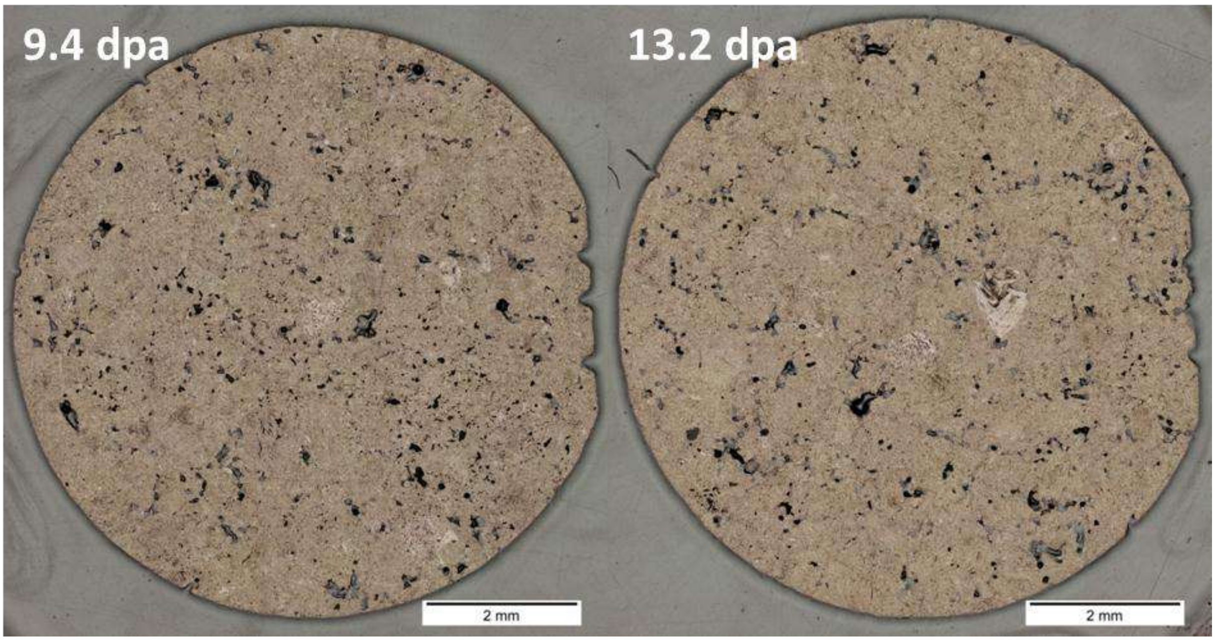

Figure 3-3 Bright field overview optical micrographs of irradiated NBG-17 samples

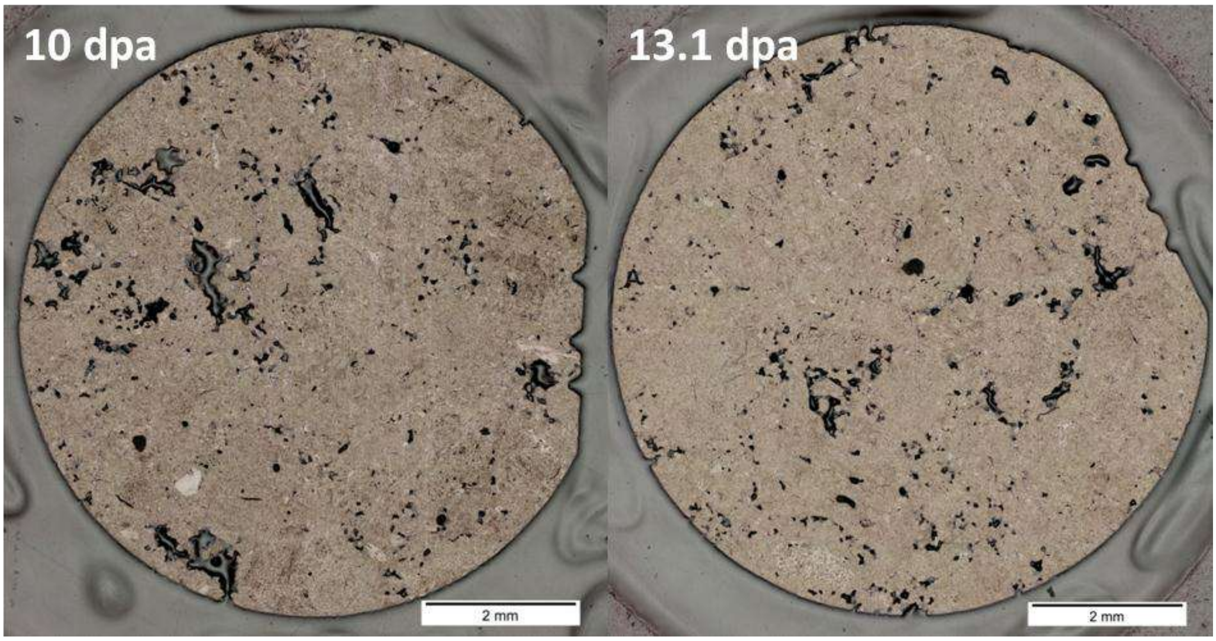

Figure 3-4 Bright field overview optical micrographs of irradiated NBG-18 samples

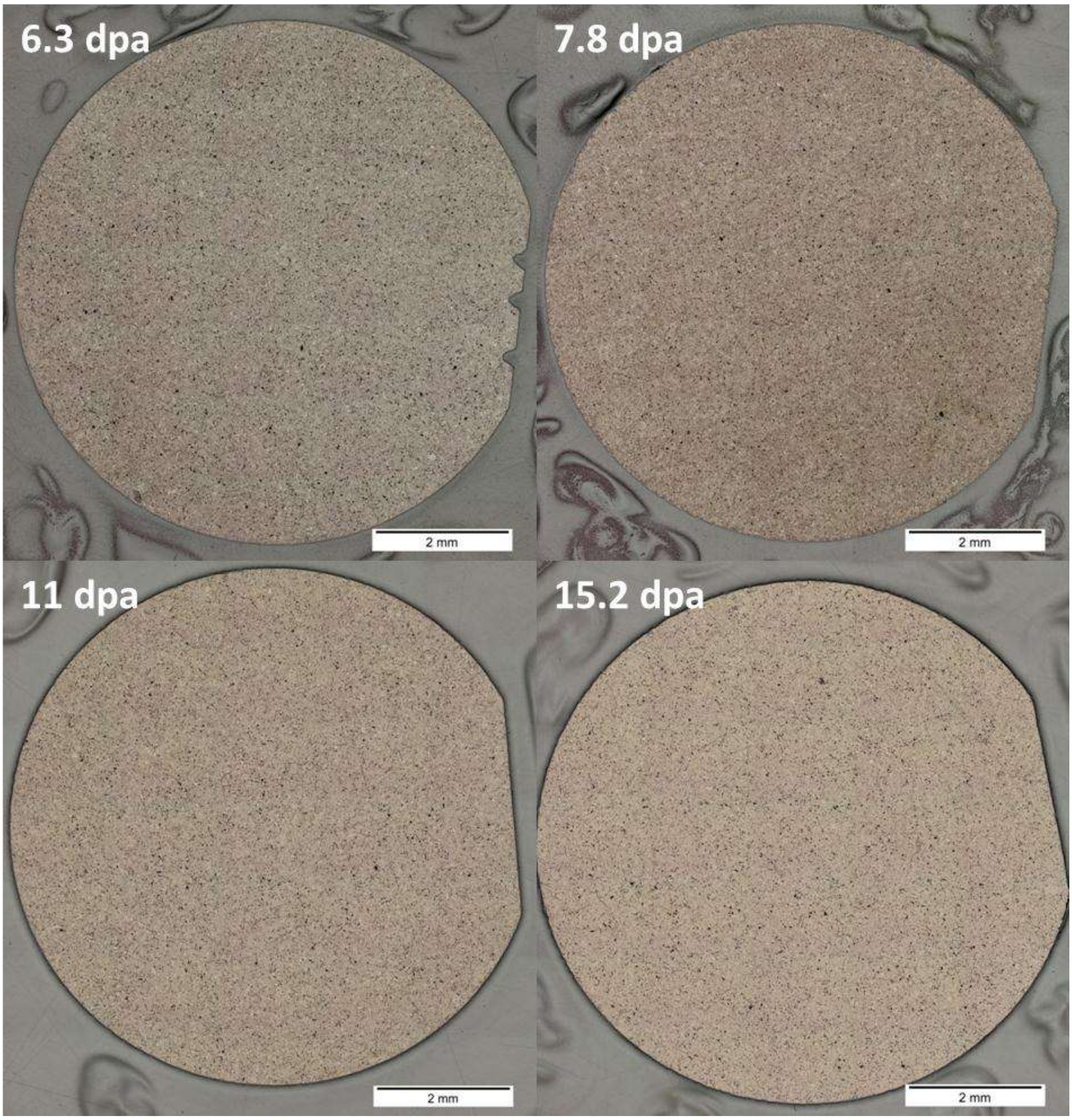

Figure 3-5 Bright field overview optical micrographs of irradiated NBG-25 samples

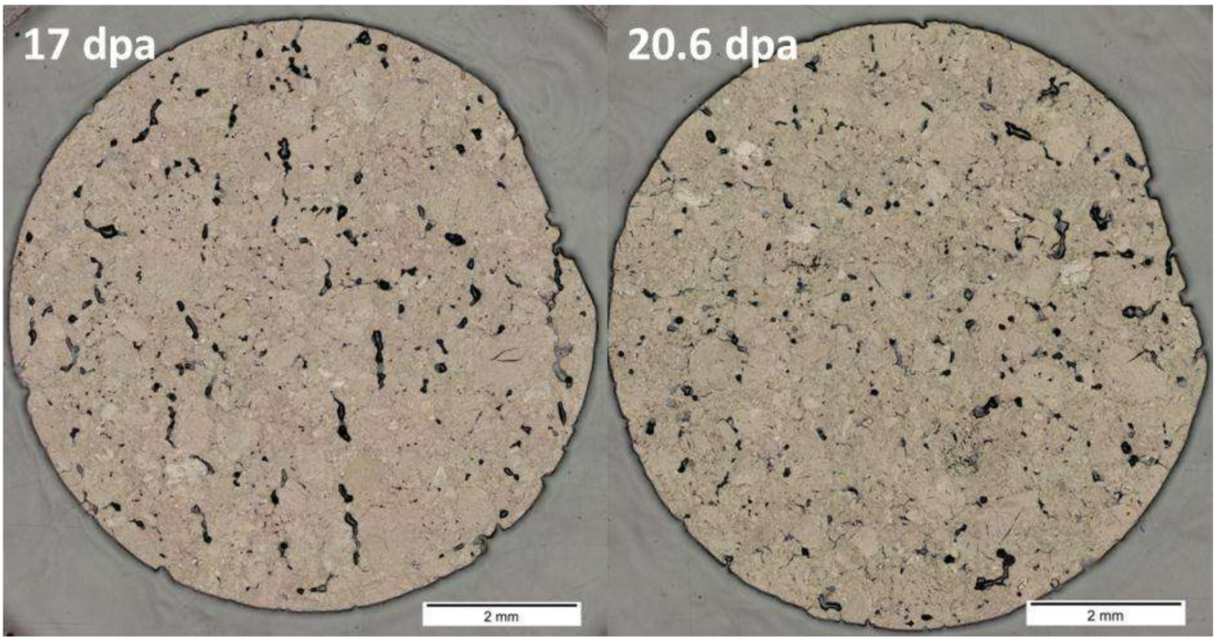

Figure 3-6 Bright field overview optical micrographs of irradiated PCEA samples

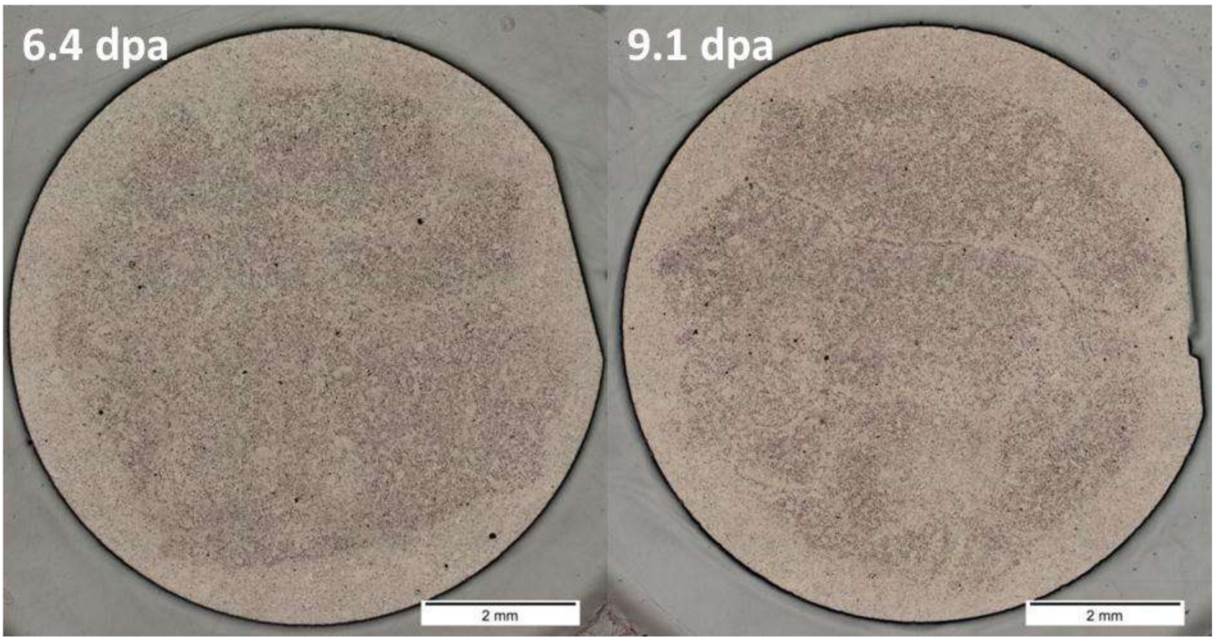

Figure 3-7 Bright field overview optical micrographs of irradiated PCIB samples

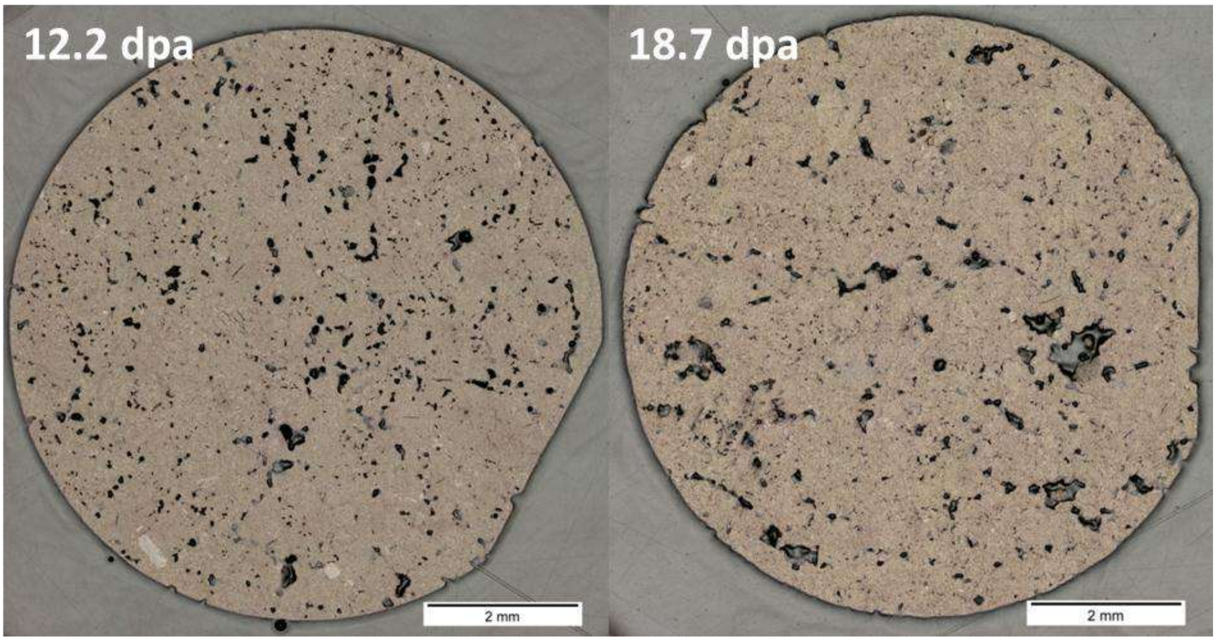

Figure 3-8 Bright field overview optical micrographs of irradiated PPEA samples

3.1.2 NBG-10 detail micrographs

Figure 3-9 to Figure 3-24 show the detail micrographs of the irradiated NBG-10 graphite specimens.

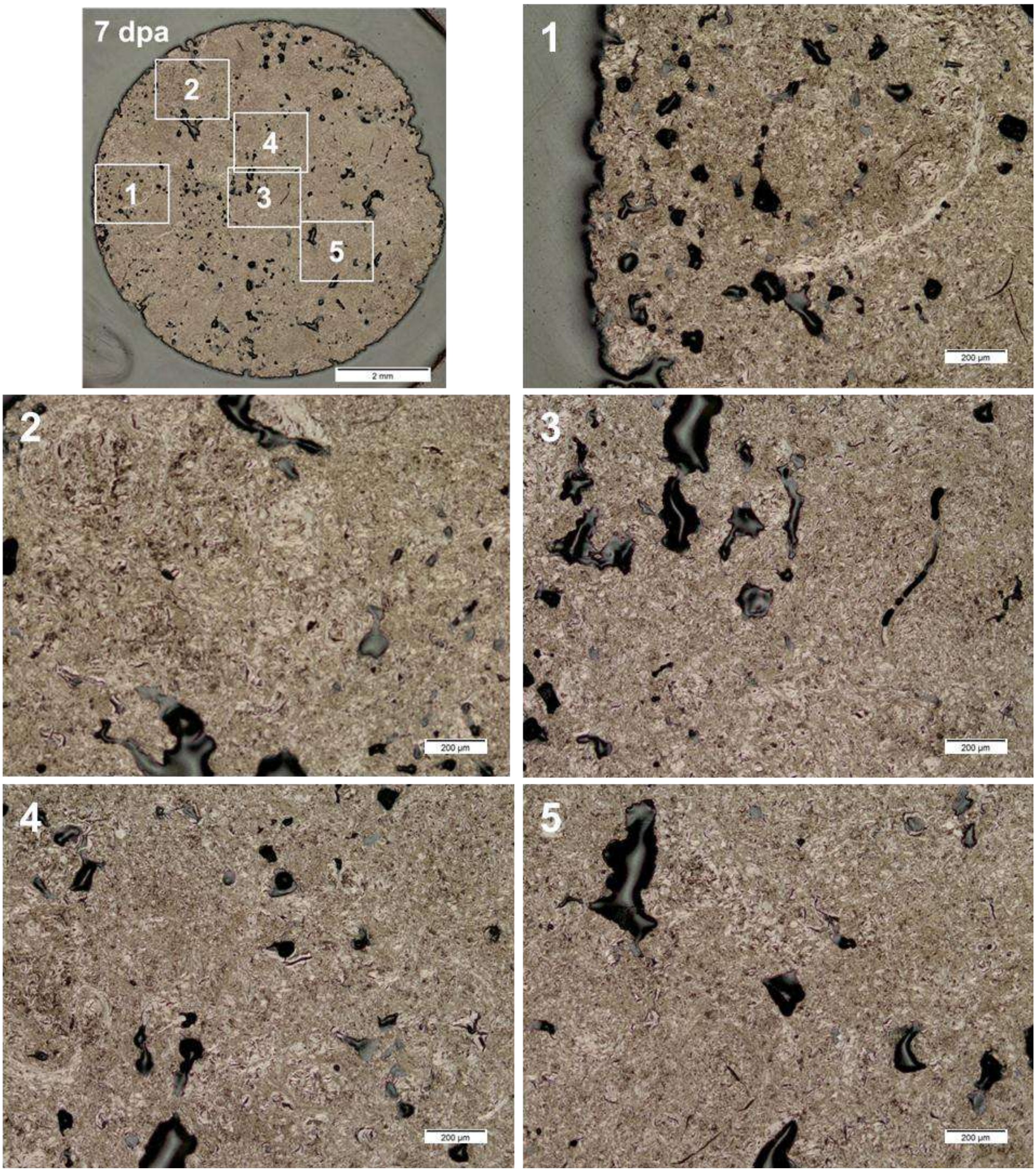

Figure 3-9 Bright field optical micrographs at 5x magnification of NBG-10 specimen S040 (7 dpa) and overview micrograph (top left) with indicated the locations of these micrographs on the sample

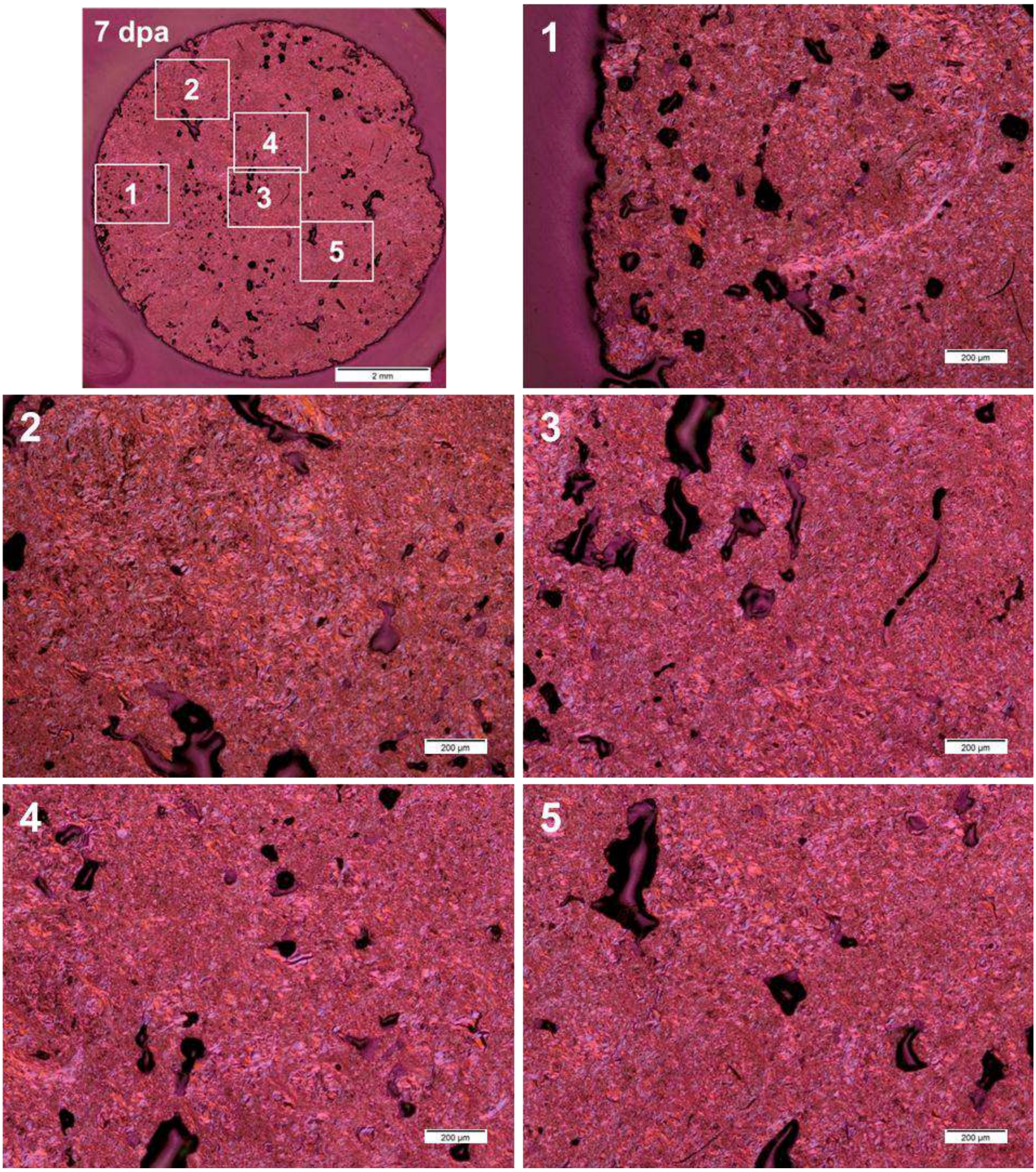

Figure 3-10 Polarisation microscopy images at 5x magnification of NBG-10 specimen S040 (7 dpa) and overview micrograph (top left) with indicated the locations of these micrographs on the sample

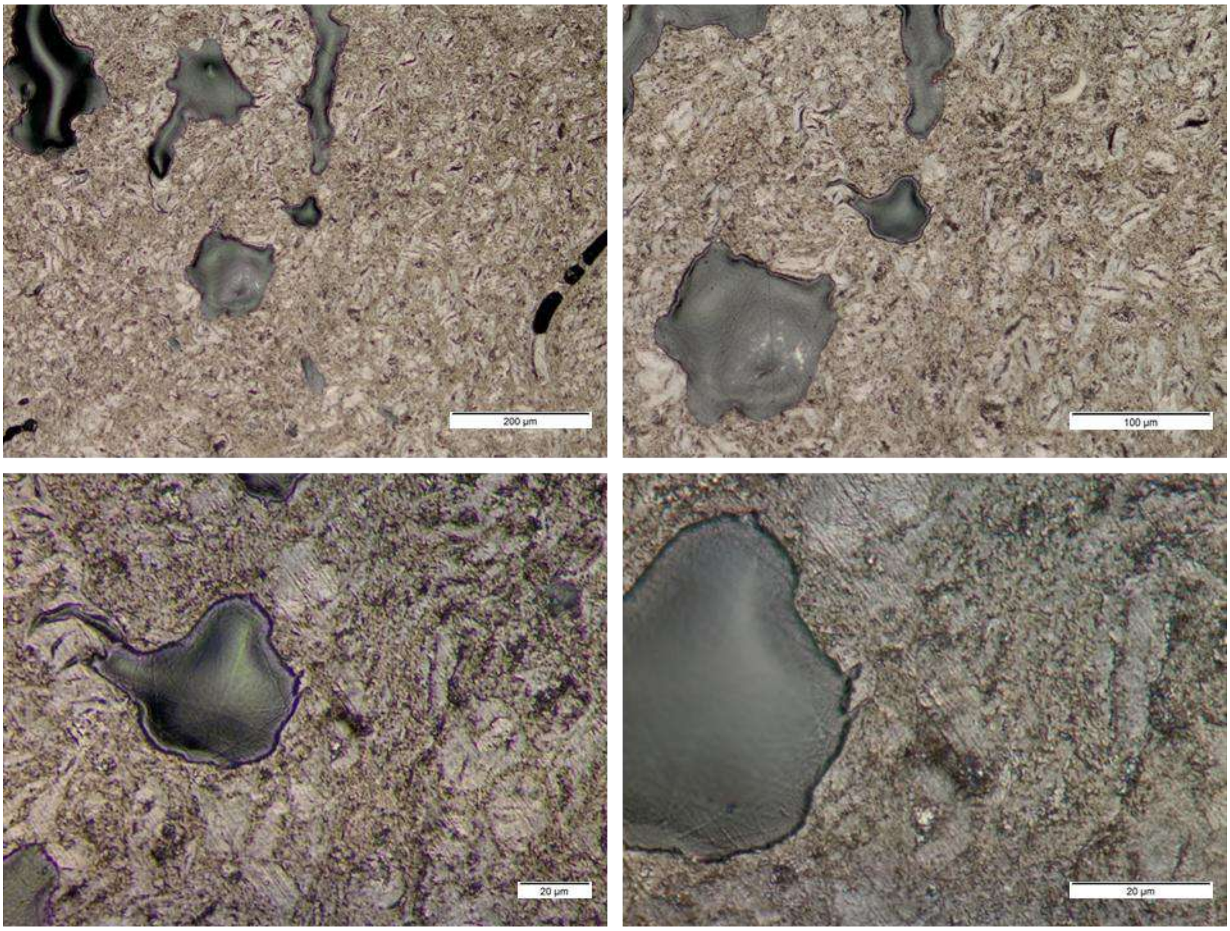

Figure 3-11 Bright field microscopy images of NBG-10 specimen S040 (7 dpa) at 10x to 100x magnification at detail location 3

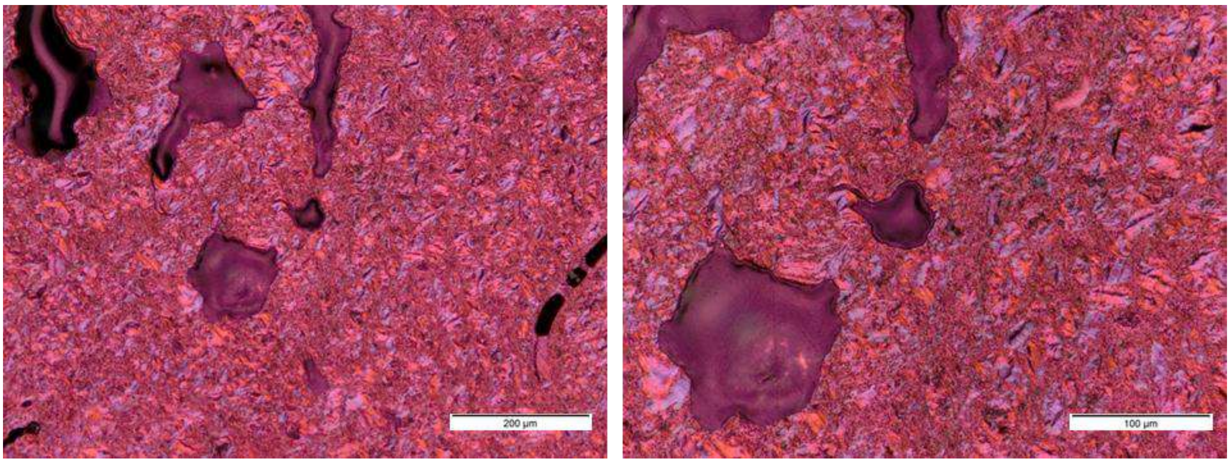

Figure 3-12 Polarisation microscopy images of NBG-10 specimen S040 (7 dpa) at 10x and 20x magnification at detail location 3

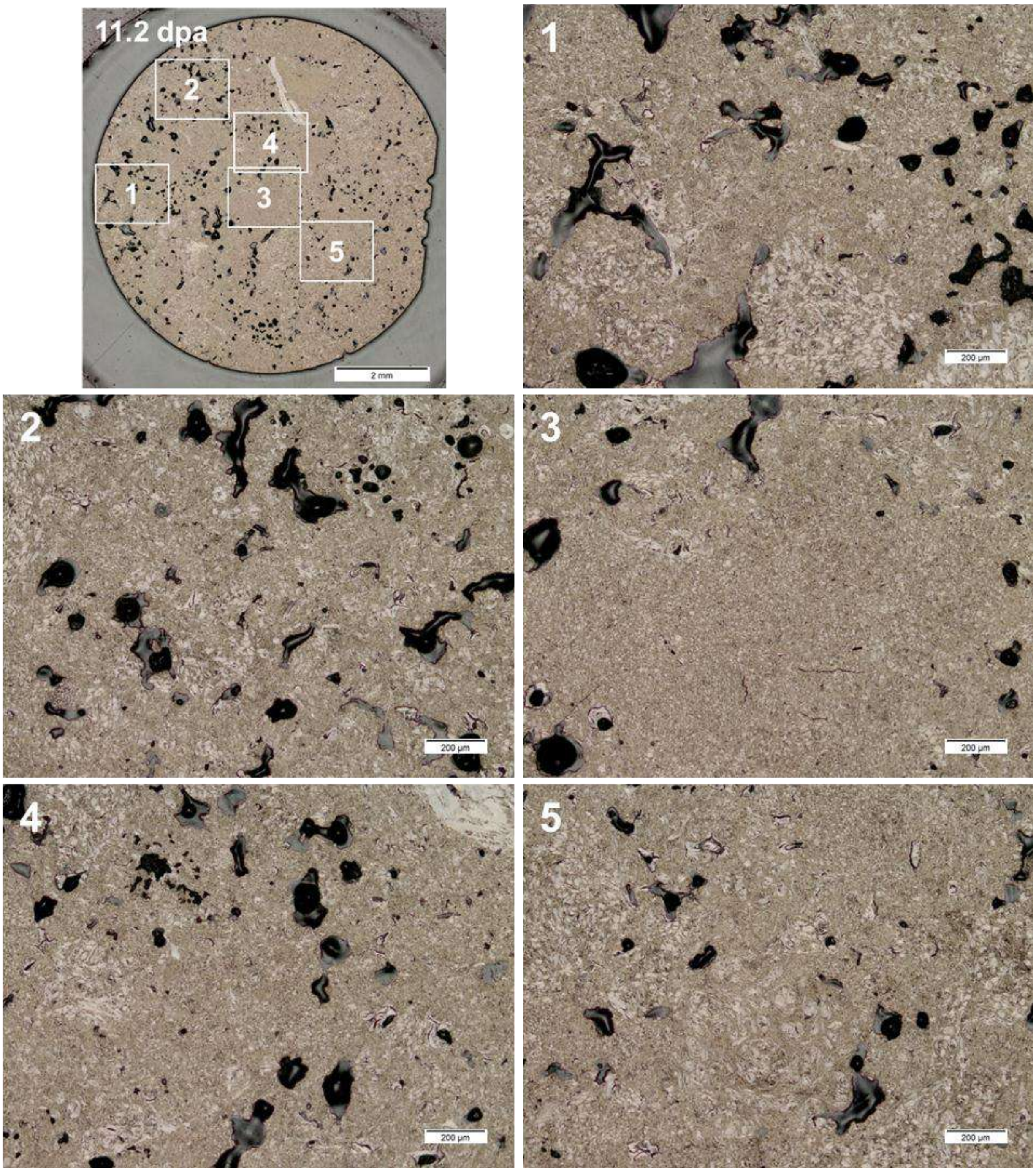

Figure 3-13 Bright field optical micrographs at 5x magnification of NBG-10 specimen S078 (11.2 dpa) and overview micrograph (top left) with indicated the locations of these micrographs on the sample

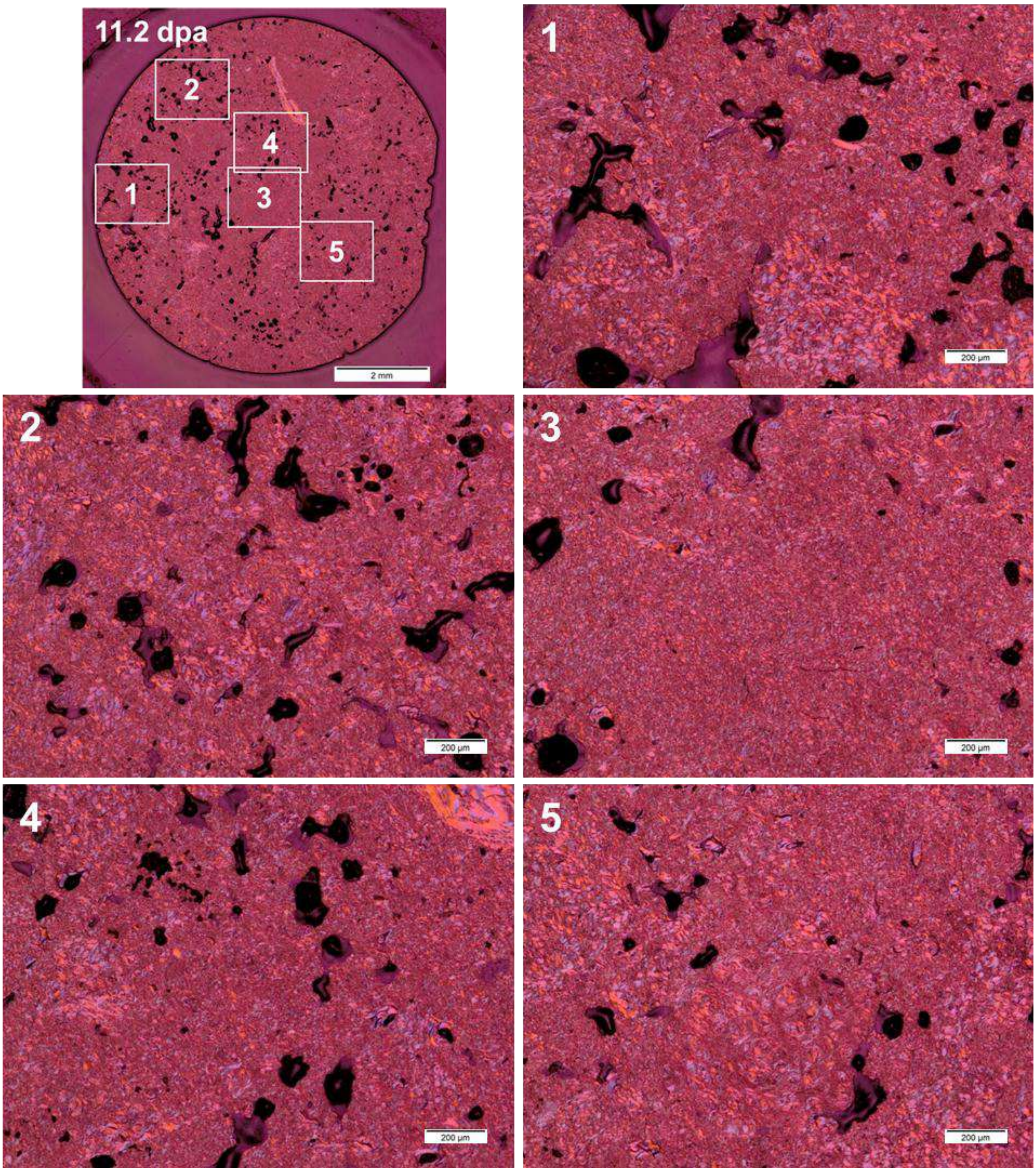

Figure 3-14 Polarisation microscopy images at 5x magnification of NBG-10 specimen S078 (11.2 dpa) and overview micrograph (top left) with indicated the locations of these micrographs on the sample

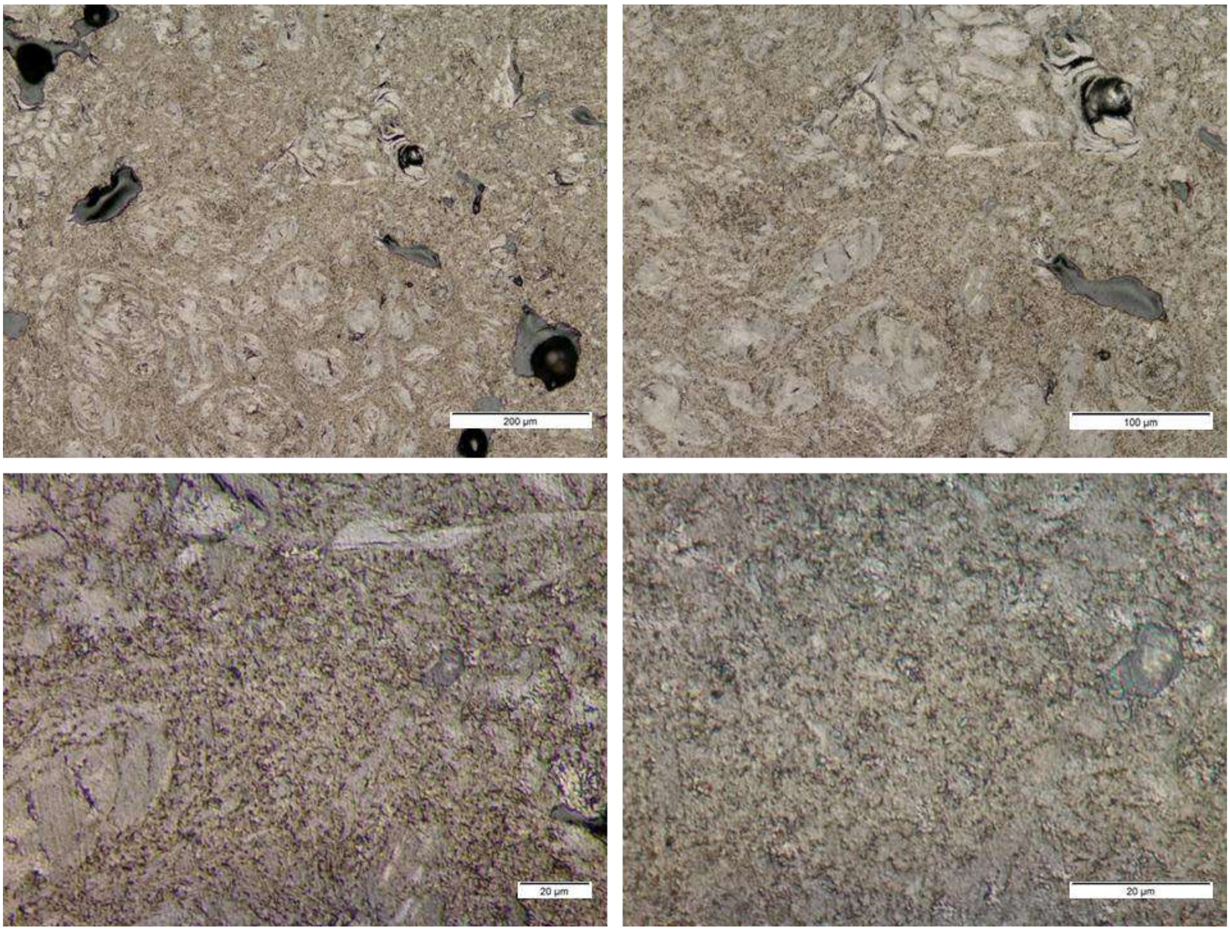

Figure 3-15 Bright field microscopy images of NBG-10 specimen S078 (11.2 dpa) at 10x to 100x magnification at detail location 5

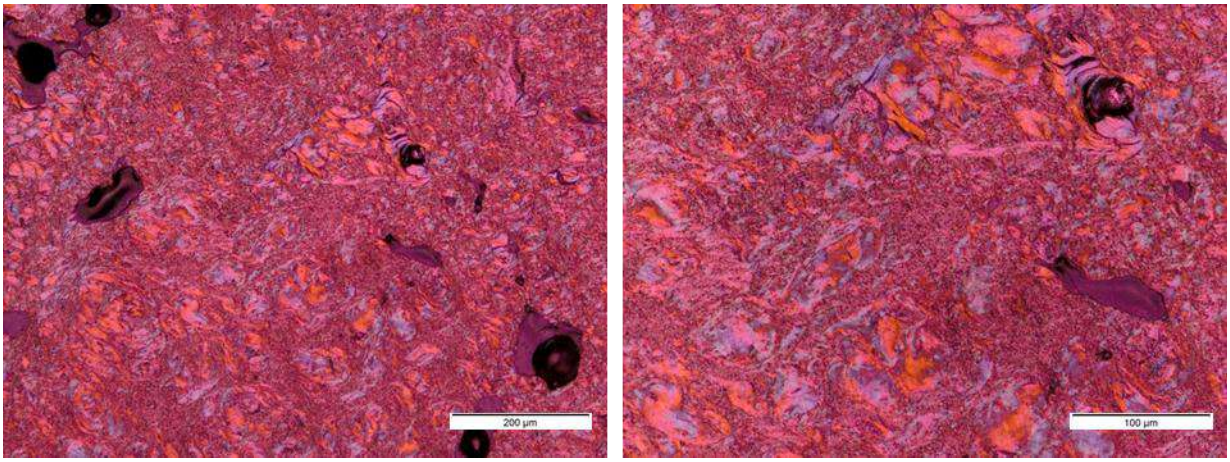

Figure 3-16 Polarisation microscopy images of NBG-10 specimen S078 (11.2 dpa) at 10x and 20x magnification at detail location 5

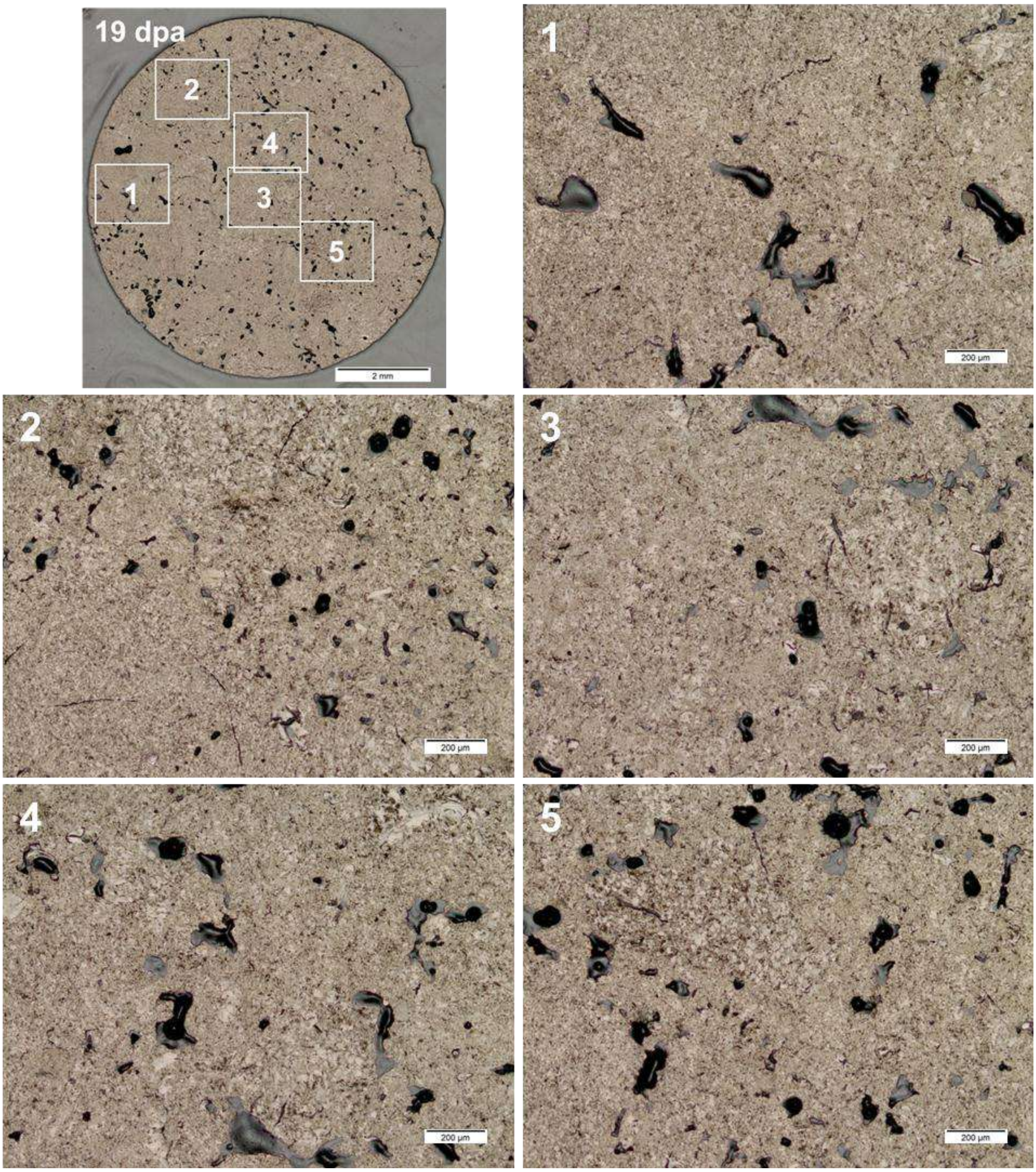

Figure 3-17 Bright field optical micrographs at 5x magnification of NBG-10 specimen S074 (19 dpa) and overview micrograph (top left) with indicated the locations of these micrographs on the sample

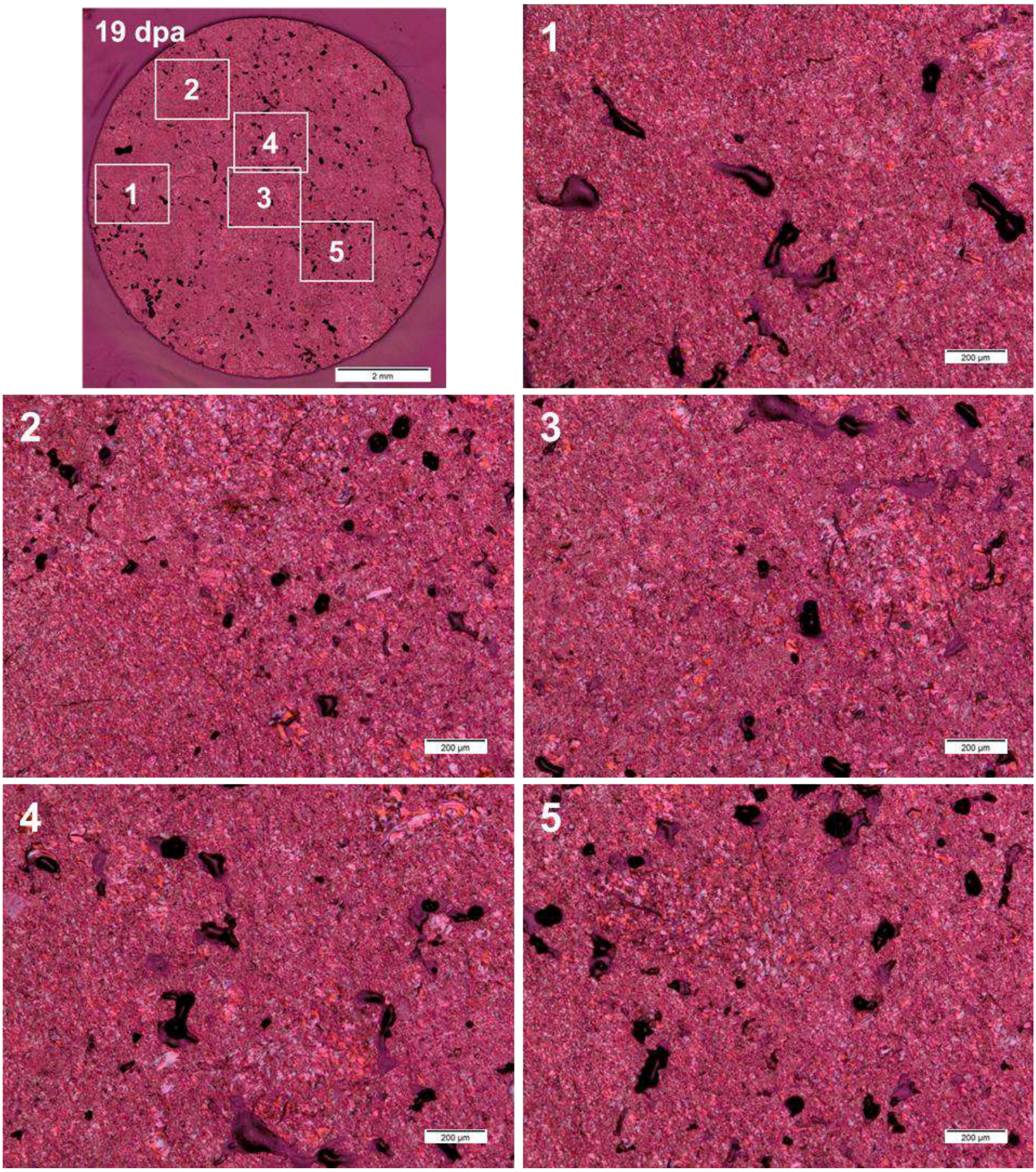

Figure 3-18 Polarisation microscopy images at 5x magnification of NBG-10 specimen S074 (19 dpa) and overview micrograph (top left) with indicated the locations of these micrographs on the sample

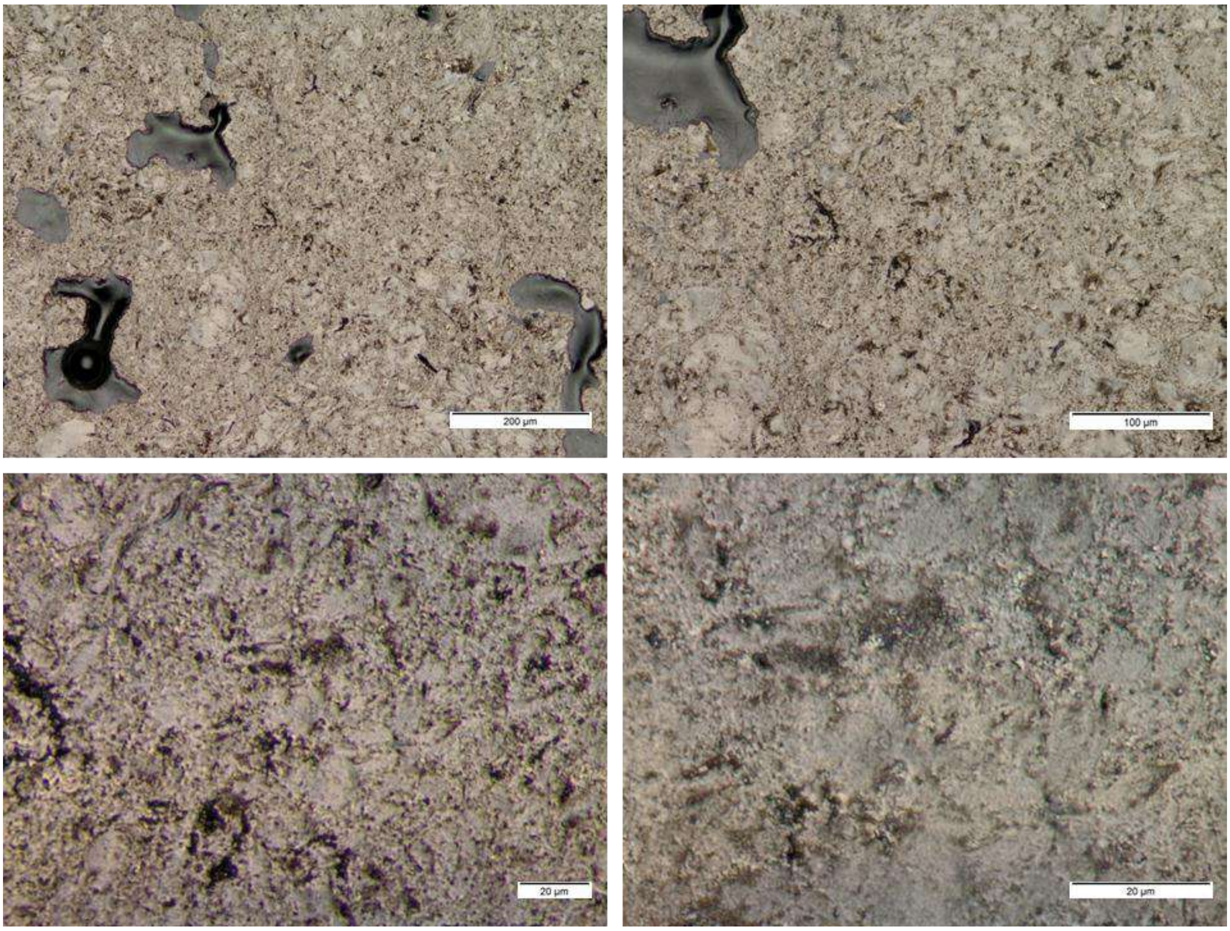

Figure 3-19 Bright field microscopy images of NBG-10 specimen S074 (19 dpa) at 10x to 100x magnification at detail location 4

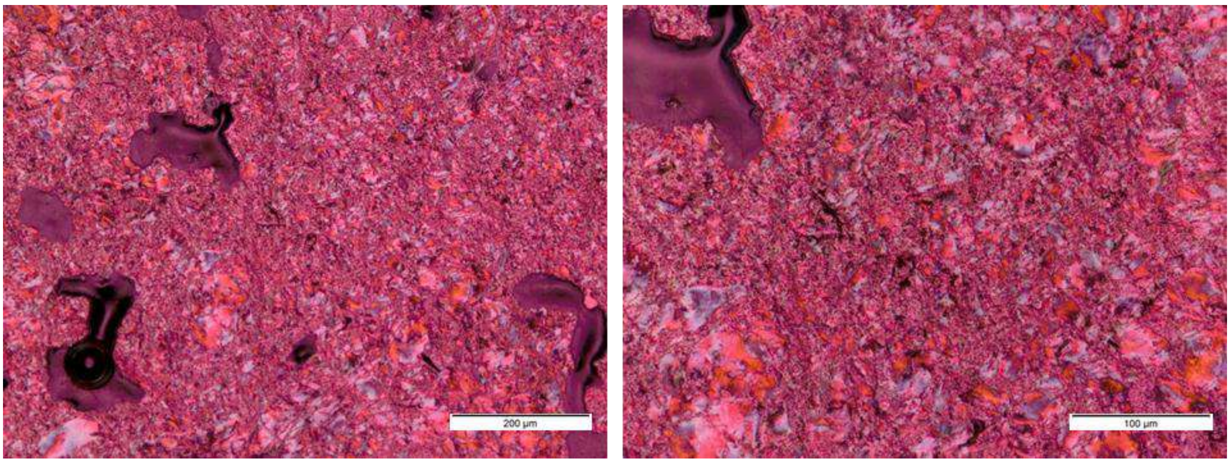

Figure 3-20 Polarisation microscopy images of NBG-10 specimen S074 (19 dpa) at 10x and 20x magnification at detail location 4

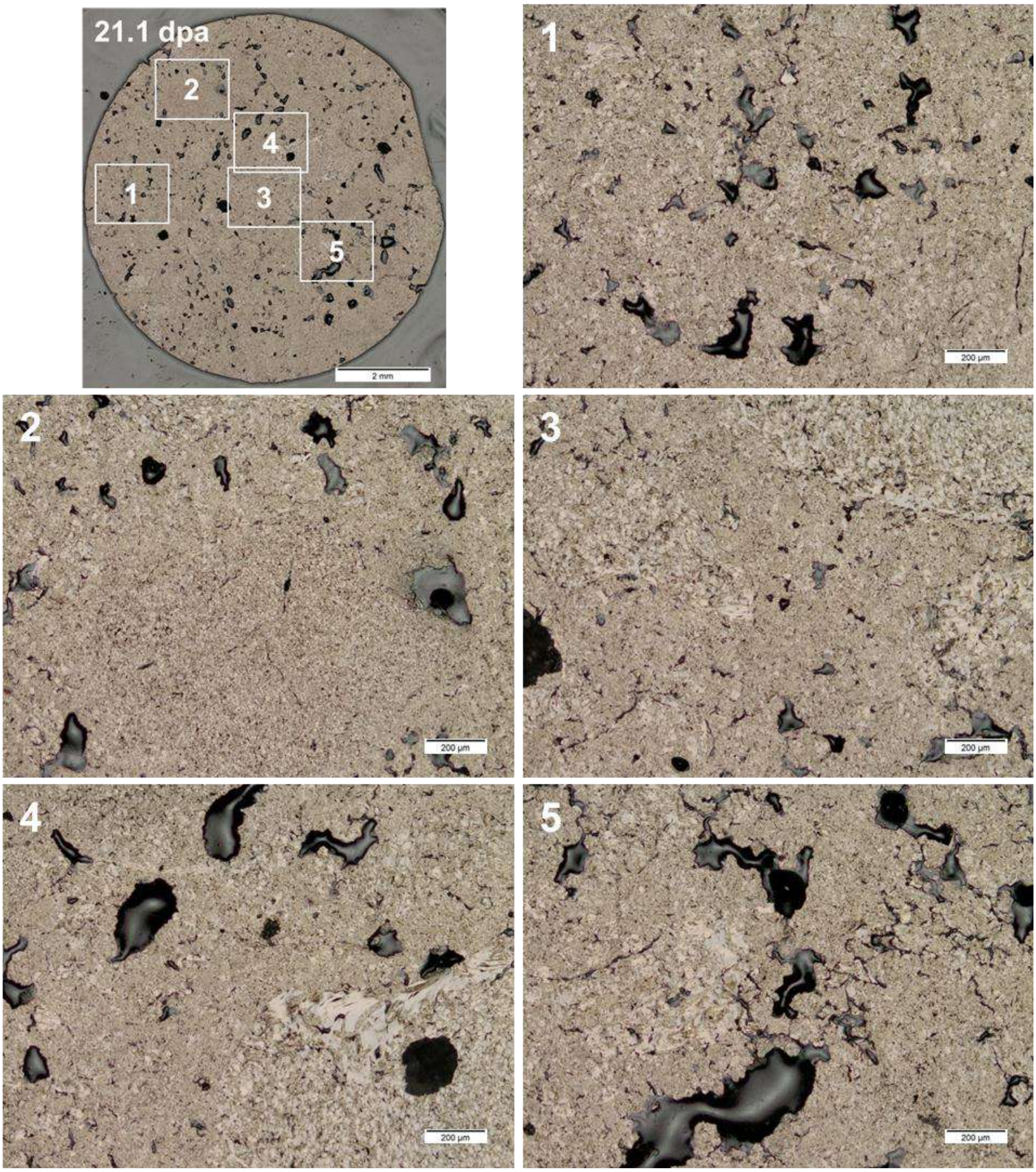

Figure 3-21 Bright field optical micrographs at 5x magnification of NBG-10 specimen S041 (21.1 dpa) and overview micrograph (top left) with indicated the locations of these micrographs on the sample

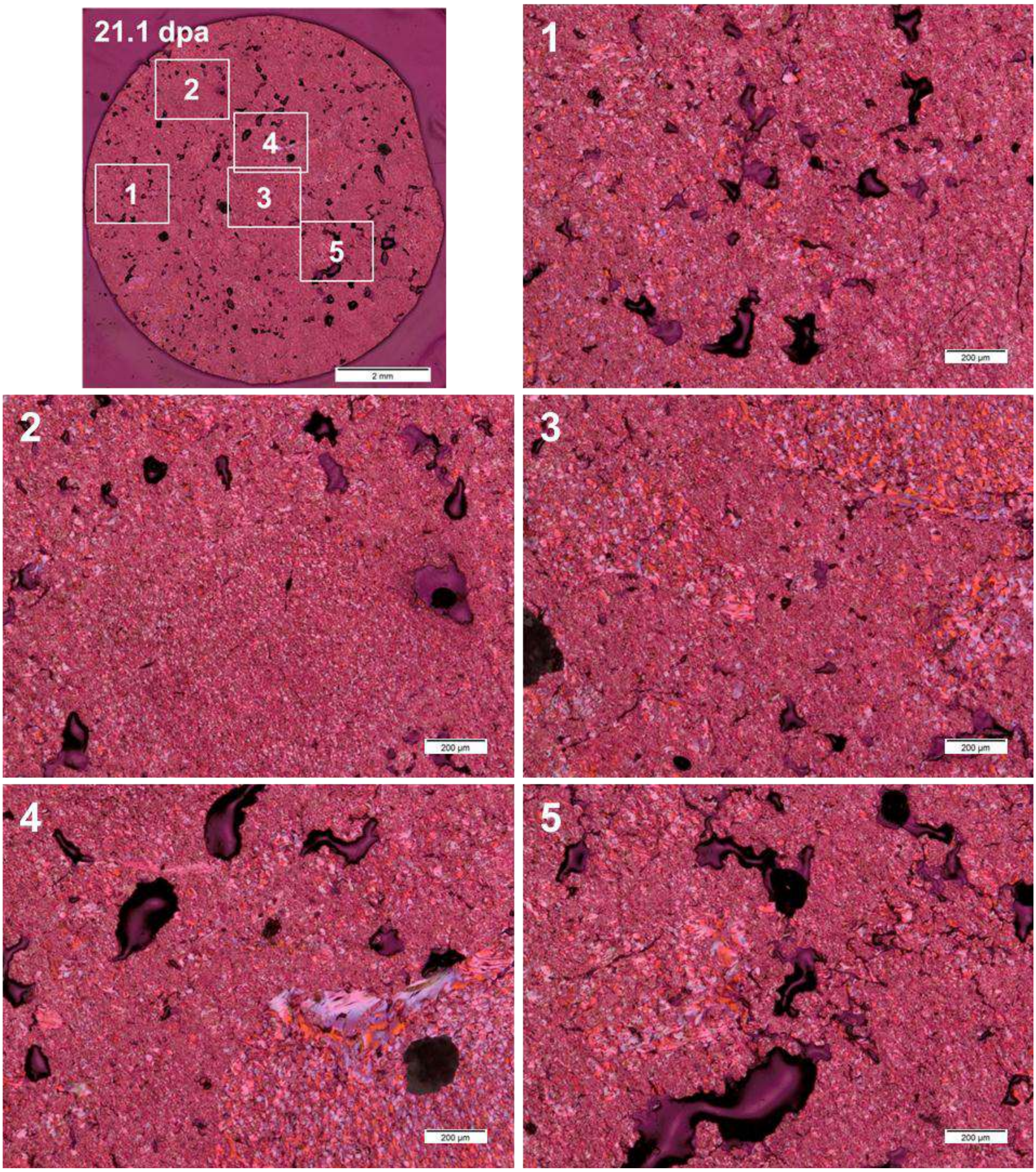

Figure 3-22 Polarisation microscopy images at 5x magnification of NBG-10 specimen S041 (21.1 dpa) and overview micrograph (top left) with indicated the locations of these micrographs on the sample

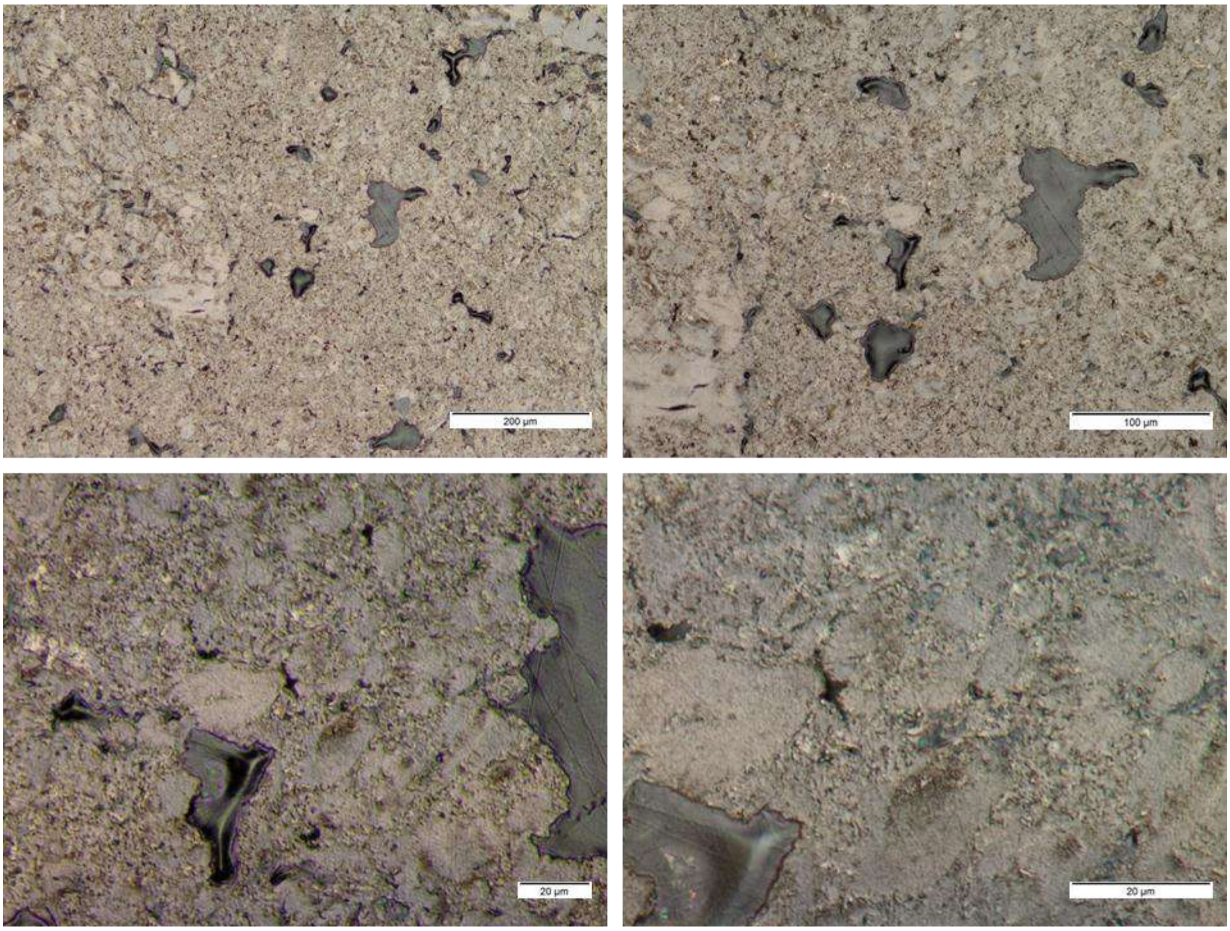

Figure 3-23 Bright field microscopy images of NBG-10 specimen S041 (21.1 dpa) at 10x to 100x magnification at detail location 3

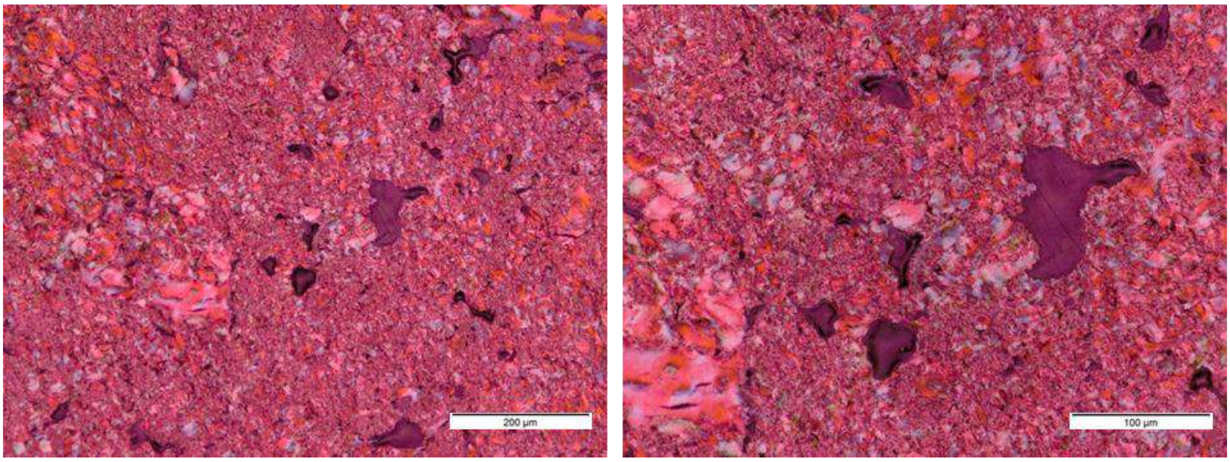

Figure 3-24 Polarisation microscopy images of NBG-10 specimen S041 (21.1 dpa) at 10x and 20x magnification at detail location 3

3.1.3 NBG-17 detail micrographs

Figure 3-25 to Figure 3-32 show the detail micrographs of the irradiated NBG-17 graphite specimens.

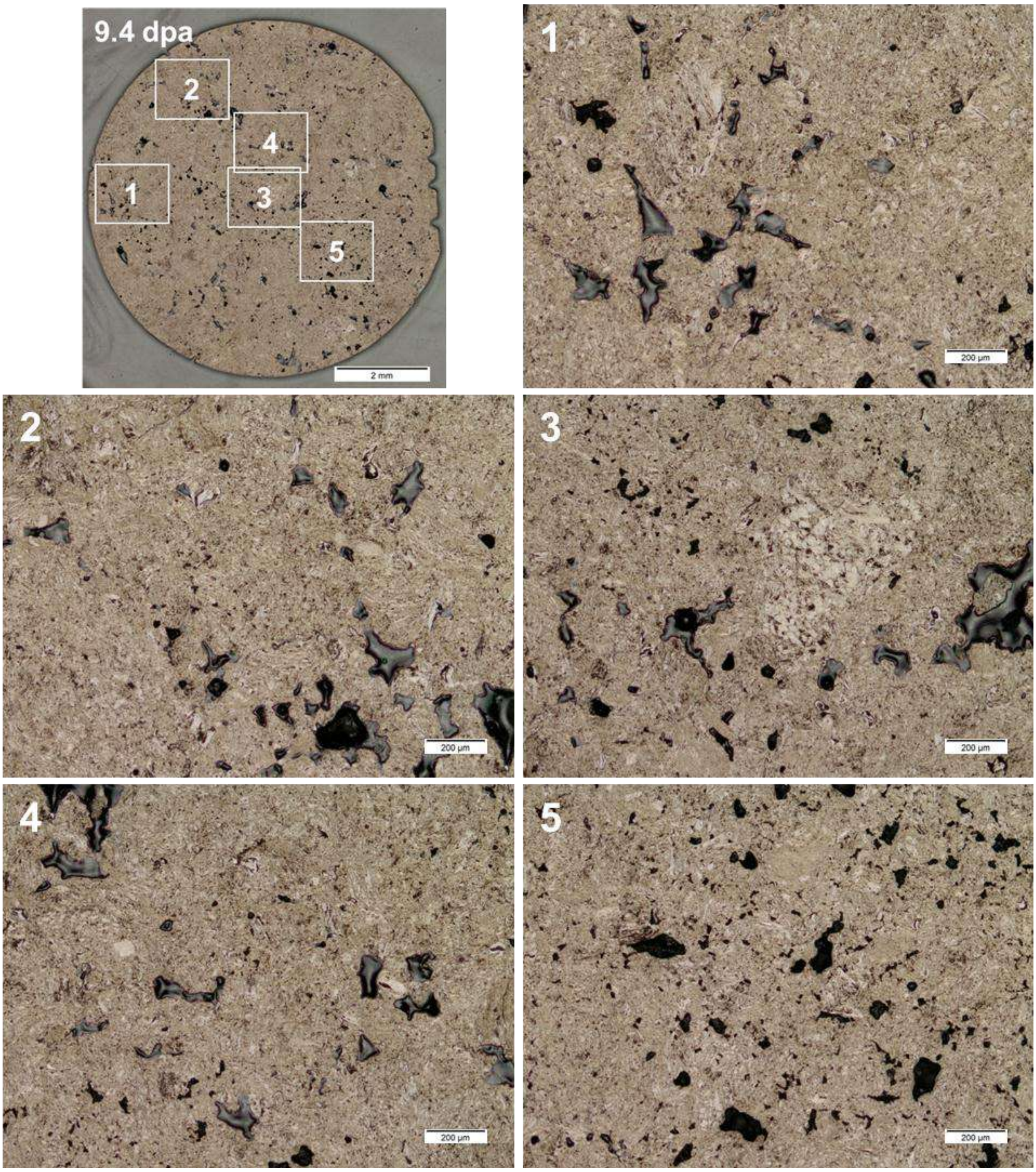

Figure 3-25 Bright field optical micrographs at 5x magnification of NBG-17 specimen S626 (9.4 dpa) and overview micrograph (top left) with indicated the locations of these micrographs on the sample

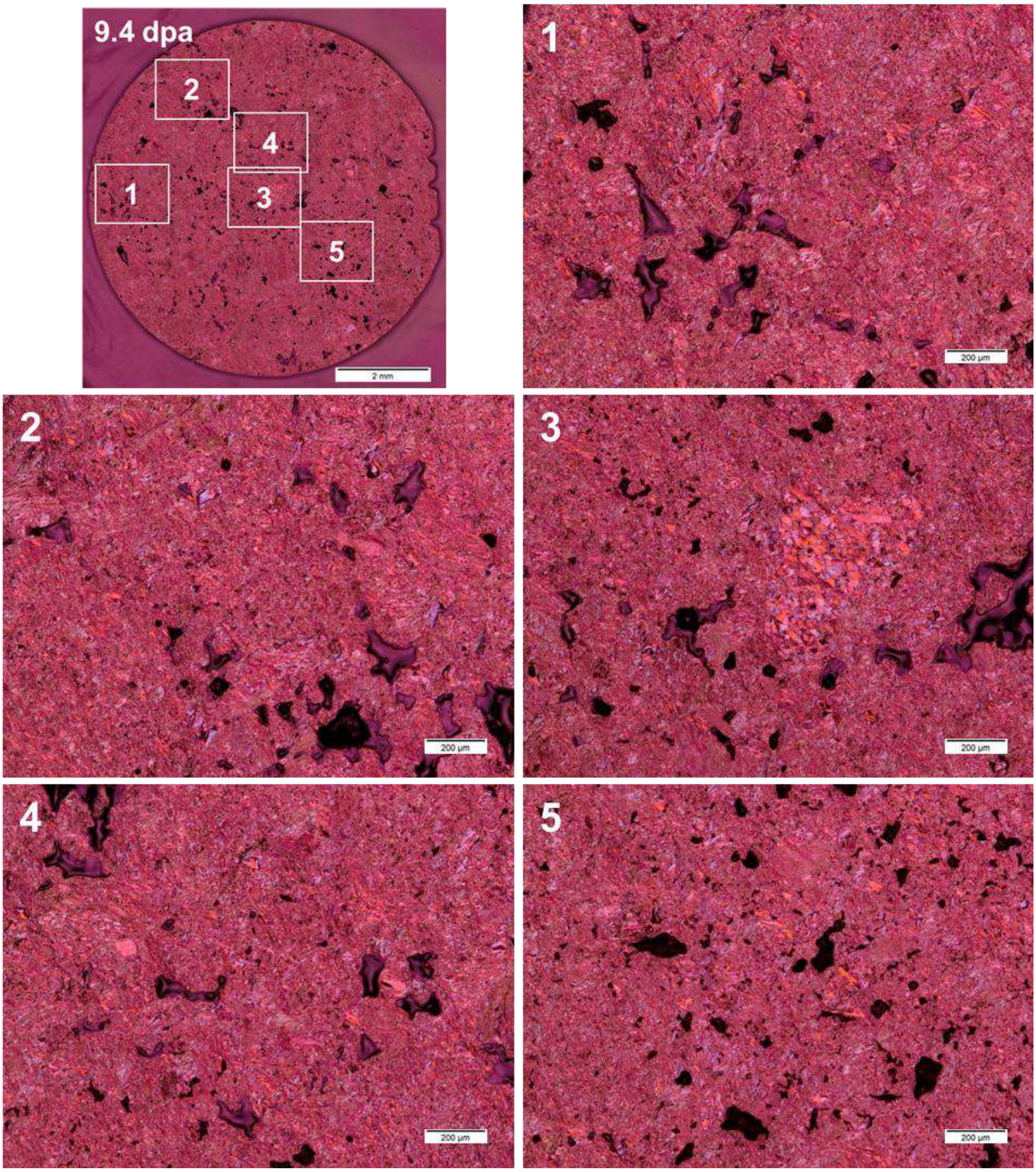

Figure 3-26 Polarisation microscopy images at 5x magnification of NBG-17 specimen S626 (9.4 dpa) and overview micrograph (top left) with indicated the locations of these micrographs on the sample

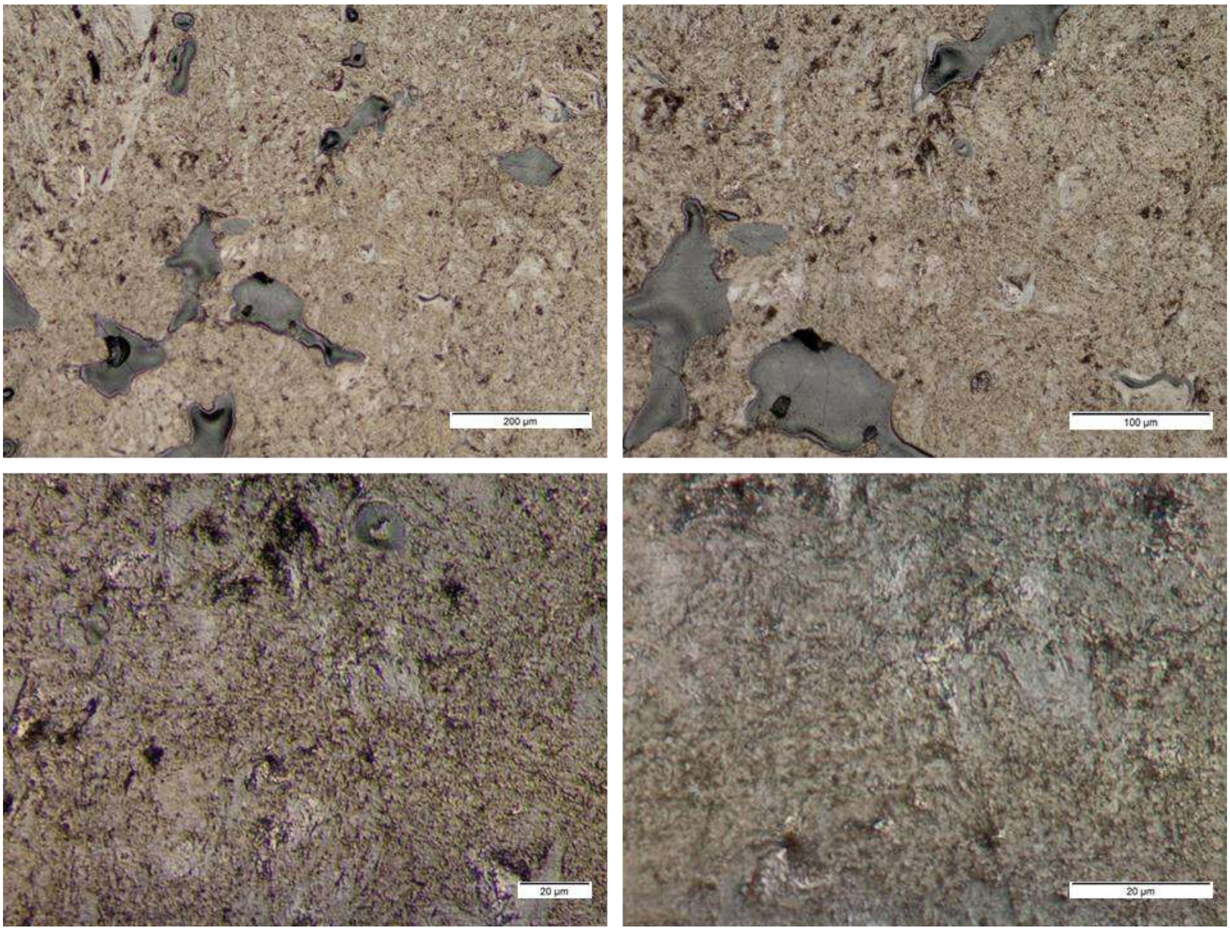

Figure 3-27 Bright field microscopy images of NBG-17 specimen S626 (9.4 dpa) at 10x to 100x magnification at detail location 1

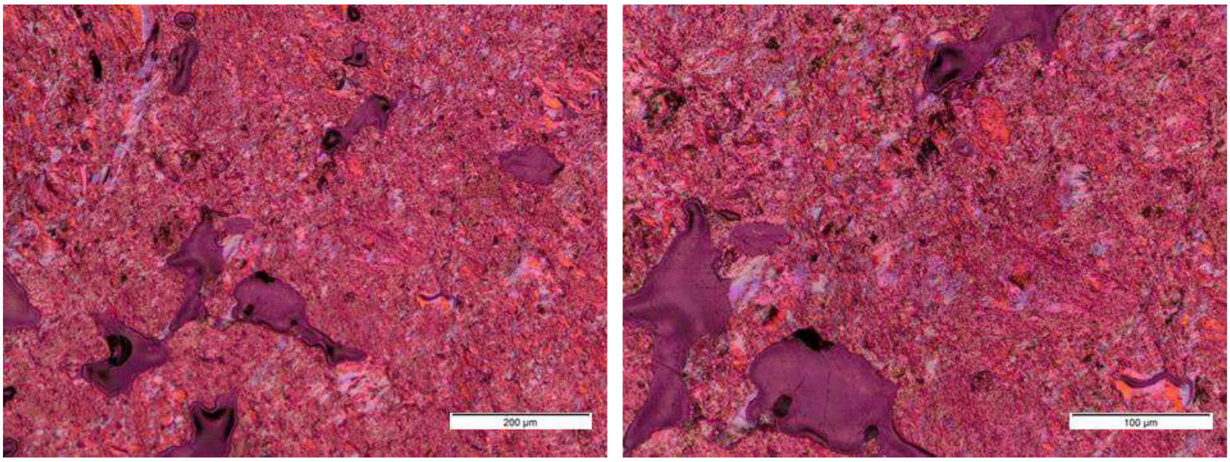

Figure 3-28 Polarisation microscopy images of NBG-17 specimen S626 (9.4 dpa) at 10x and 20x magnification at detail location 1

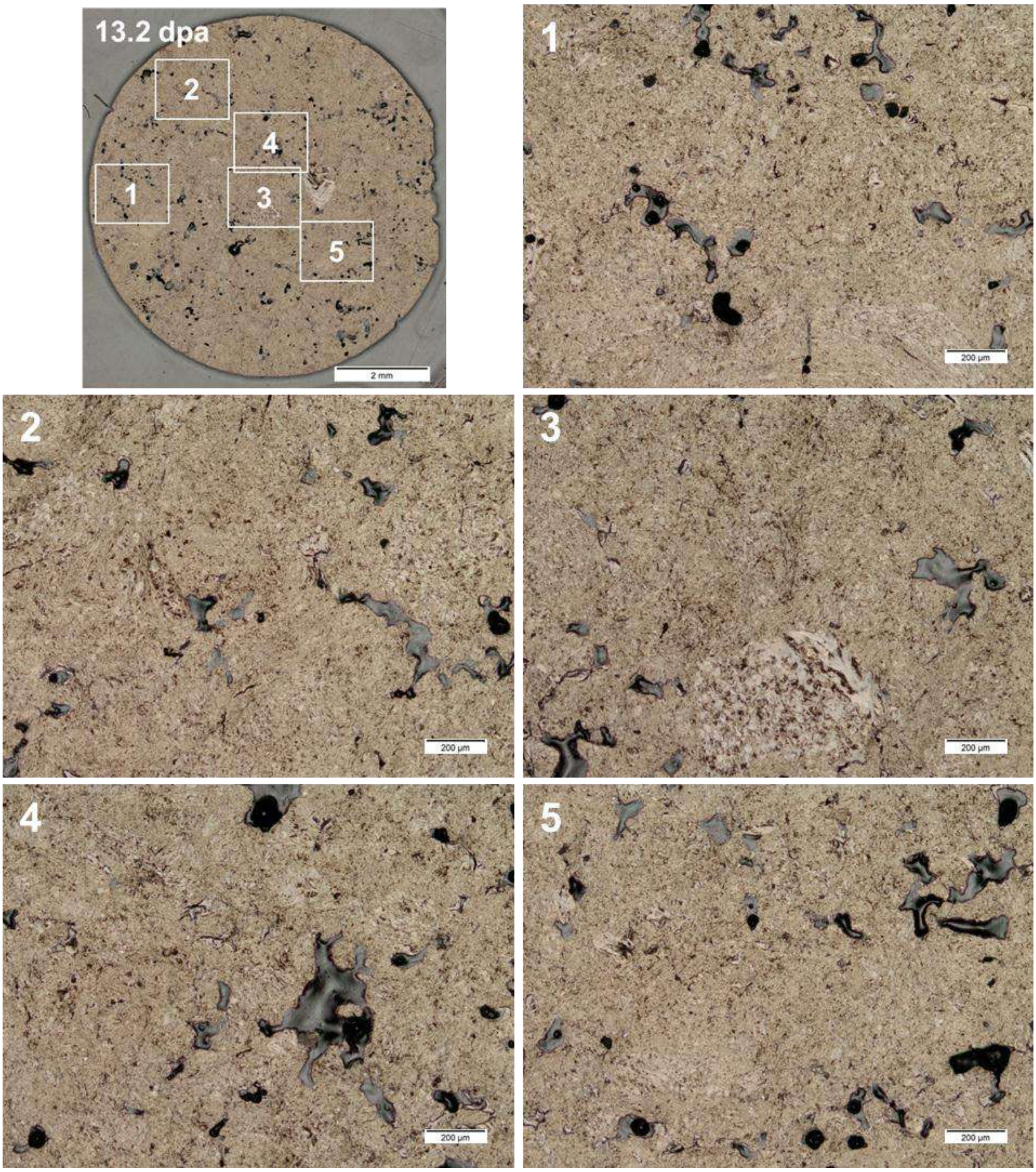

Figure 3-29 Bright field optical micrographs at 5x magnification of NBG-17 specimen S579 (13.2 dpa) and overview micrograph (top left) with indicated the locations of these micrographs on the sample

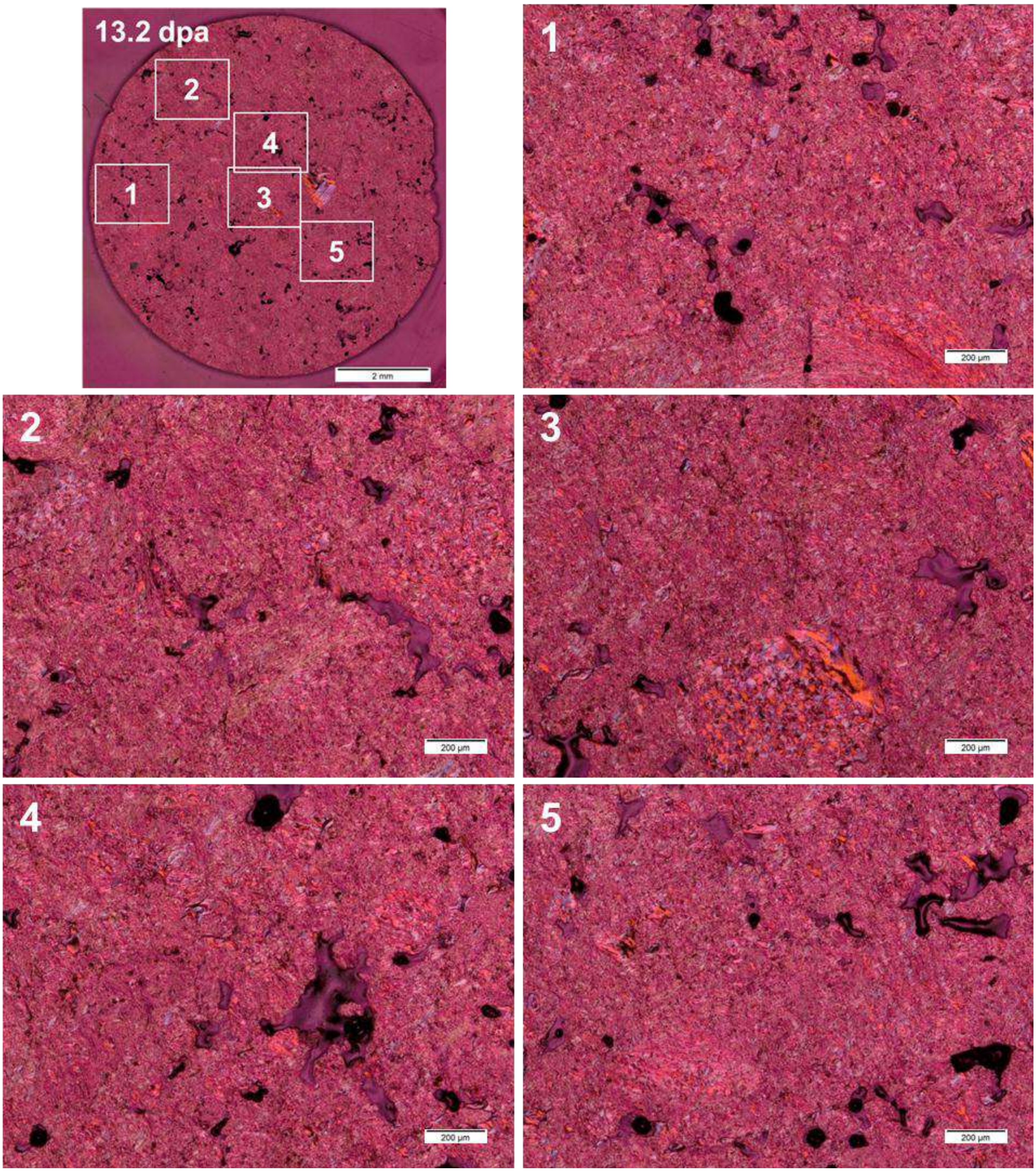

Figure 3-30 Polarisation microscopy images at 5x magnification of NBG-17 specimen S579 (13.2 dpa) and overview micrograph (top left) with indicated the locations of these micrographs on the sample

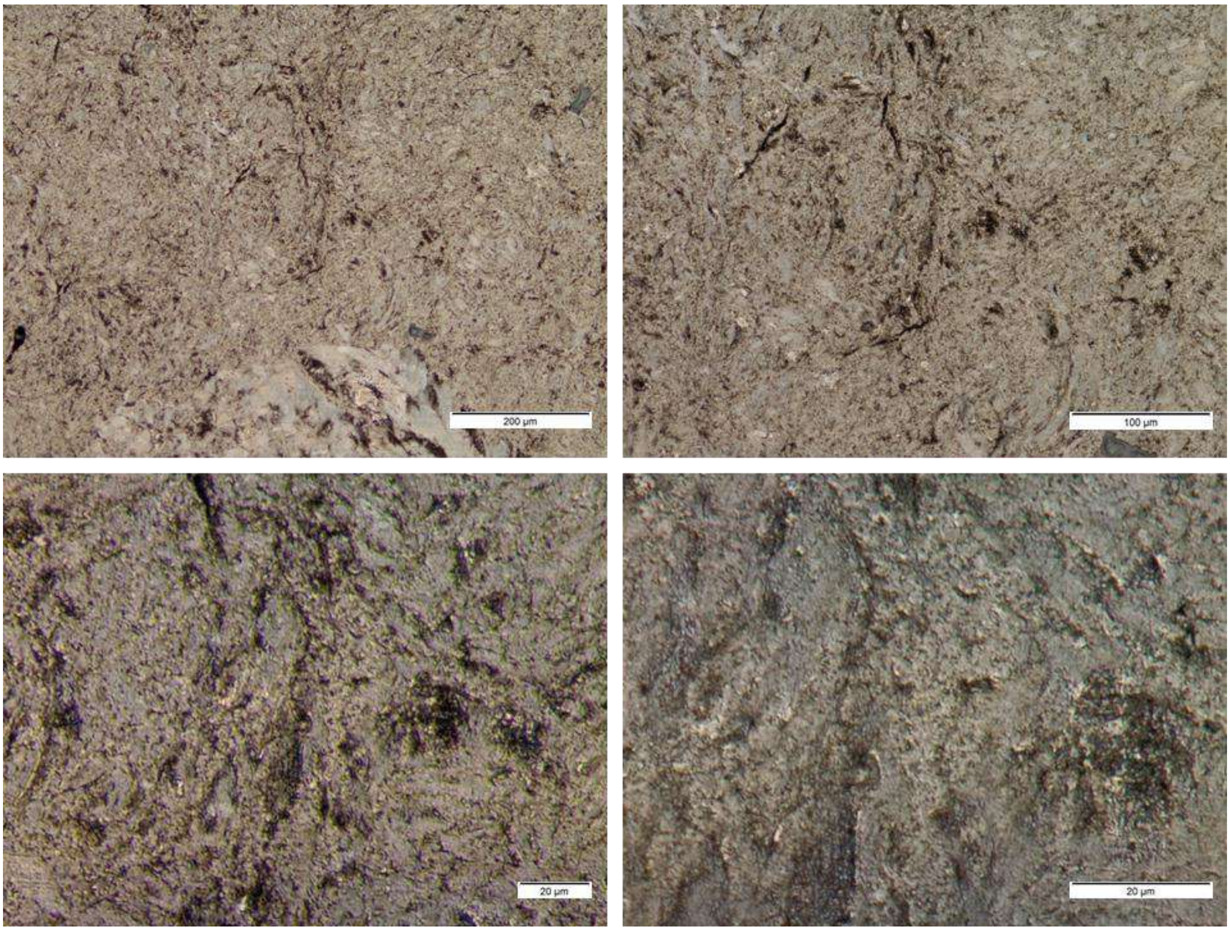

Figure 3-31 Bright field microscopy images of NBG-17 specimen S579 (13.2 dpa) at 10x to 100x magnification at detail location 3

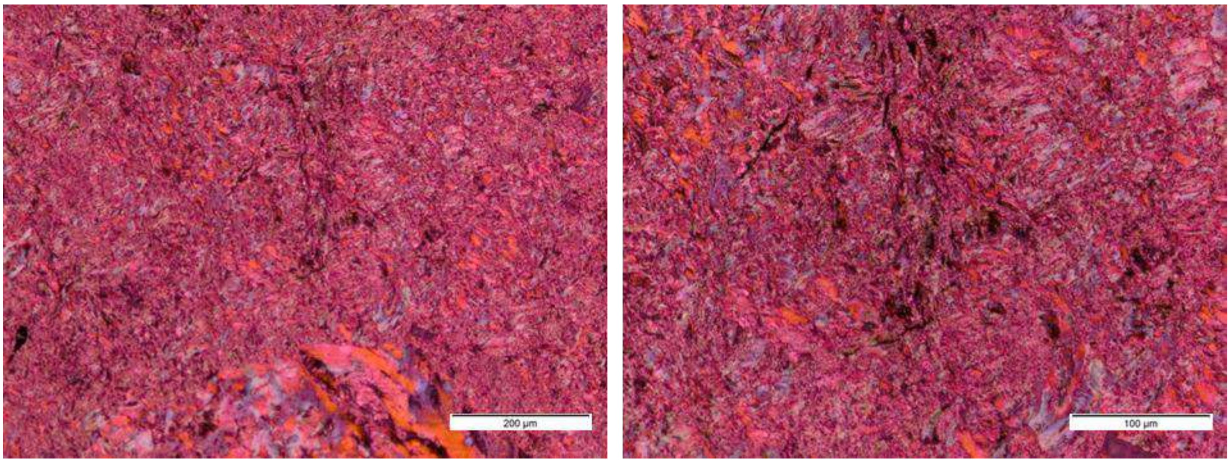

Figure 3-32 Polarisation microscopy images of NBG-17 specimen S579 (13.2 dpa) at 10x and 20x magnification at detail location 3

3.1.4 NBG-18 detail micrographs

Figure 3-33 to Figure 3-40 show the detail micrographs of the irradiated NBG-18 graphite specimens.

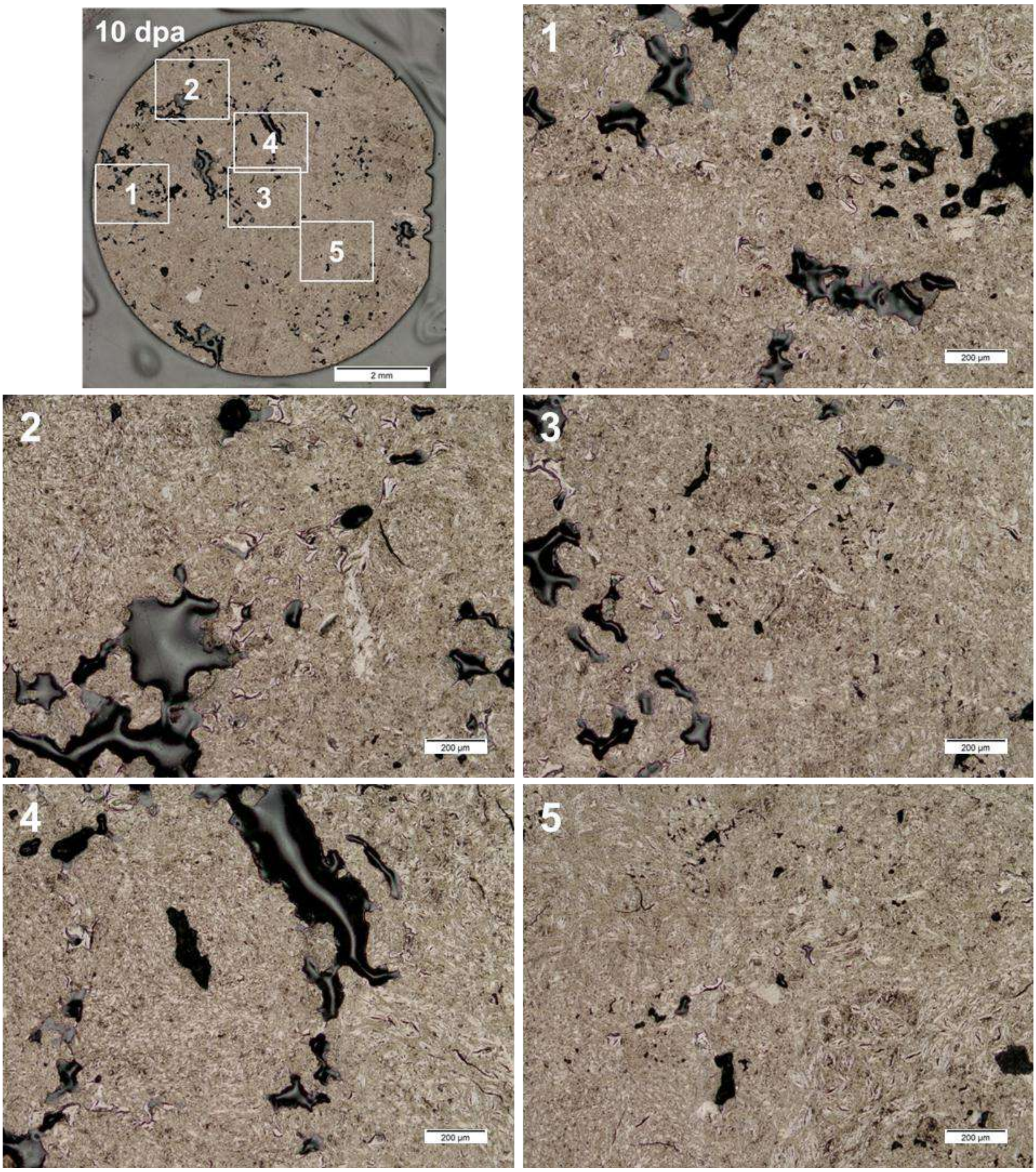

Figure 3-33 Bright field optical micrographs at 5x magnification of NBG-18 specimen S476 (10 dpa) and overview micrograph (top left) with indicated the locations of these micrographs on the sample

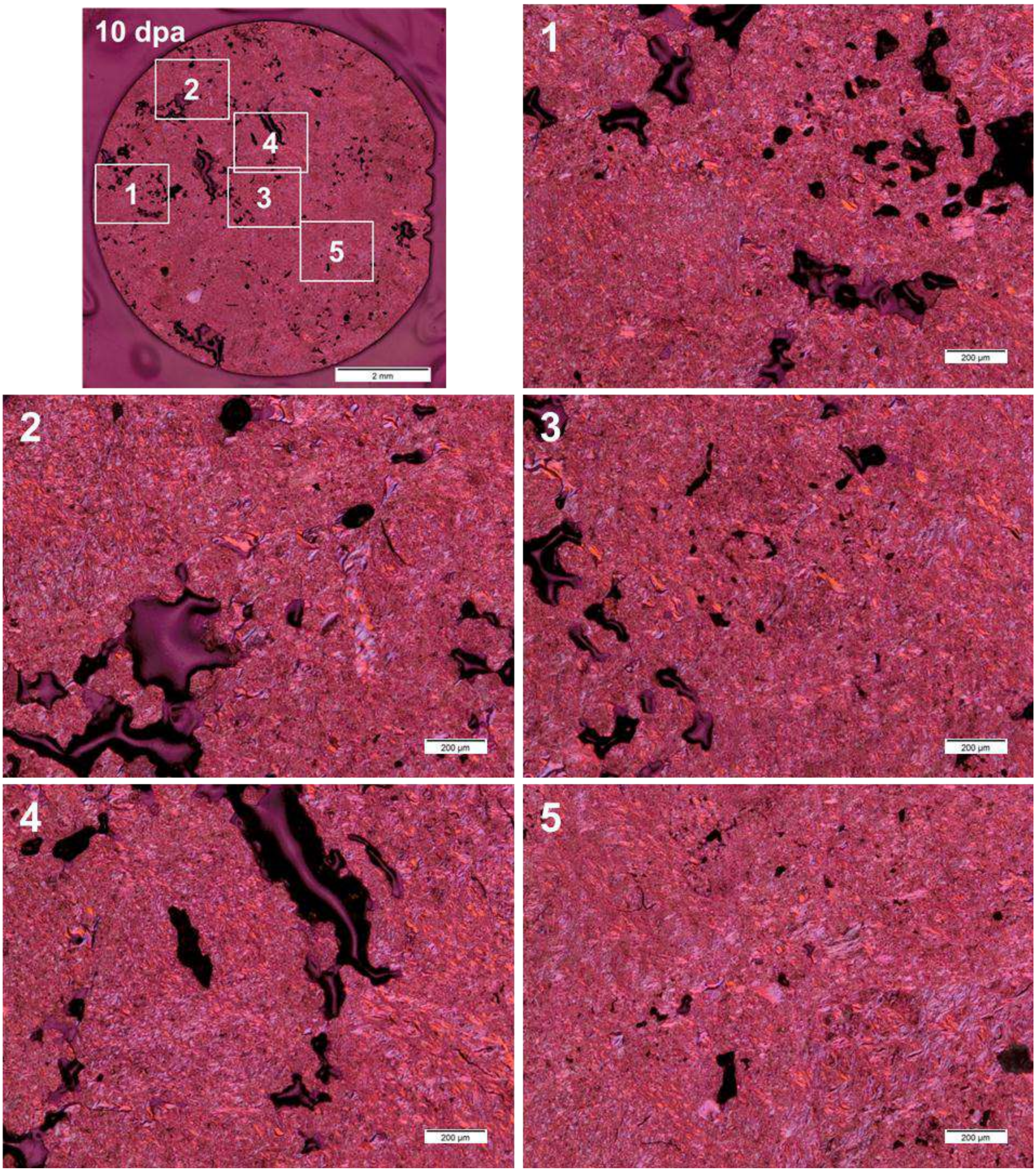

Figure 3-34 Polarisation microscopy images at 5x magnification of NBG-18 specimen S476 (10 dpa) and overview micrograph (top left) with indicated the locations of these micrographs on the sample

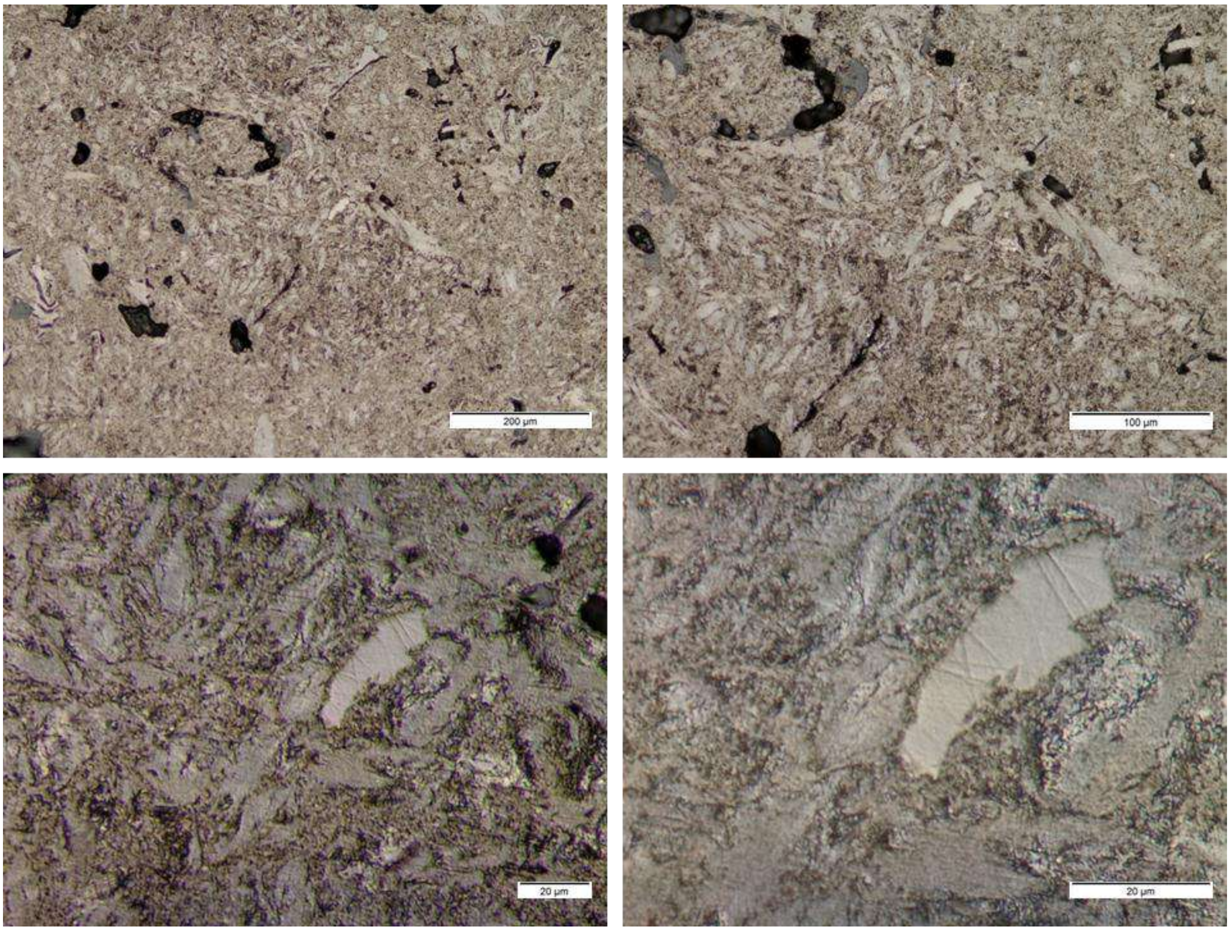

Figure 3-35 Bright field microscopy images of NBG-18 specimen S476 (10 dpa) at 10x to 100x magnification at detail location 3

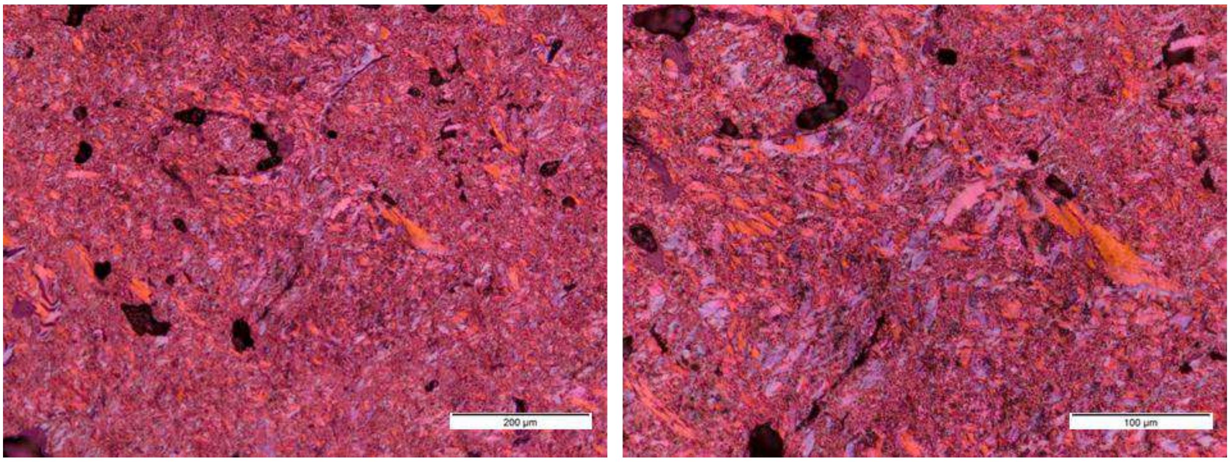

Figure 3-36 Polarisation microscopy images of NBG-18 specimen S476 (10 dpa) at 10x and 20x magnification at detail location 3

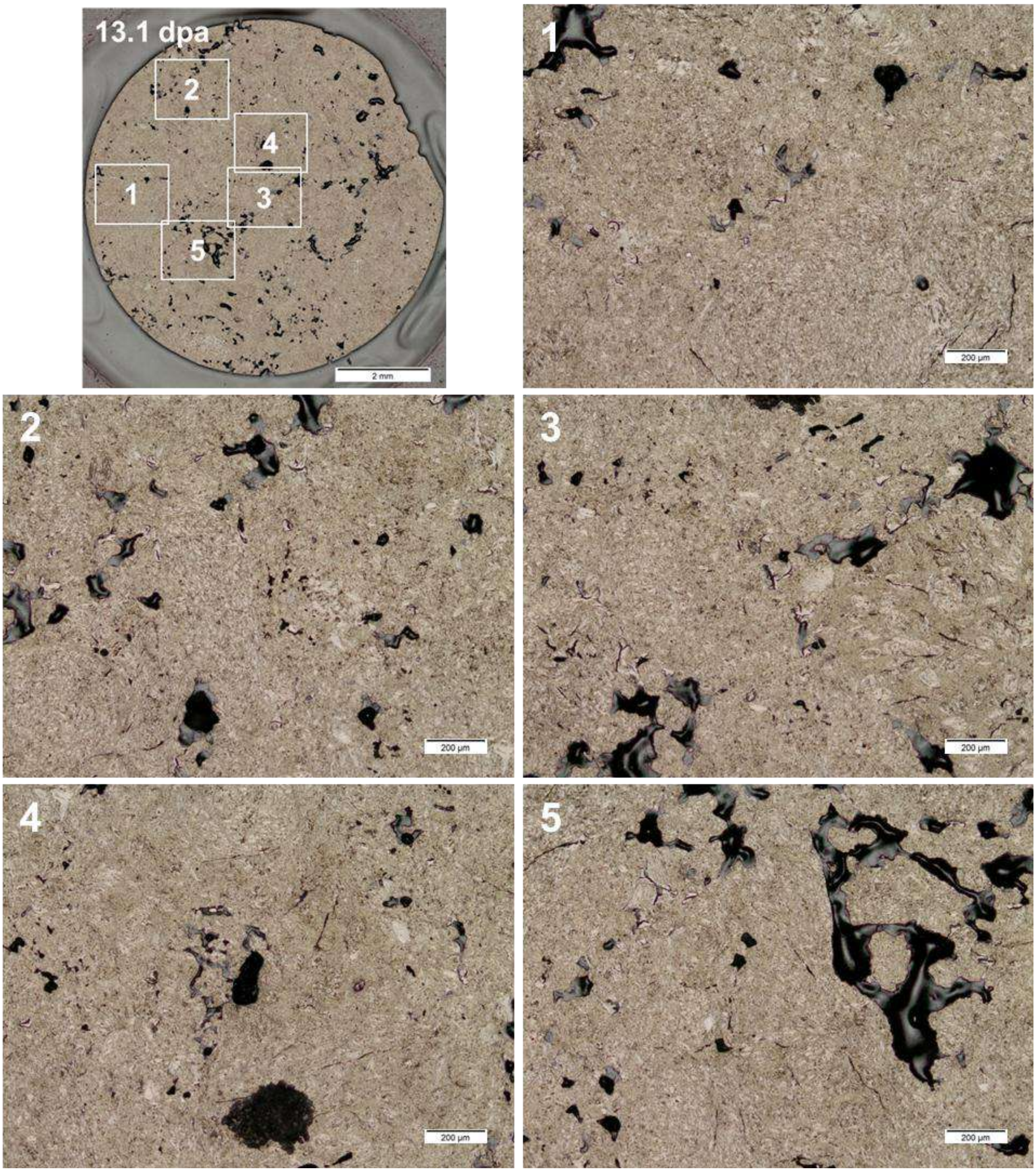

Figure 3-37 Bright field optical micrographs at 5x magnification of NBG-18 specimen S468 (13.1 dpa) and overview micrograph (top left) with indicated the locations of these micrographs on the sample

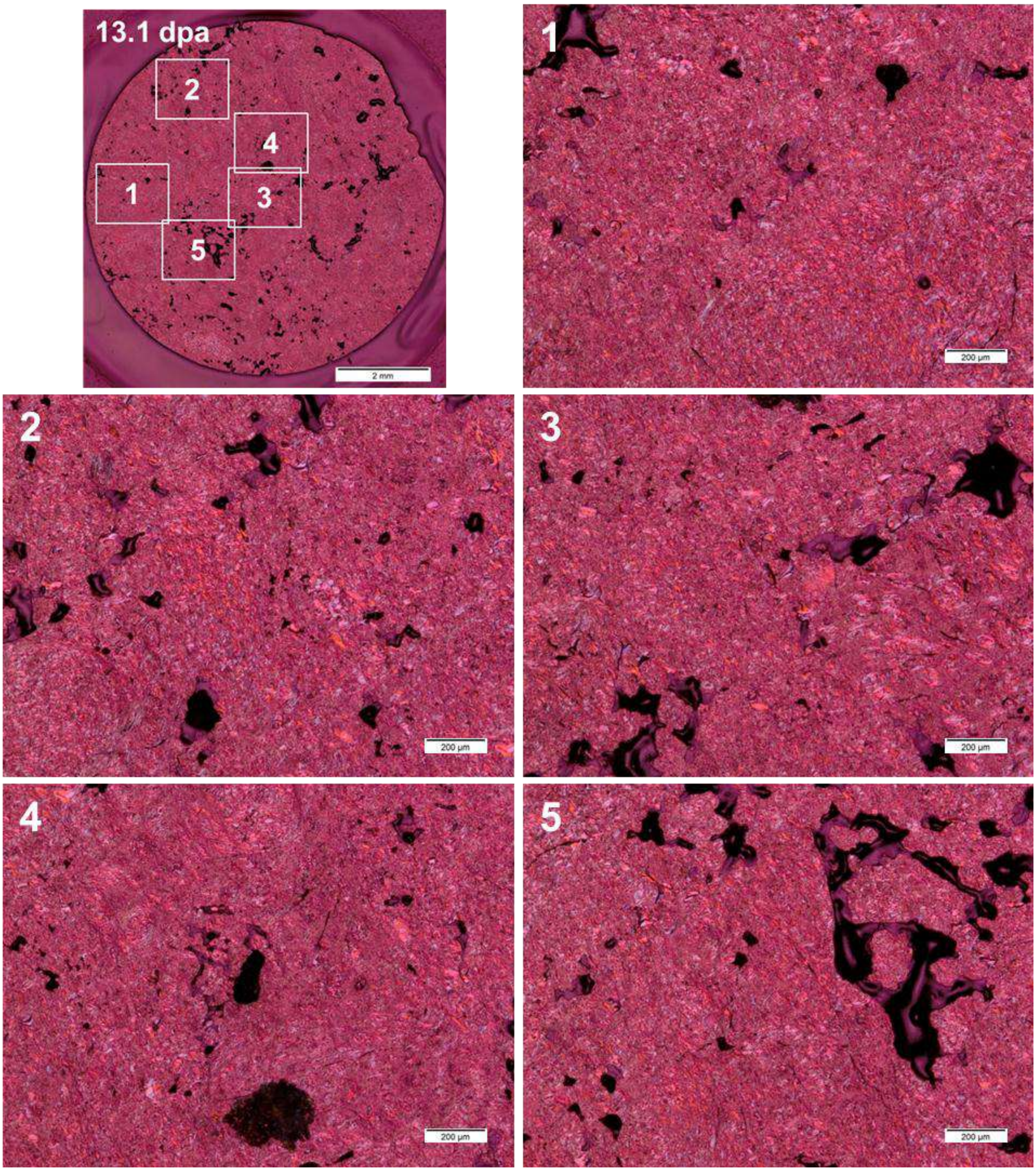

Figure 3-38 Polarisation microscopy images at 5x magnification of NBG-18 specimen S468 (13.1 dpa) and overview micrograph (top left) with indicated the locations of these micrographs on the sample

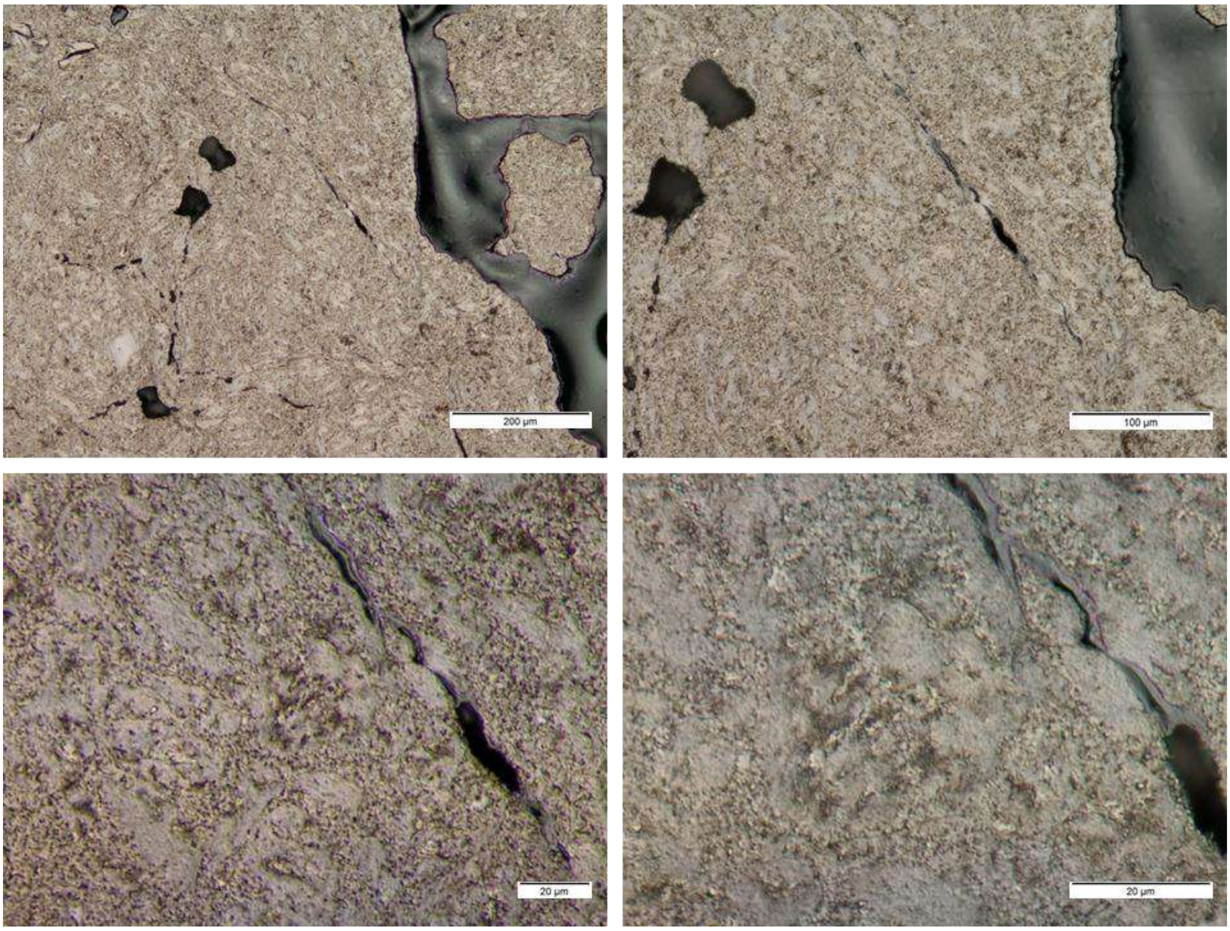

Figure 3-39 Bright field microscopy images of NBG-18 specimen S468 (13.1 dpa) at 10x to 100x magnification at detail location 5

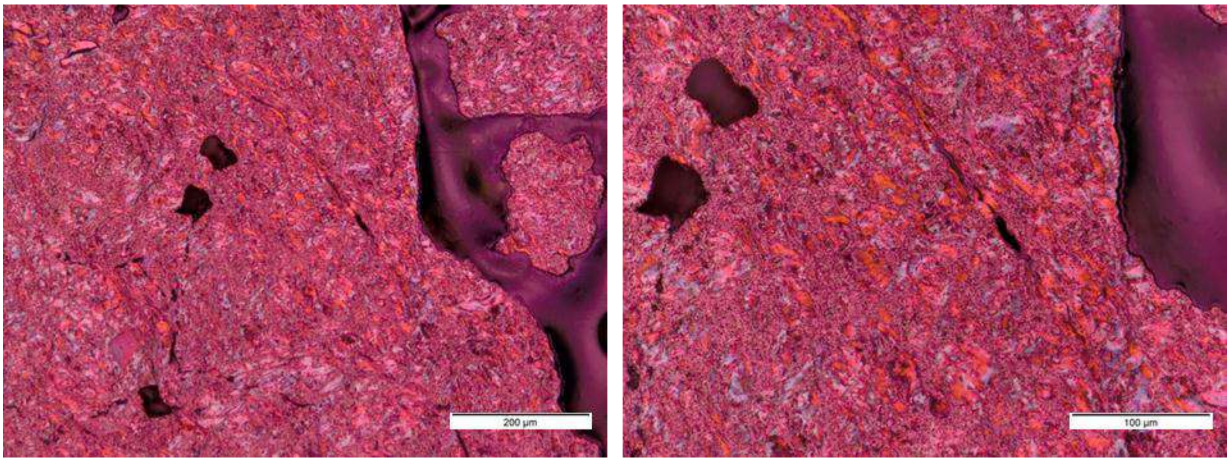

Figure 3-40 Polarisation microscopy images of NBG-18 specimen S468 (13.1 dpa) at 10x and 20x magnification at detail location 5

3.1.5 NBG-25 detail micrographs

Figure 3-41 to Figure 3-56 show the detail micrographs of the irradiated NBG-25 graphite specimens.

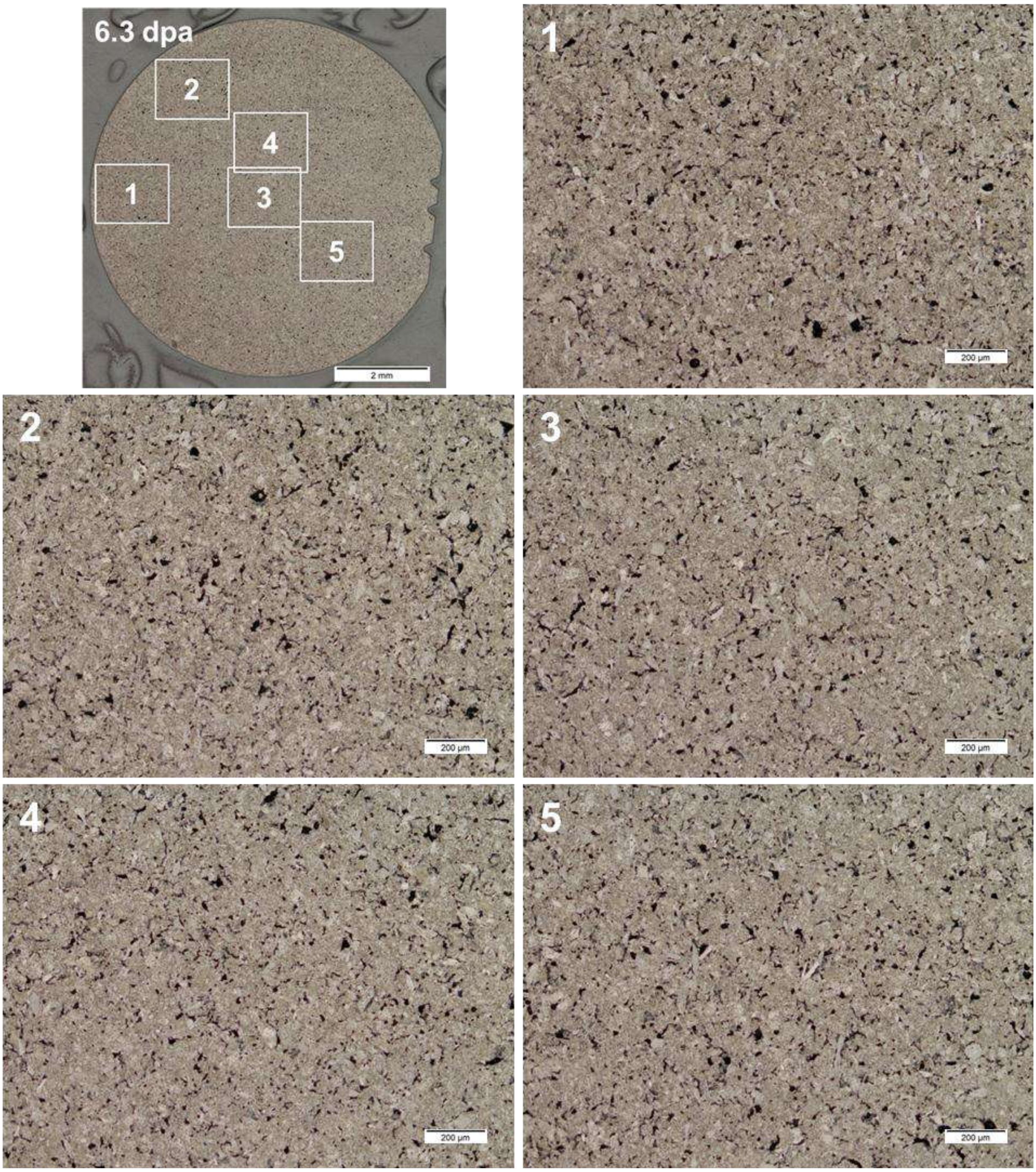

Figure 3-41 Bright field optical micrographs at 5x magnification of NBG-25 specimen S114 (6.3 dpa) and overview micrograph (top left) with indicated the locations of these micrographs on the sample

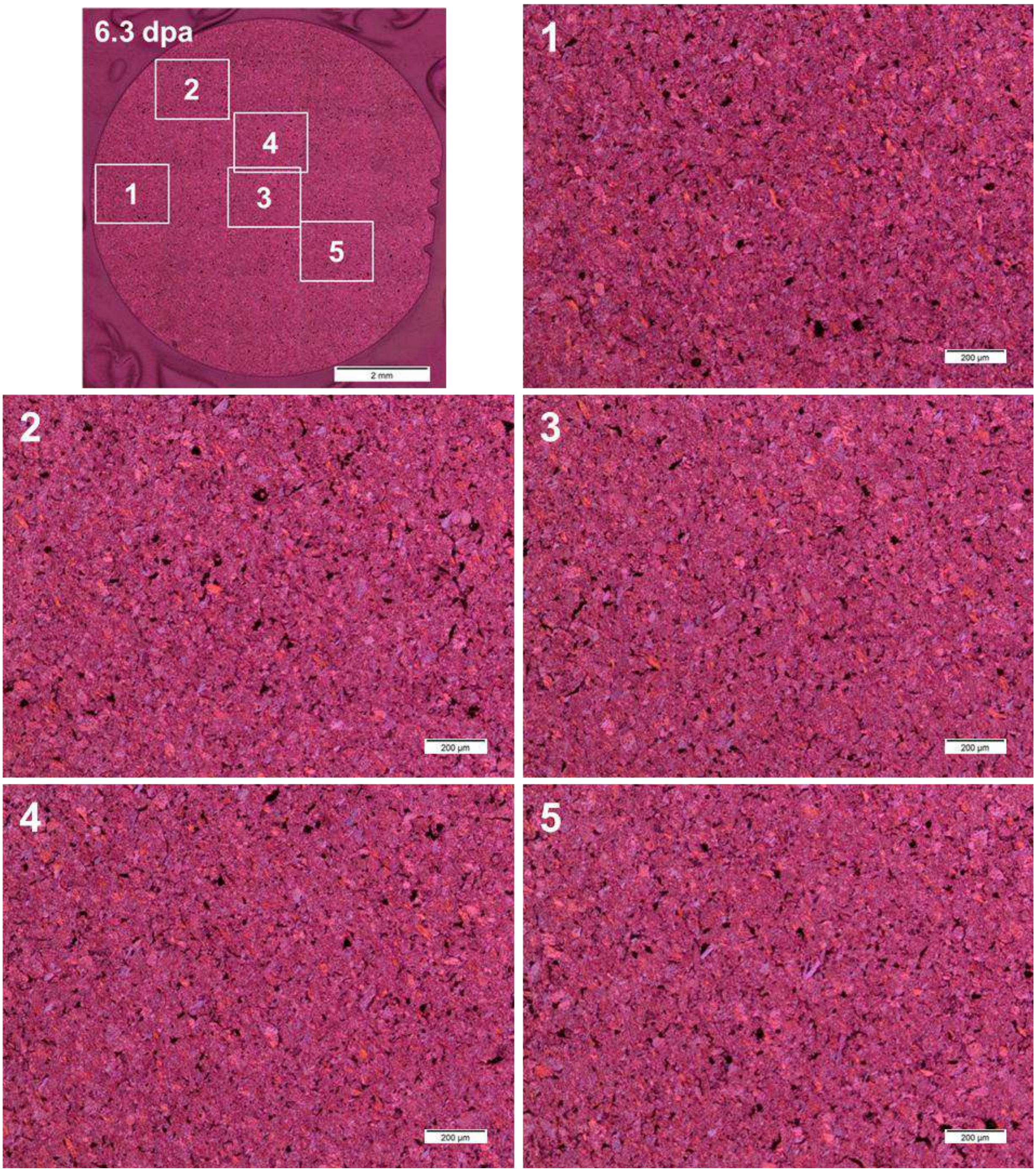

Figure 3-42 Polarisation microscopy images at 5x magnification of NBG-25 specimen S114 (6.3 dpa) and overview micrograph (top left) with indicated the locations of these micrographs on the sample

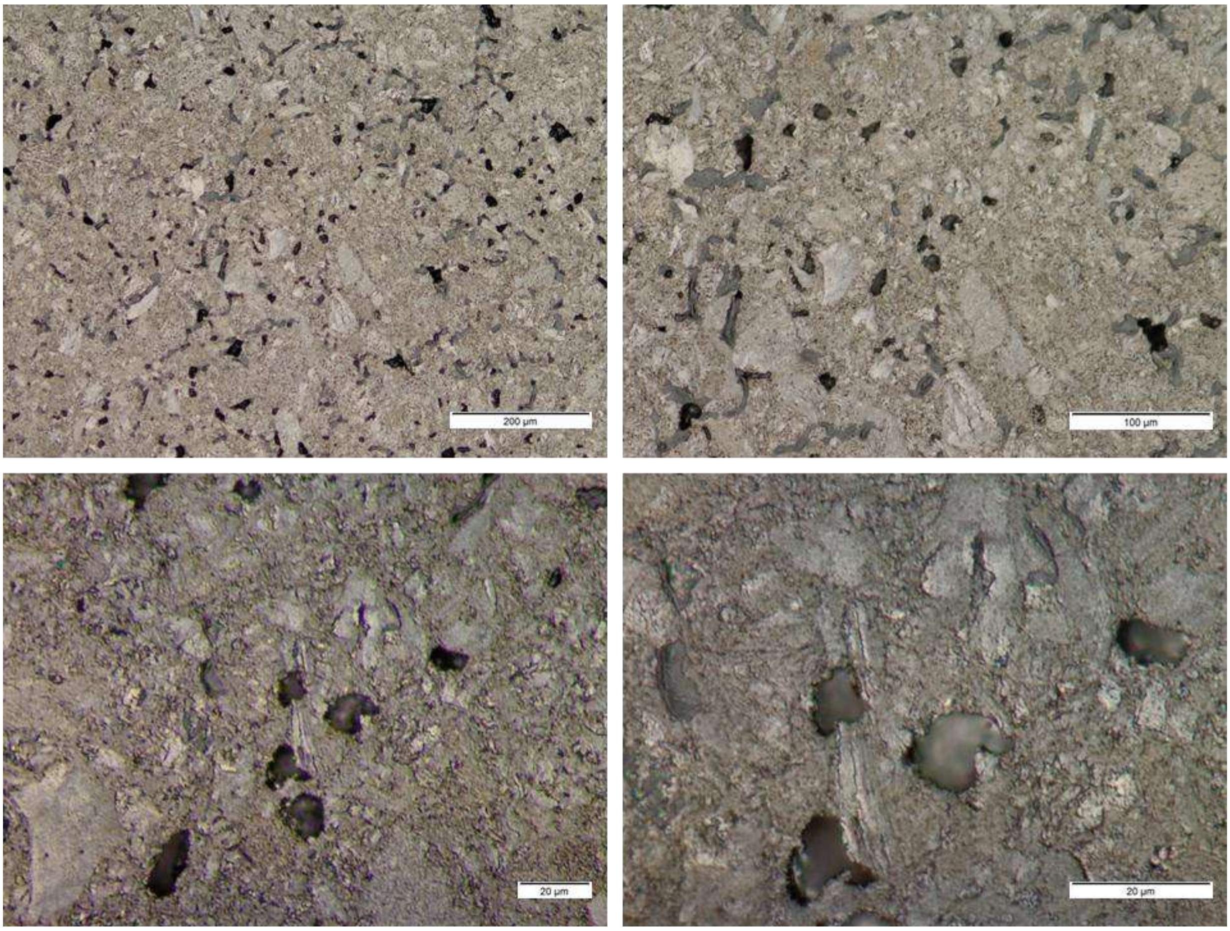

Figure 3-43 Bright field microscopy images of NBG-25 specimen S114 (6.3 dpa) at 10x to 100x magnification at detail location 3

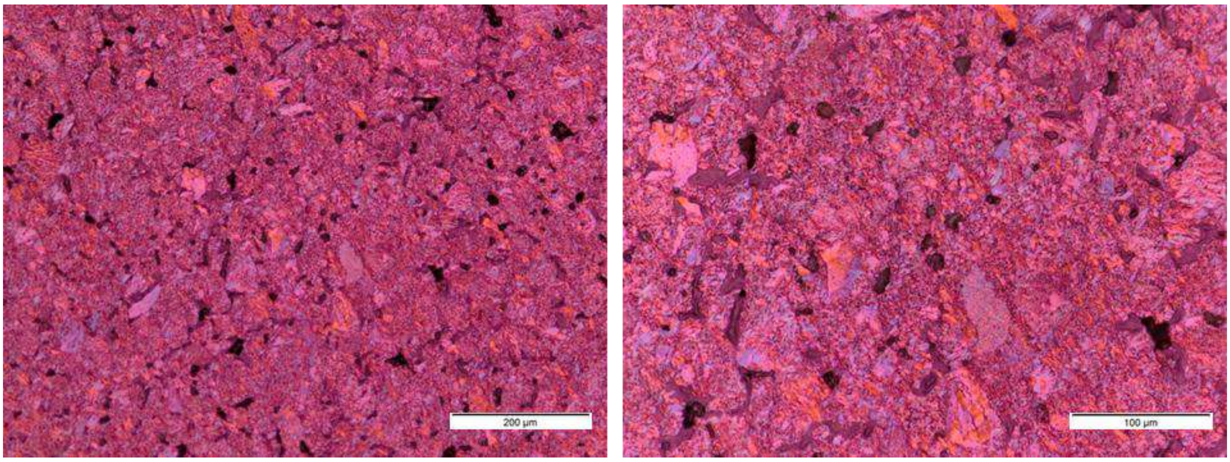

Figure 3-44 Polarisation microscopy images of NBG-25 specimen S114 (6.3 dpa) at 10x and 20x magnification at detail location 3

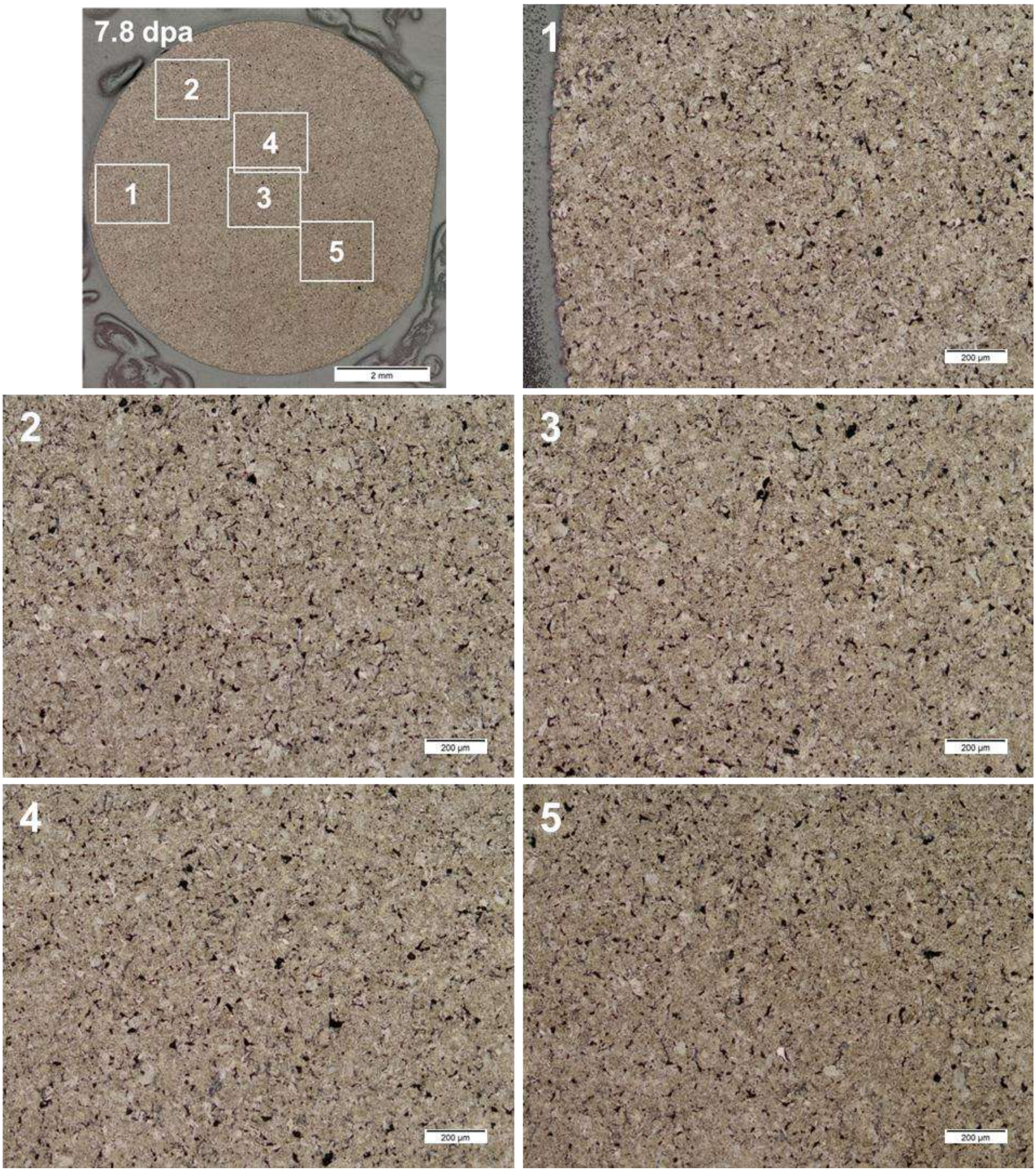

Figure 3-45 Bright field optical micrographs at 5x magnification of NBG-25 specimen S141 (7.8 dpa) and overview micrograph (top left) with indicated the locations of these micrographs on the sample

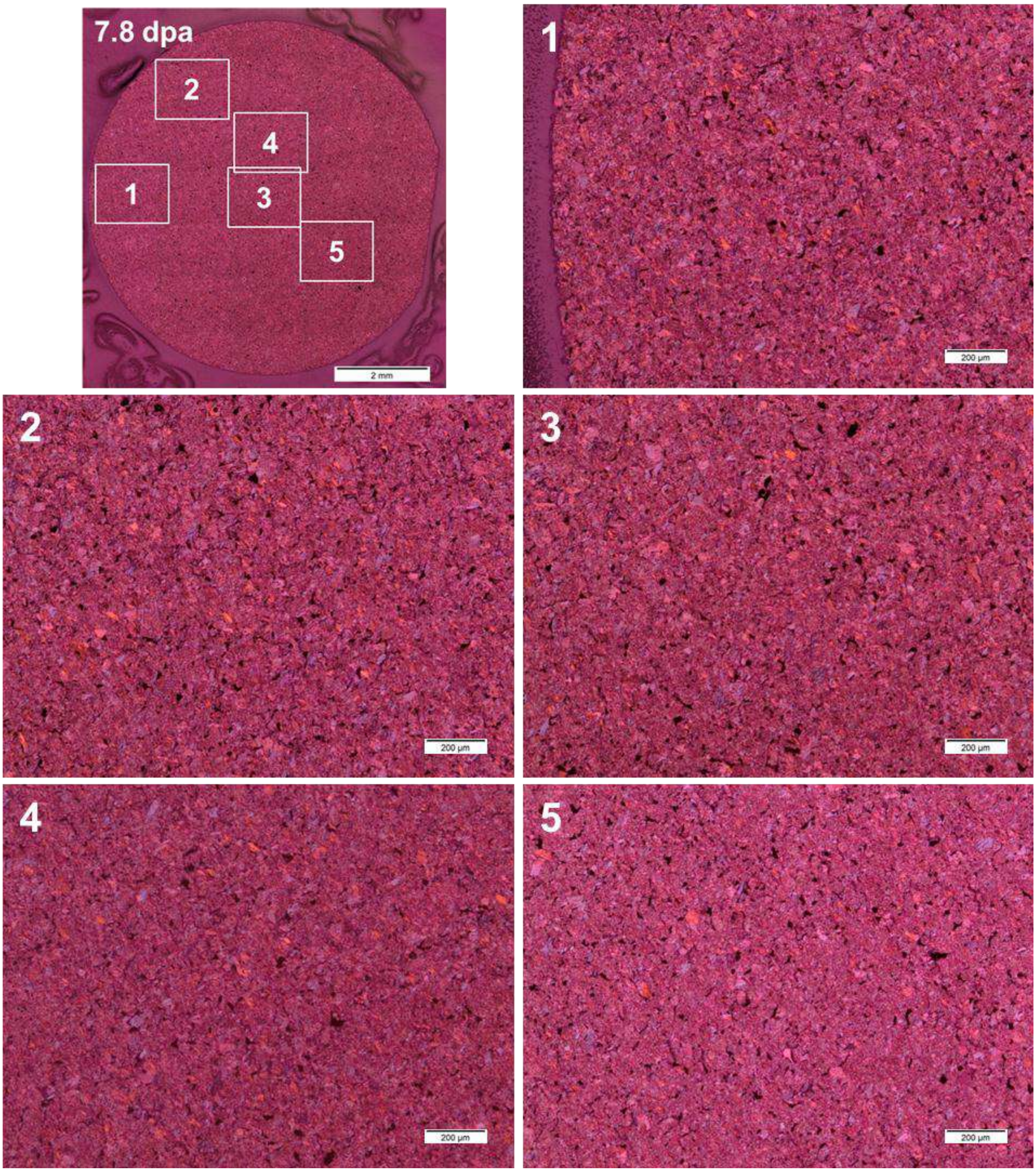

Figure 3-46 Polarisation microscopy images at 5x magnification of NBG-25 specimen S141 (7.8 dpa) and overview micrograph (top left) with indicated the locations of these micrographs on the sample

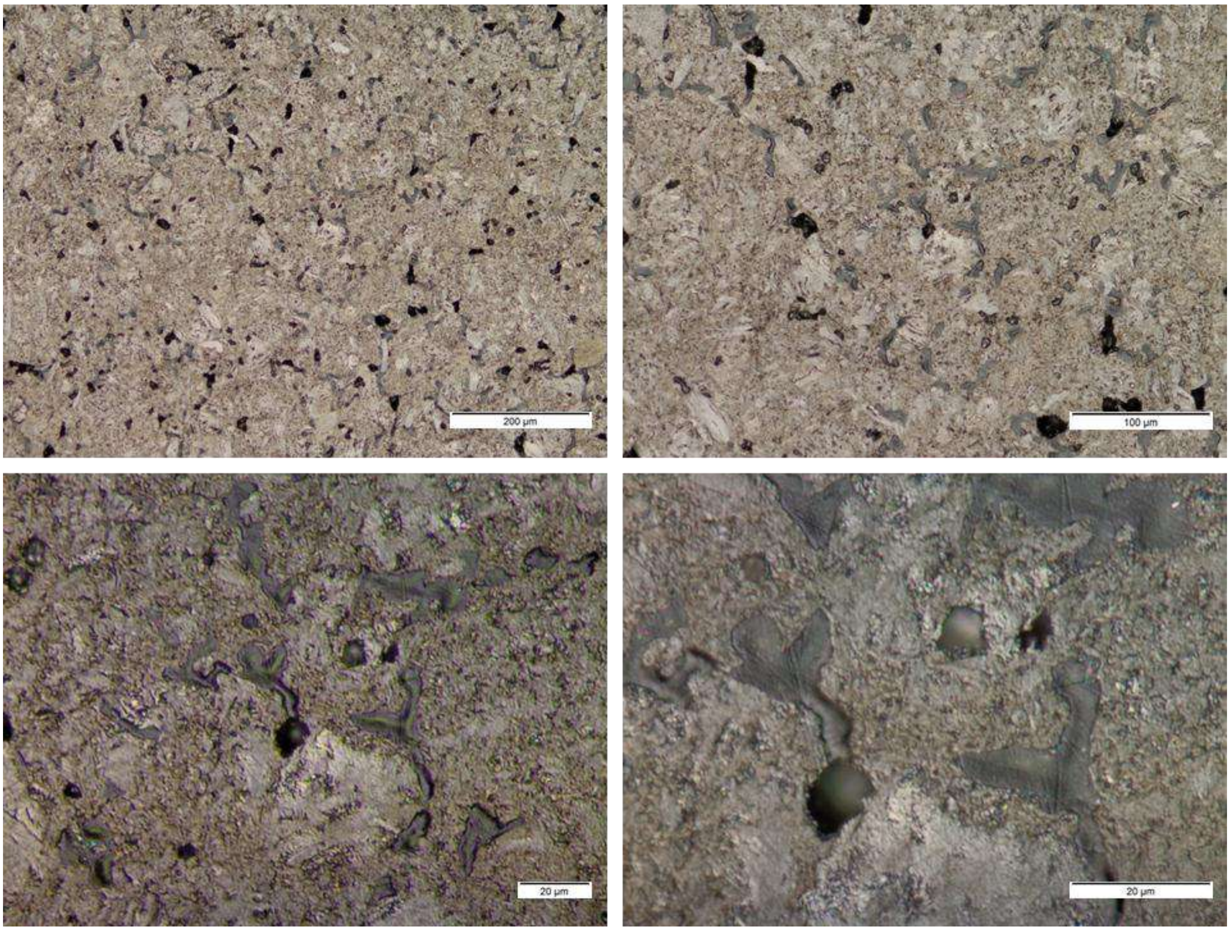

Figure 3-47 Bright field microscopy images of NBG-25 specimen S141 (7.8 dpa) at 10x to 100x magnification at detail location 2

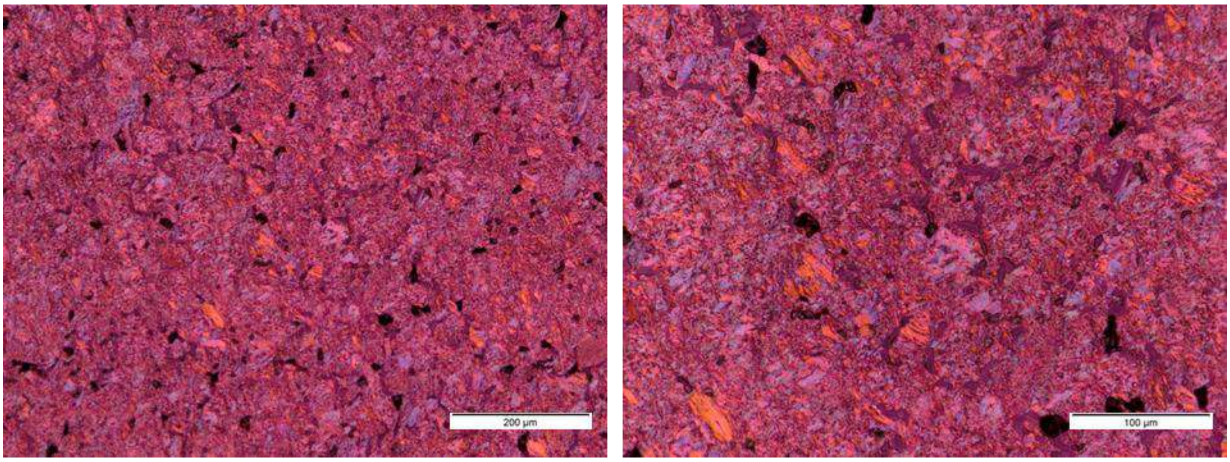

Figure 3-48 Polarisation microscopy images of NBG-25 specimen S141 (7.8 dpa) at 10x and 20x magnification at detail location 2

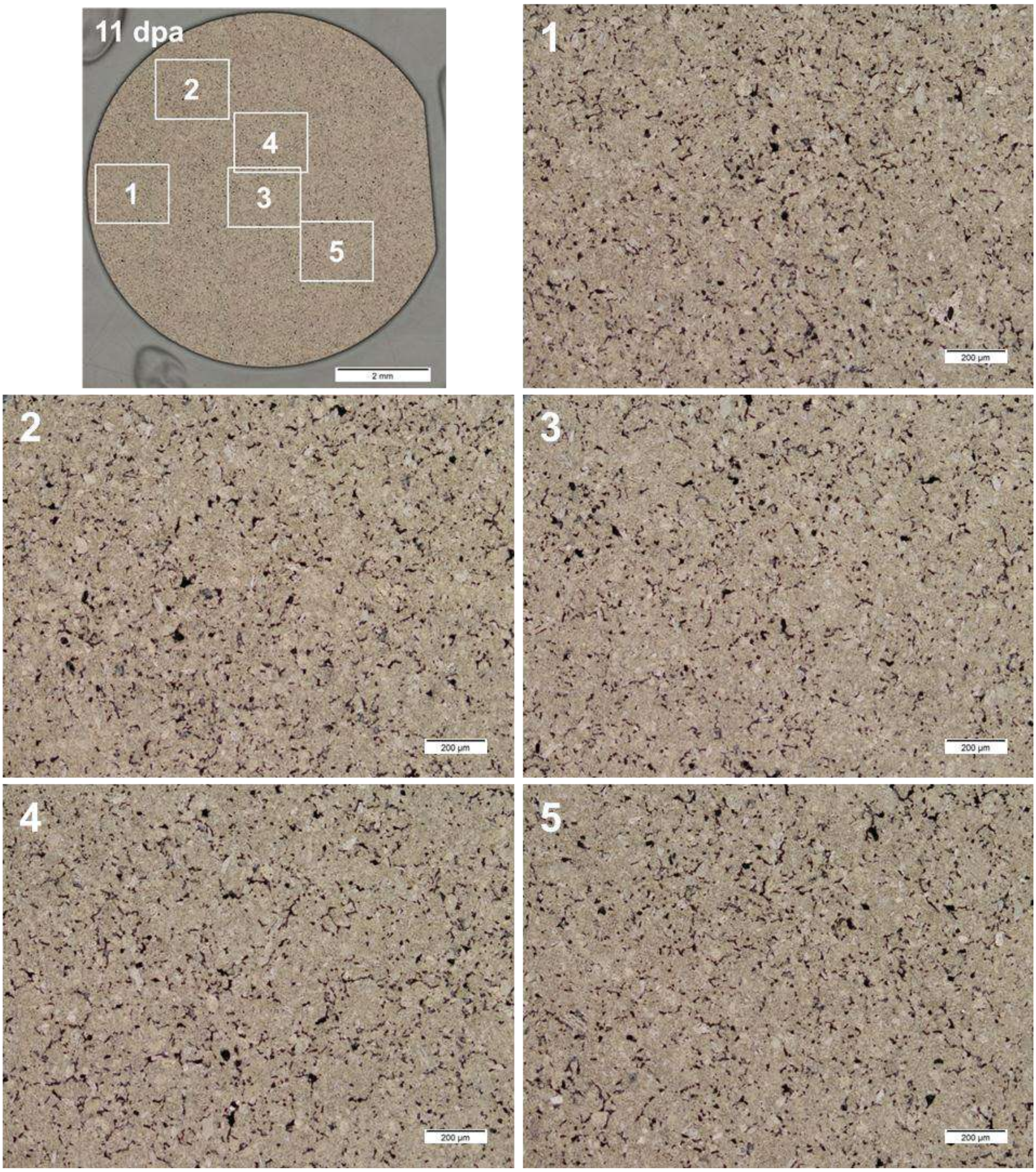

Figure 3-49 Bright field optical micrographs at 5x magnification of NBG-25 specimen S107 (11 dpa) and overview micrograph (top left) with indicated the locations of these micrographs on the sample

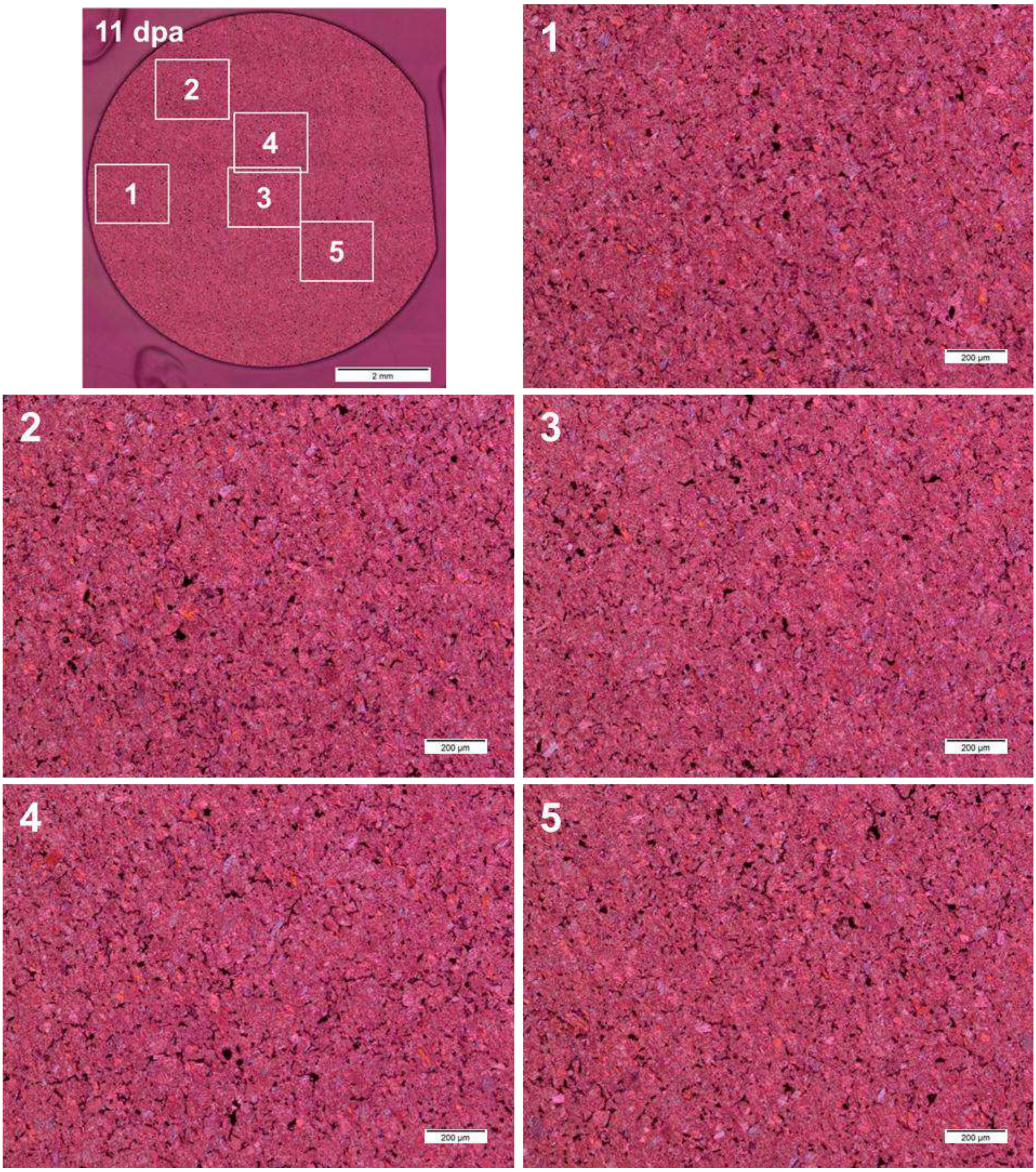

Figure 3-50 Polarisation microscopy images at 5x magnification of NBG-25 specimen S107 (11 dpa) and overview micrograph (top left) with indicated the locations of these micrographs on the sample

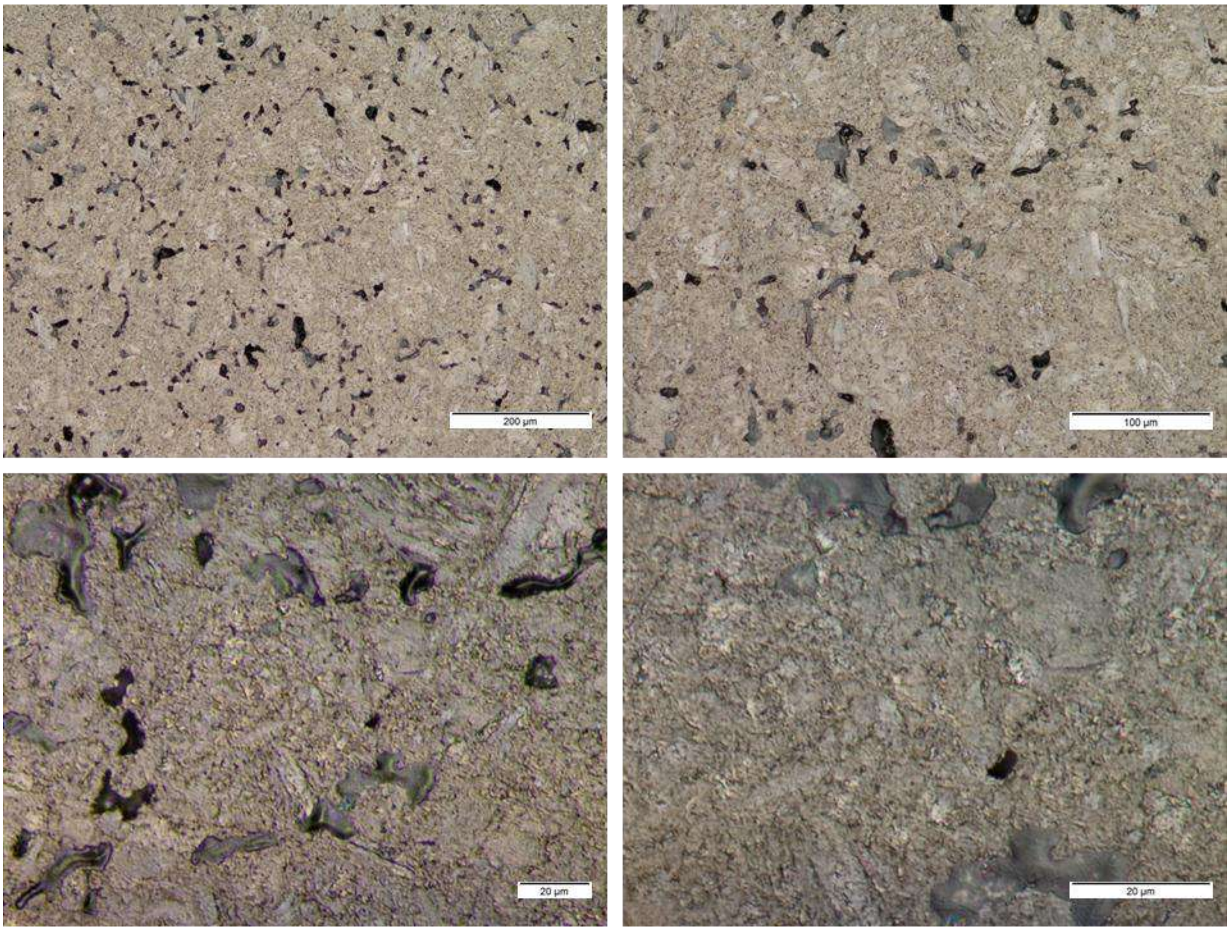

Figure 3-51 Bright field microscopy images of NBG-25 specimen S107 (11 dpa) at 10x to 100x magnification at detail location 3

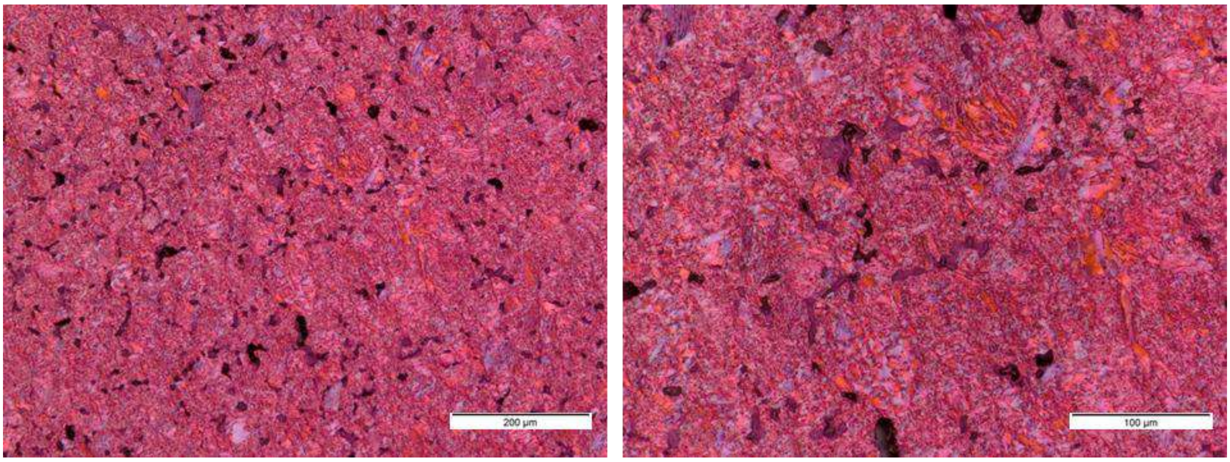

Figure 3-52 Polarisation microscopy images of NBG-25 specimen S107 (11 dpa) at 10x and 20x magnification at detail location 3

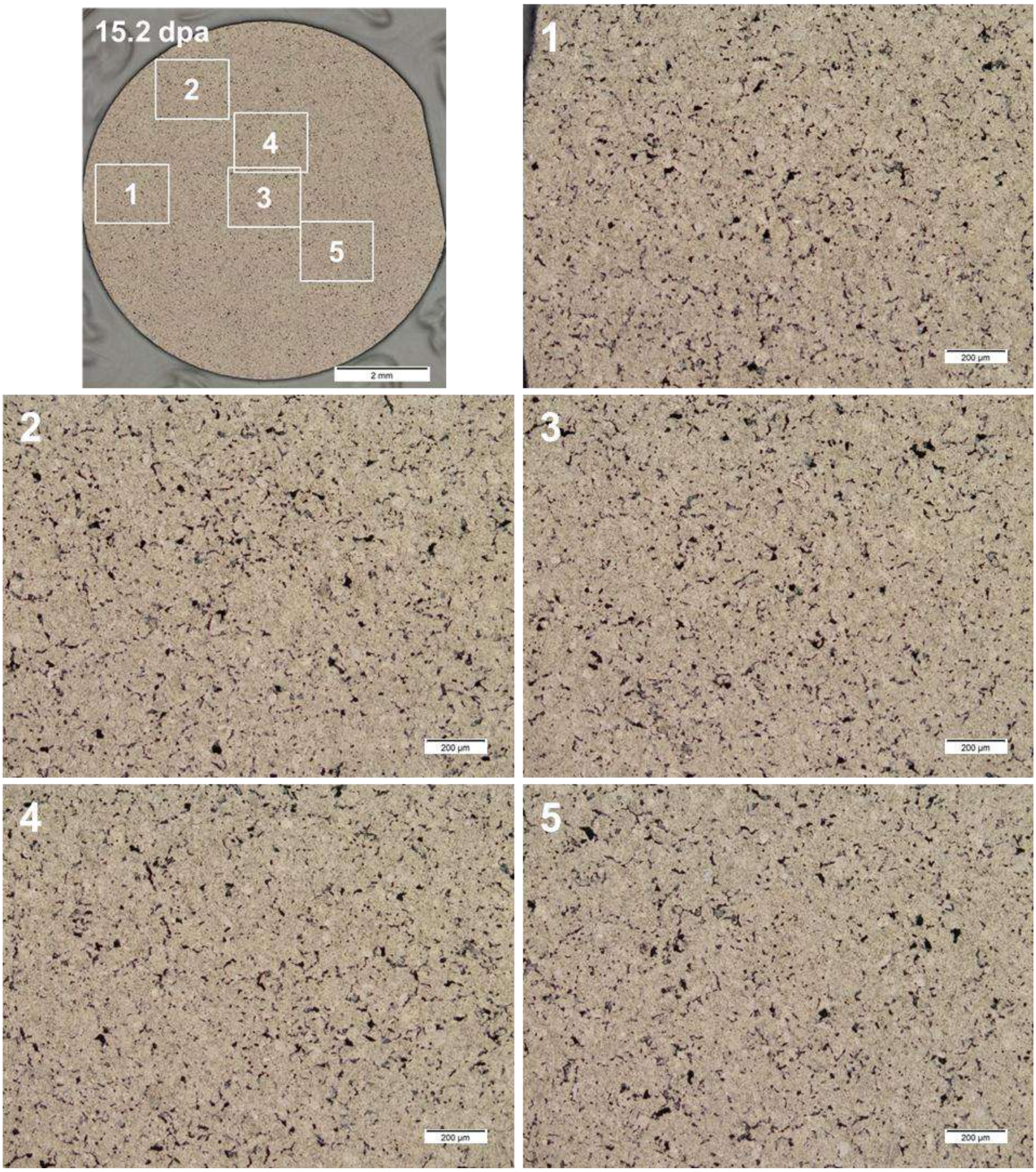

Figure 3-53 Bright field optical micrographs at 5x magnification of NBG-25 specimen S111 (15.2 dpa) and overview micrograph (top left) with indicated the locations of these micrographs on the sample

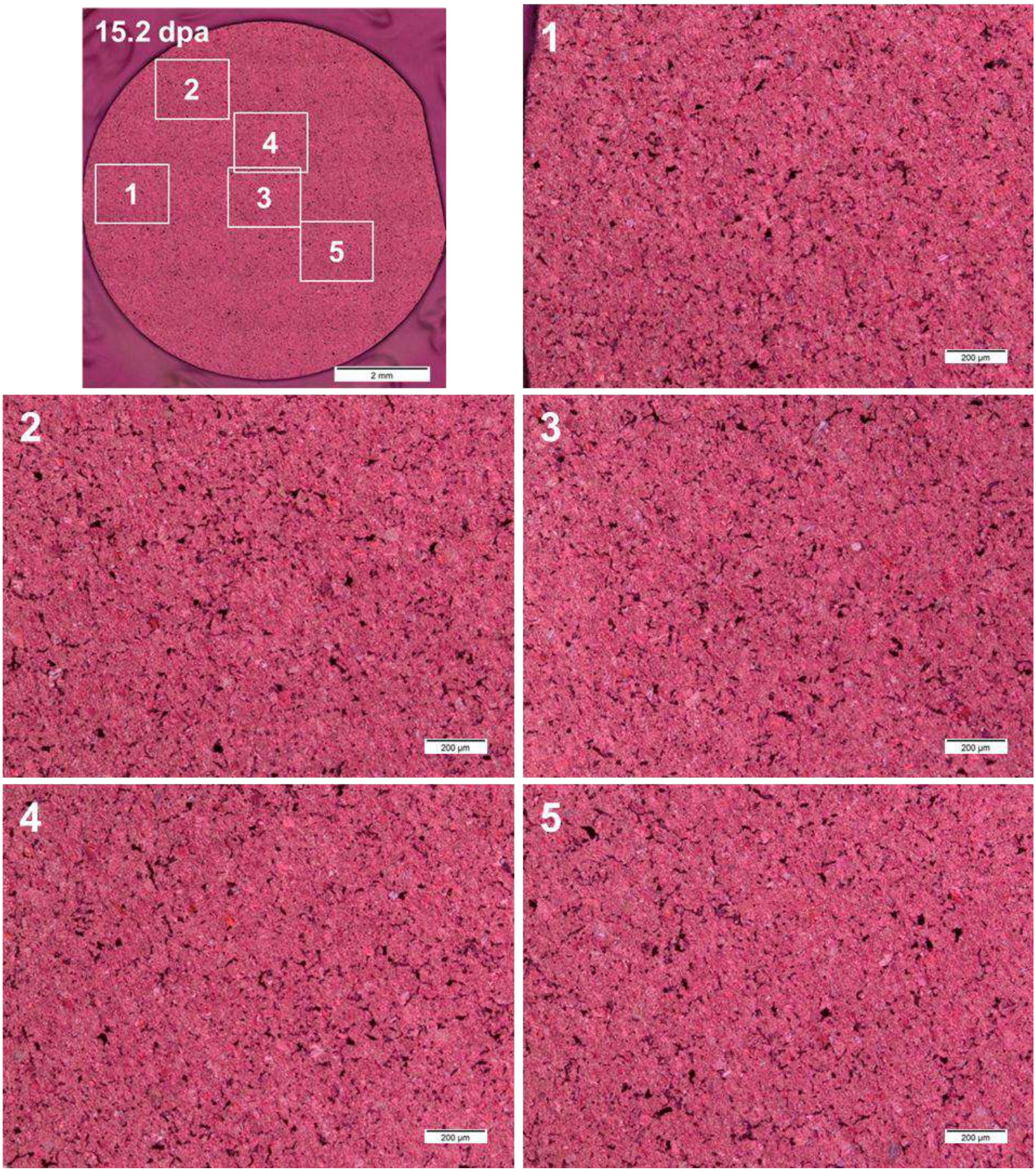

Figure 3-54 Polarisation microscopy images at 5x magnification of NBG-25 specimen S111 (15.2 dpa) and overview micrograph (top left) with indicated the locations of these micrographs on the sample

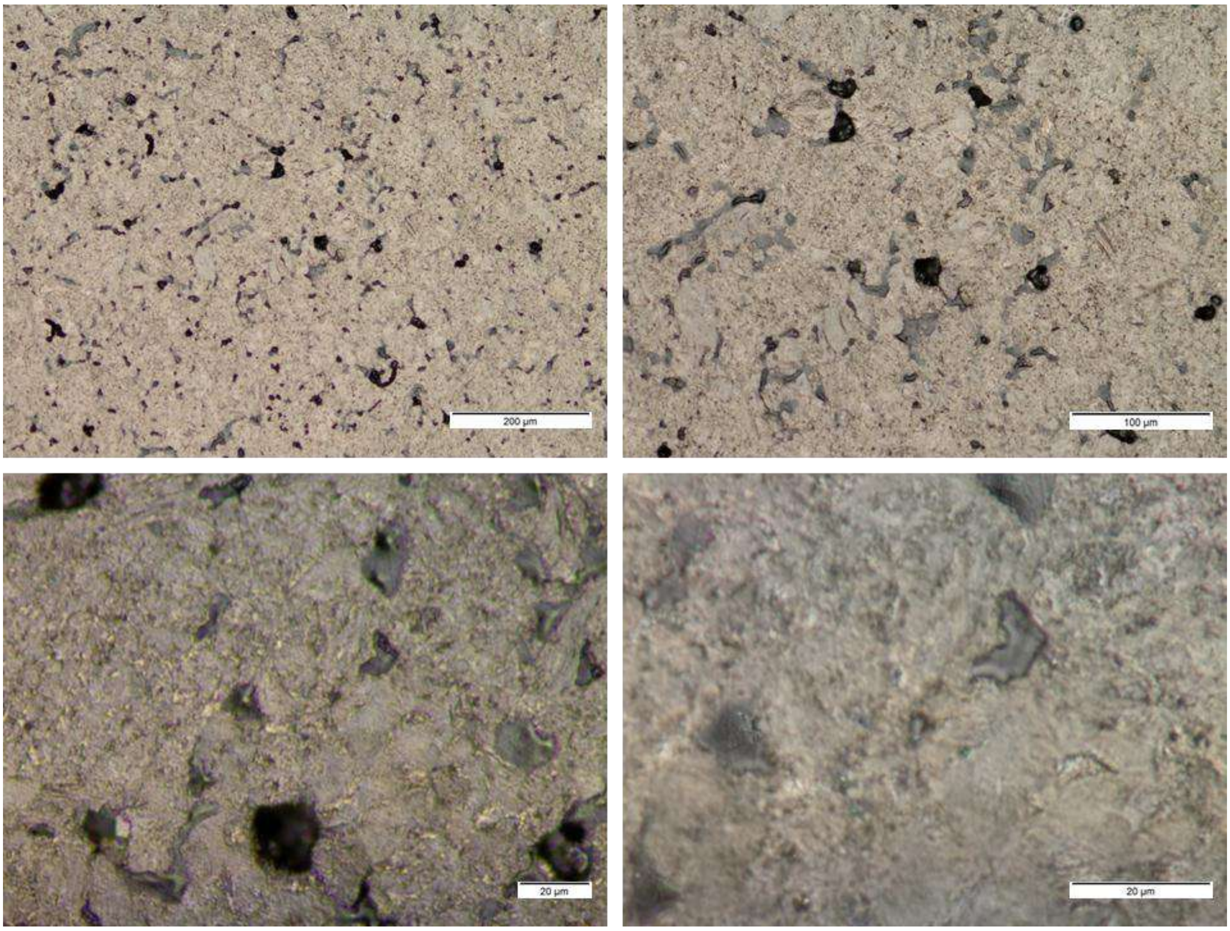

Figure 3-55 Bright field microscopy images of NBG-25 specimen S111 (15.2 dpa) at 10x to 100x magnification at detail location 3

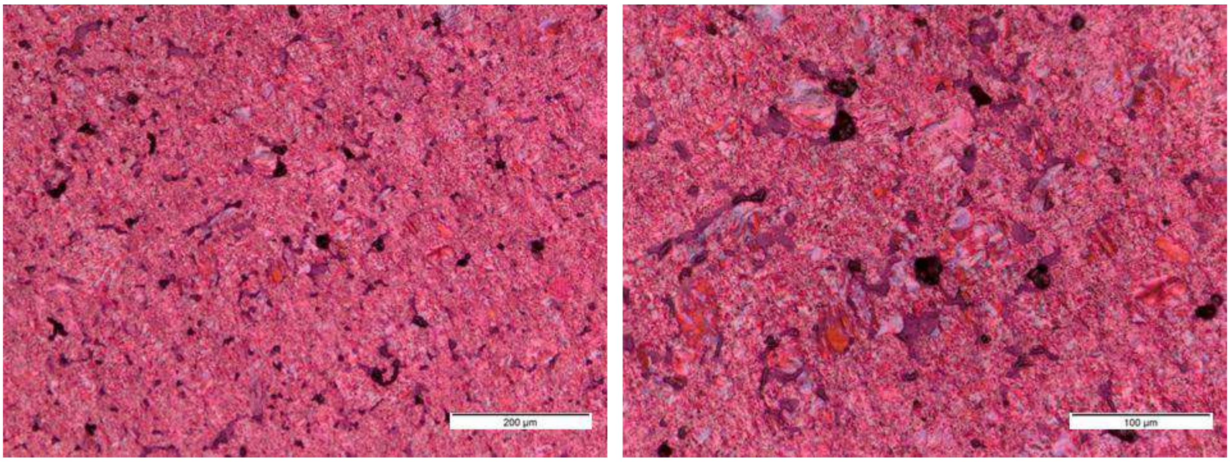

Figure 3-56 Polarisation microscopy images of NBG-25 specimen S111 (15.2 dpa) at 10x and 20x magnification at detail location 3

3.1.6 PCEA detail micrographs

Figure 3-57 to Figure 3-64 show the detail micrographs of the irradiated PCEA graphite specimens.

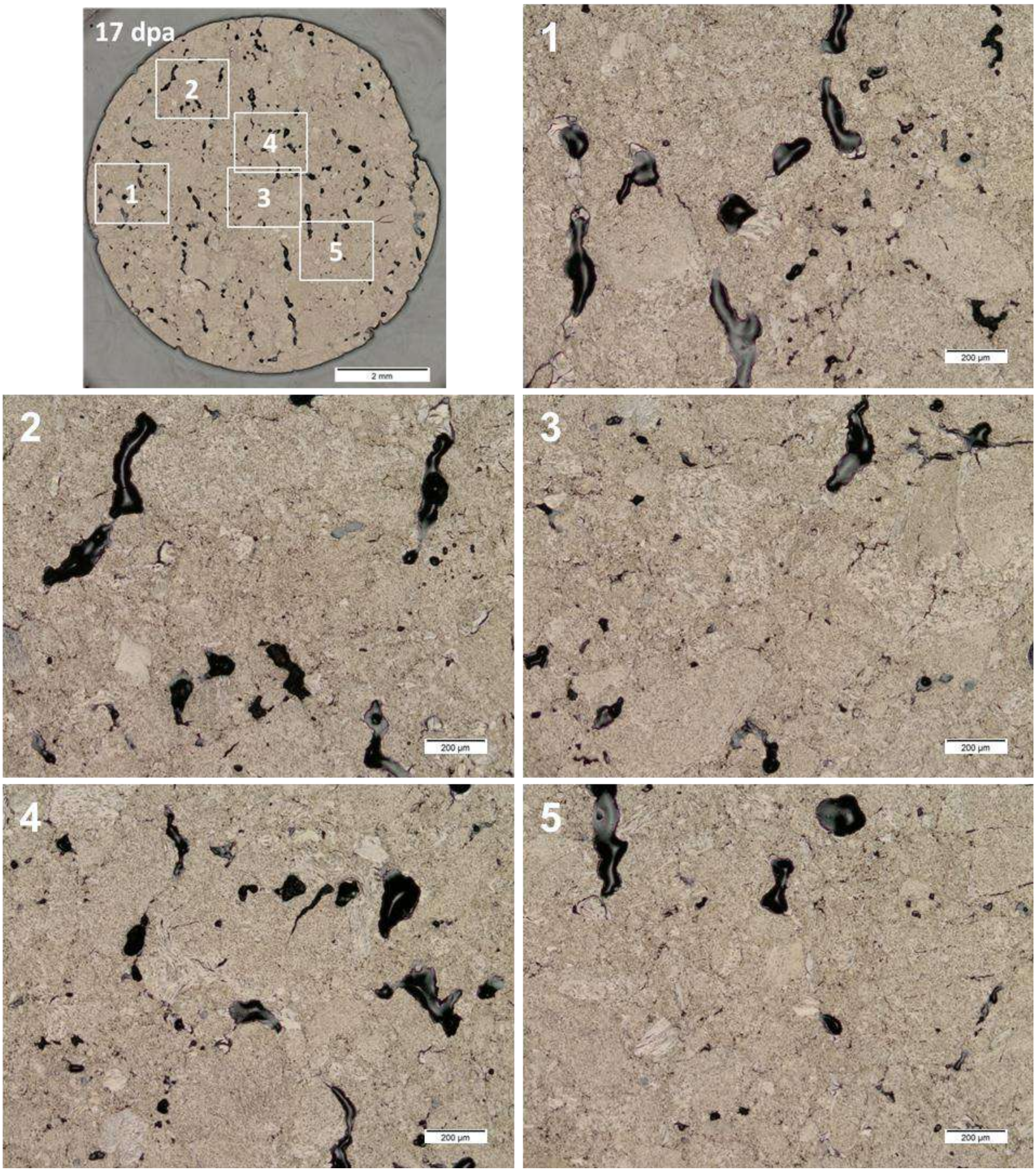

Figure 3-57 Bright field optical micrographs at 5x magnification of PCEA specimen U021 (17 dpa) and overview micrograph (top left) with indicated the locations of these micrographs on the sample

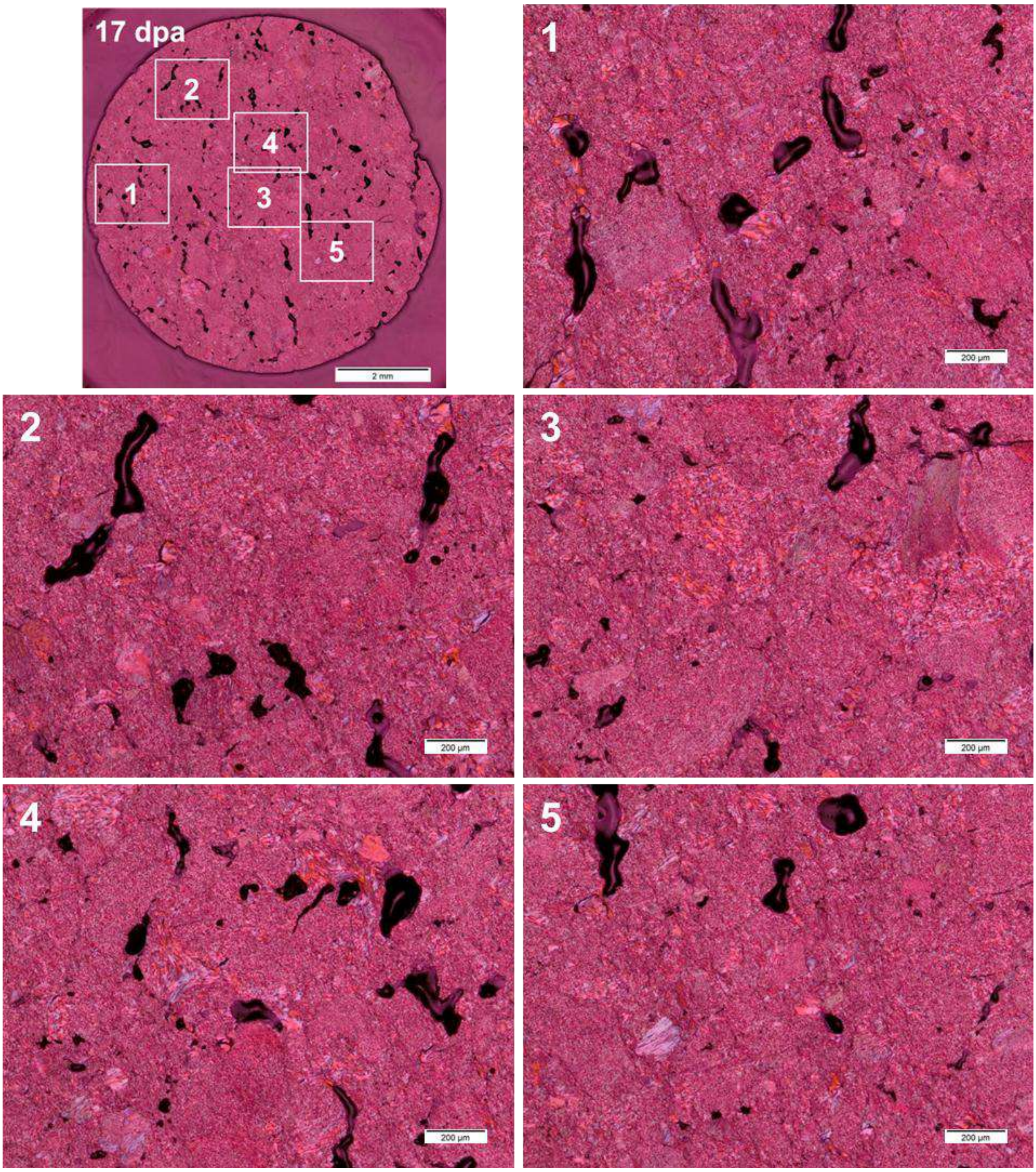

Figure 3-58 Polarisation microscopy images at 5x magnification of PCEA specimen U021 (17 dpa) and overview micrograph (top left) with indicated the locations of these micrographs on the sample

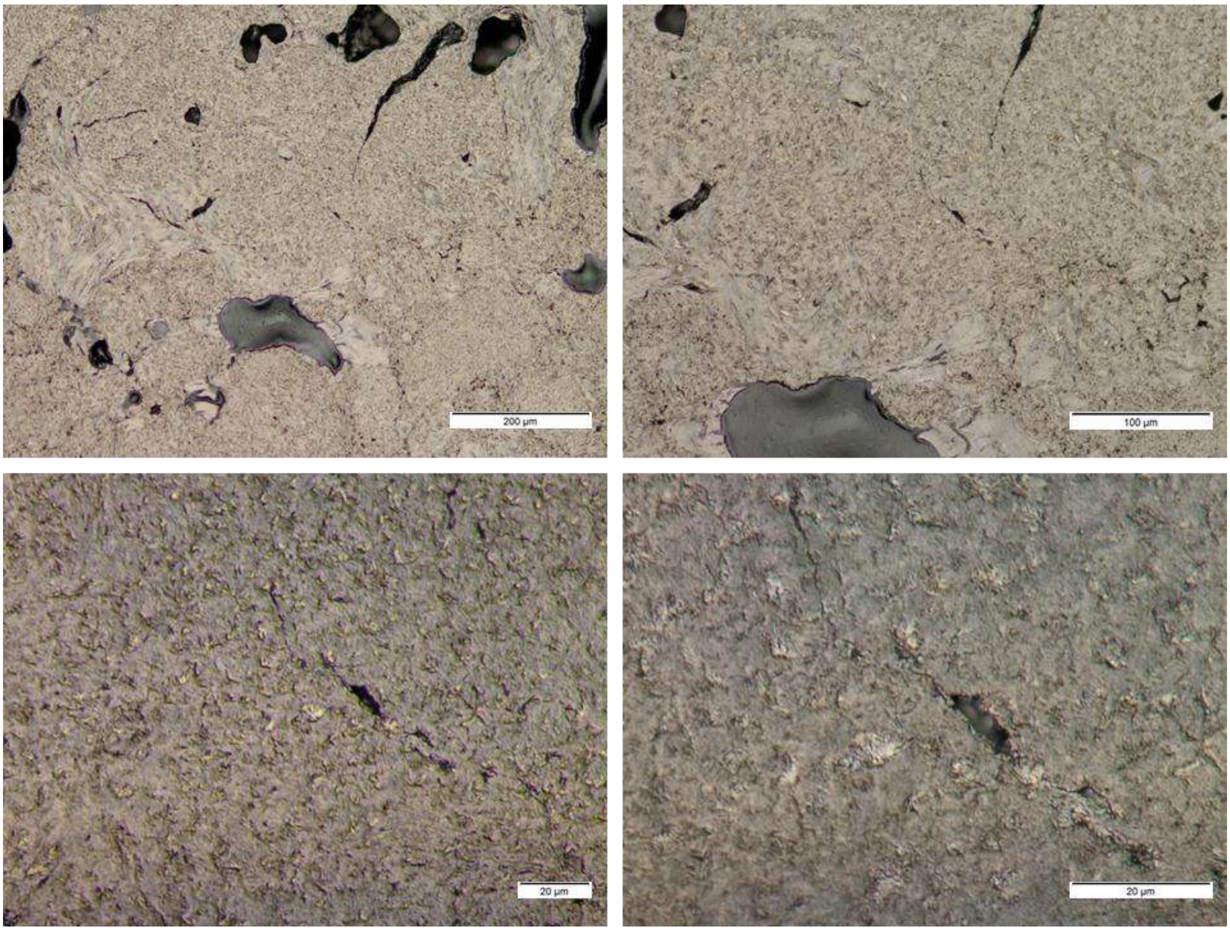

Figure 3-59 Bright field microscopy images of PCEA specimen U021 (17 dpa) at 10x to 100x magnification at detail location 4

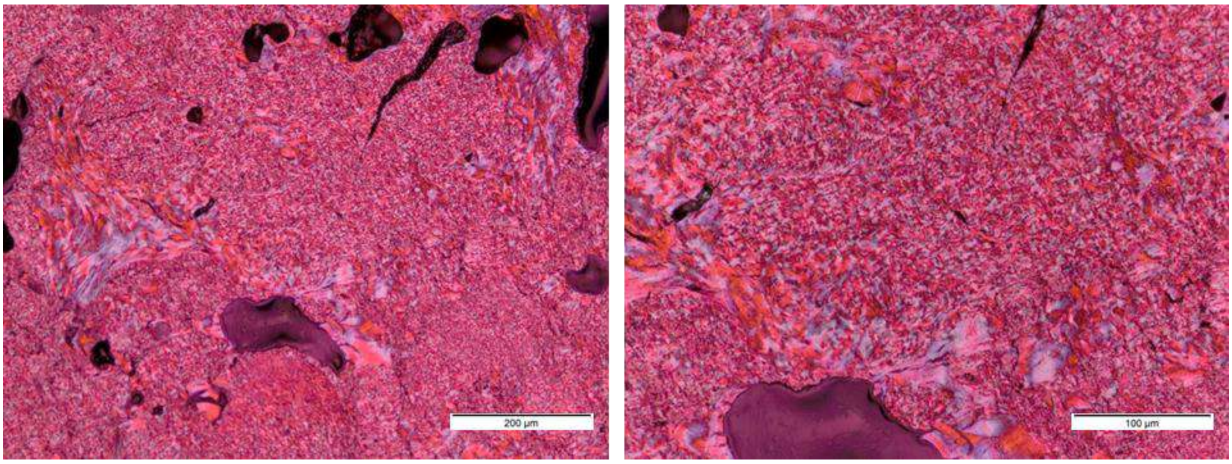

Figure 3-60 Polarisation microscopy images of PCEA specimen U021 (17 dpa) at 10x and 20x magnification at detail location 4

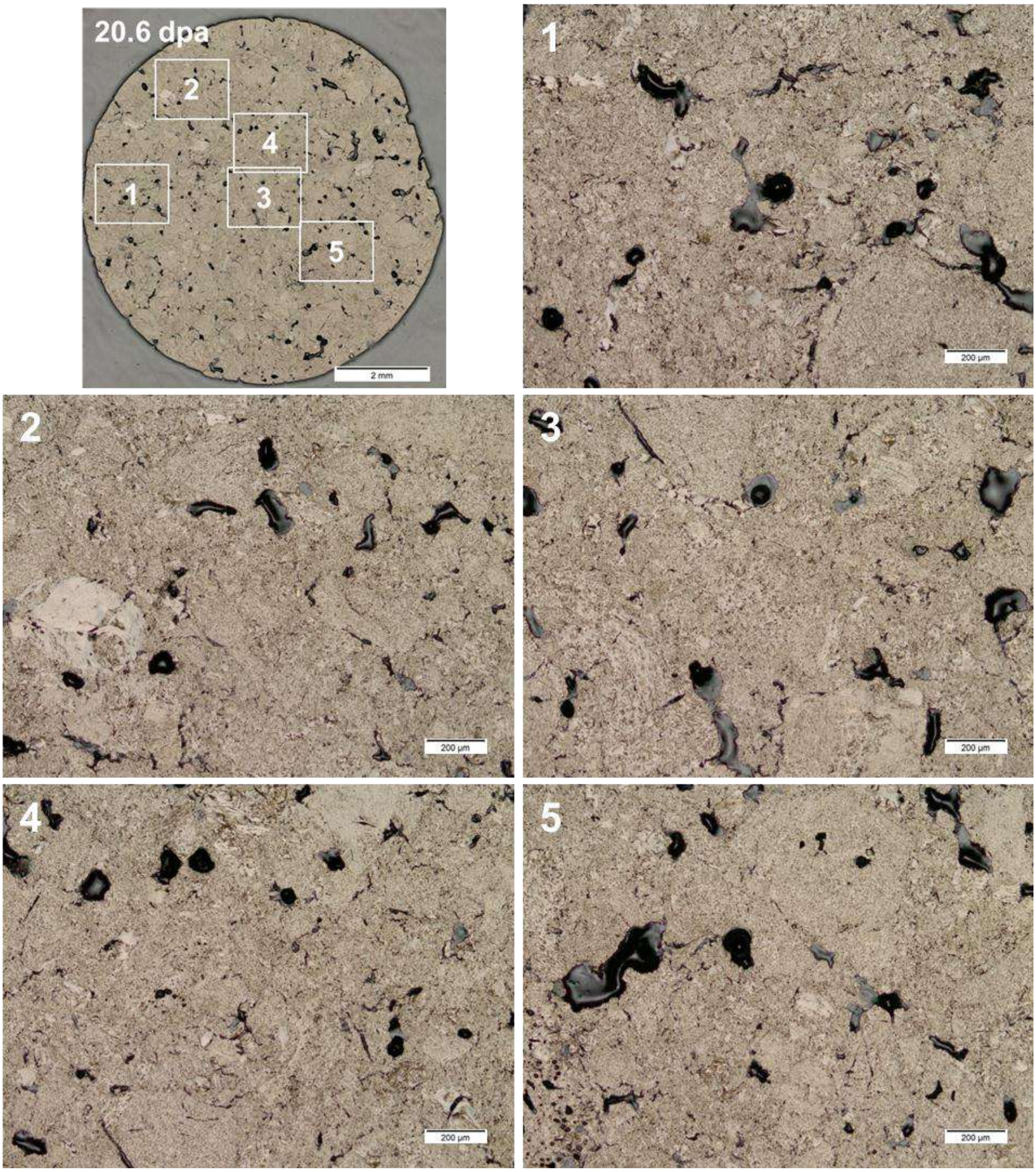

Figure 3-61 Bright field optical micrographs at 5x magnification of PCEA specimen U070 (20.6 dpa) and overview micrograph (top left) with indicated the locations of these micrographs on the sample

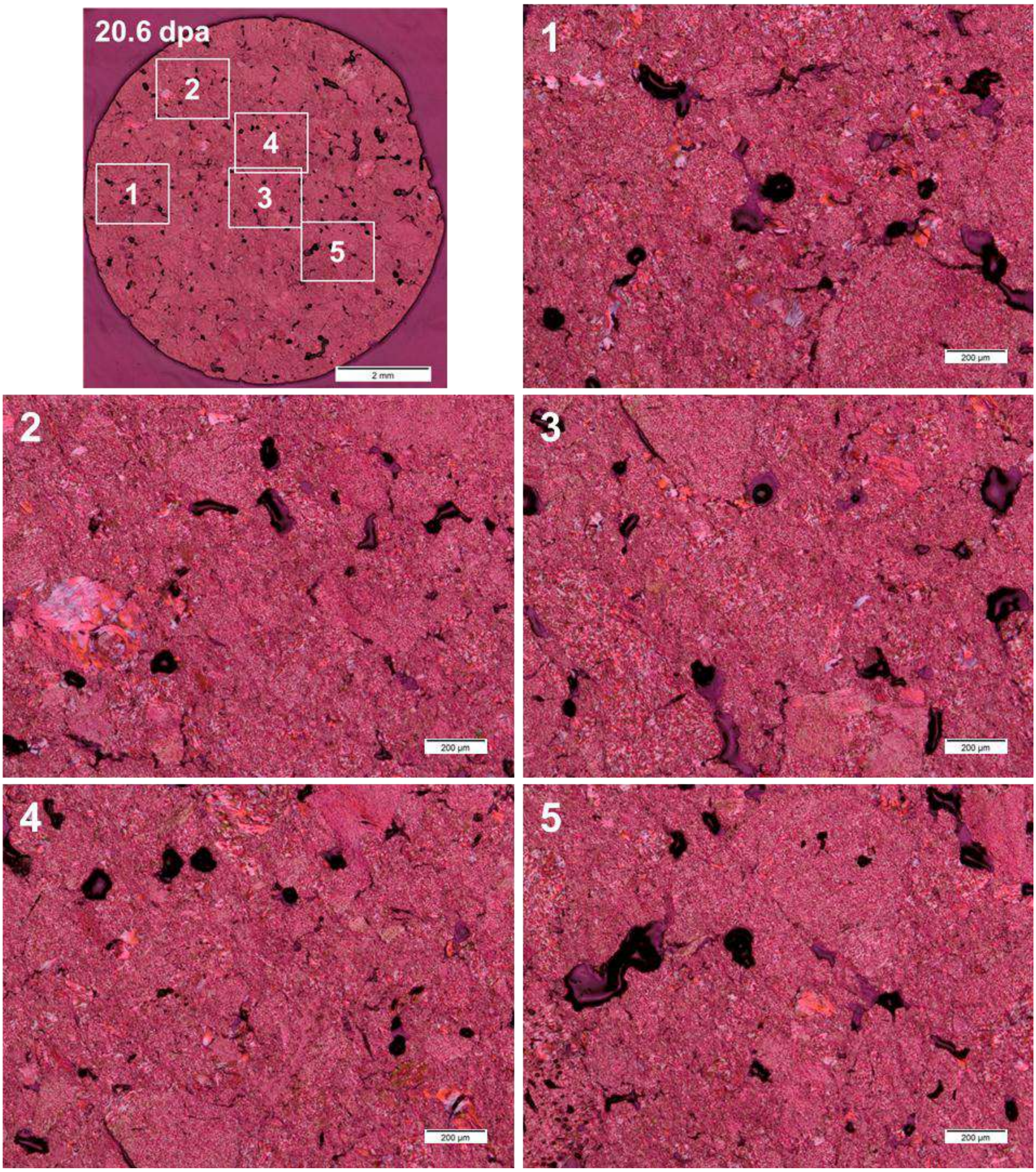

Figure 3-62 Polarisation microscopy images at 5x magnification of PCEA specimen U070 (20.6 dpa) and overview micrograph (top left) with indicated the locations of these micrographs on the sample

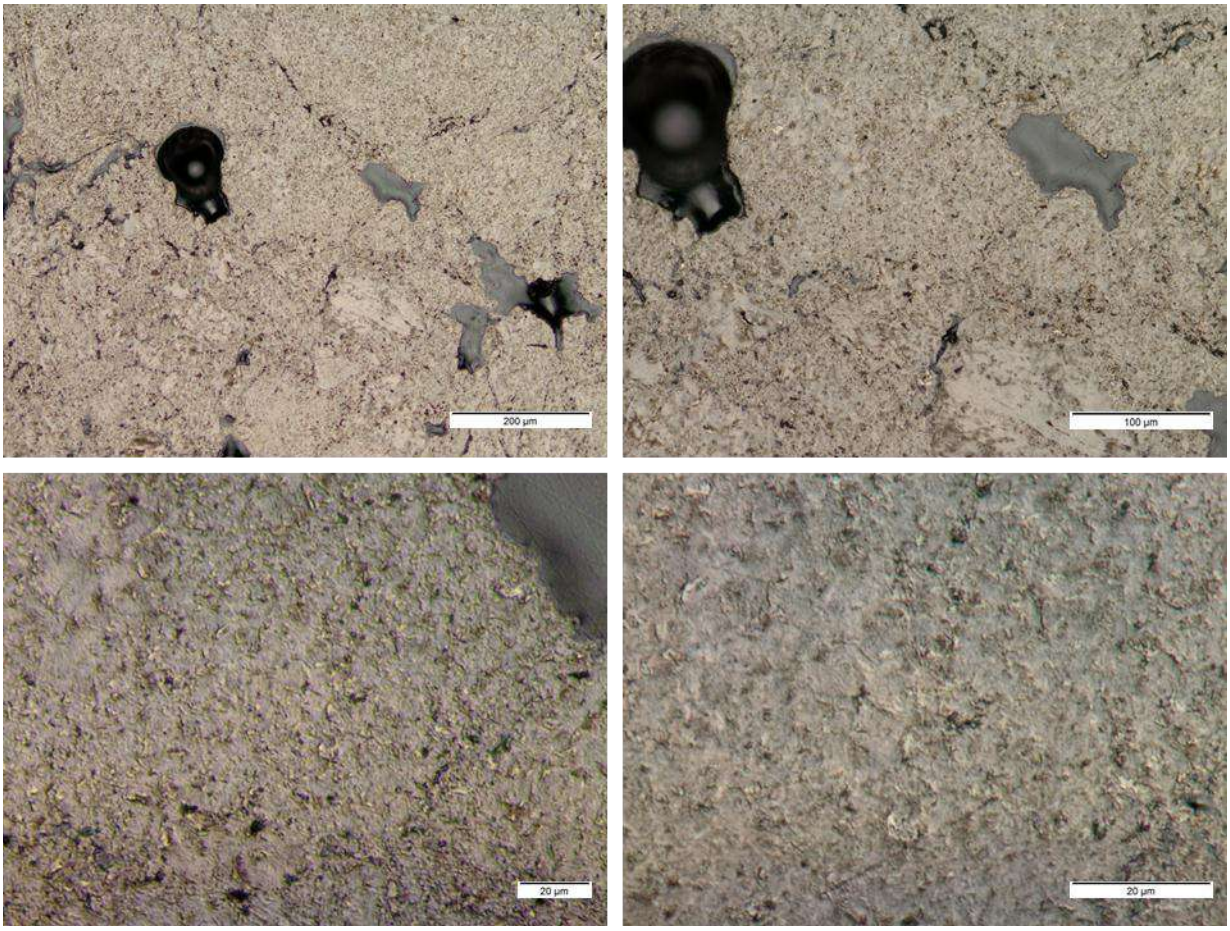

Figure 3-63 Bright field microscopy images of PCEA specimen U070 (20.6 dpa) at 10x to 100x magnification at detail location 5

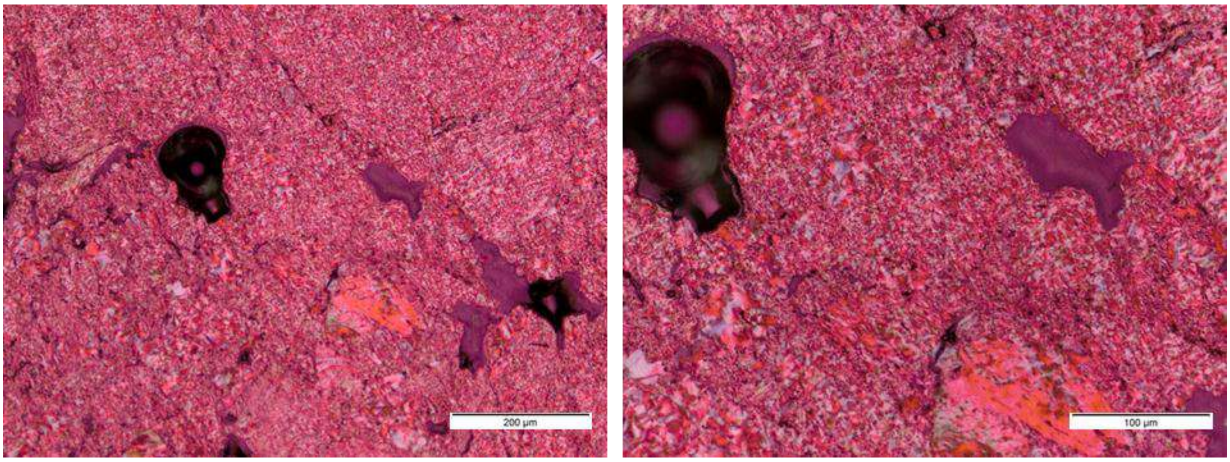

Figure 3-64 Polarisation microscopy images of PCEA specimen U070 (20.6 dpa) at 10x and 20x magnification at detail location 5

3.1.7 PCIB detail micrographs

Figure 3-65 to Figure 3-72 show the detail micrographs of the irradiated PCIB graphite specimens.

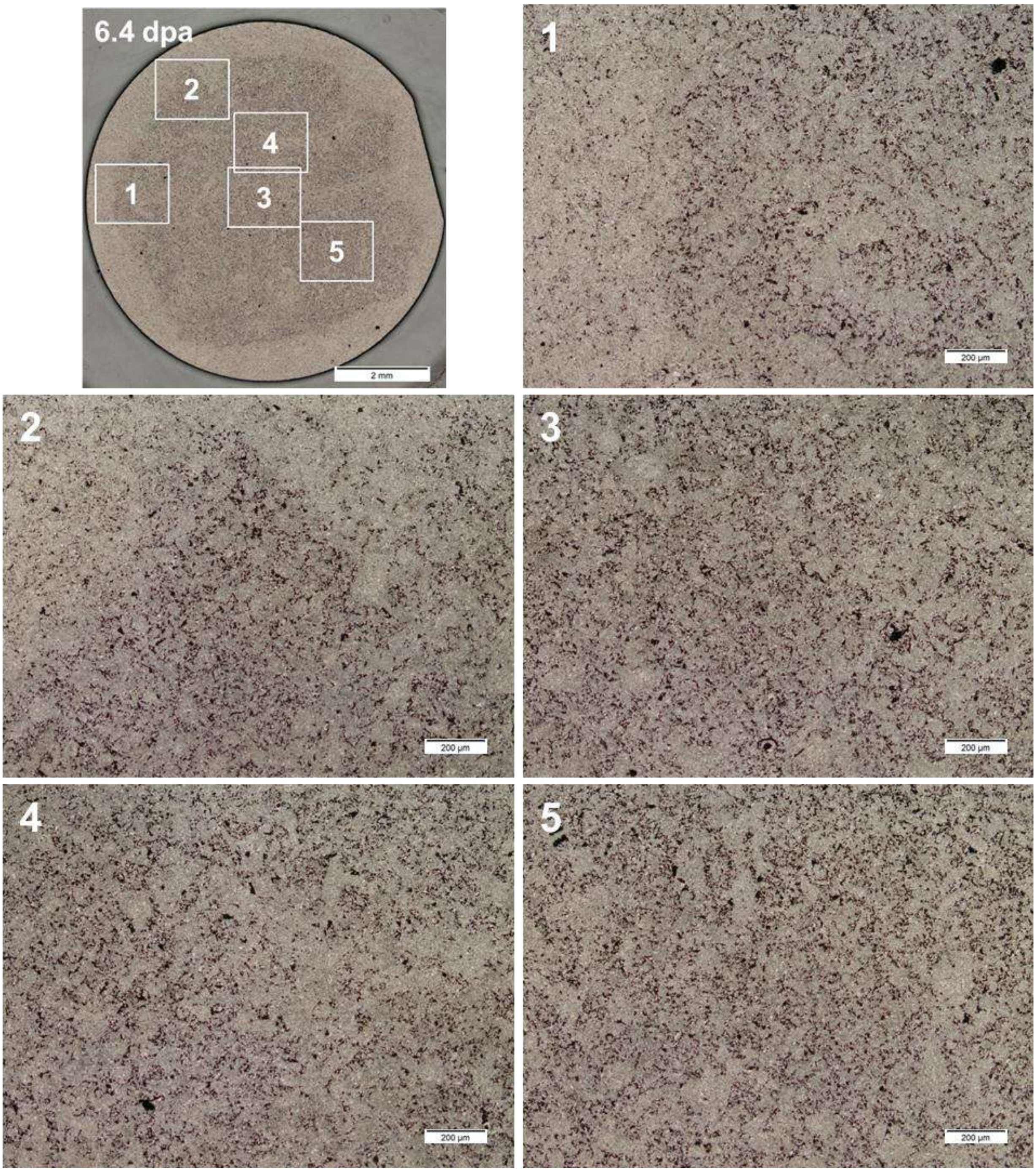

Figure 3-65 Bright field optical micrographs at 5x magnification of PCIB specimen U163 (6.4 dpa) and overview micrograph (top left) with indicated the locations of these micrographs on the sample

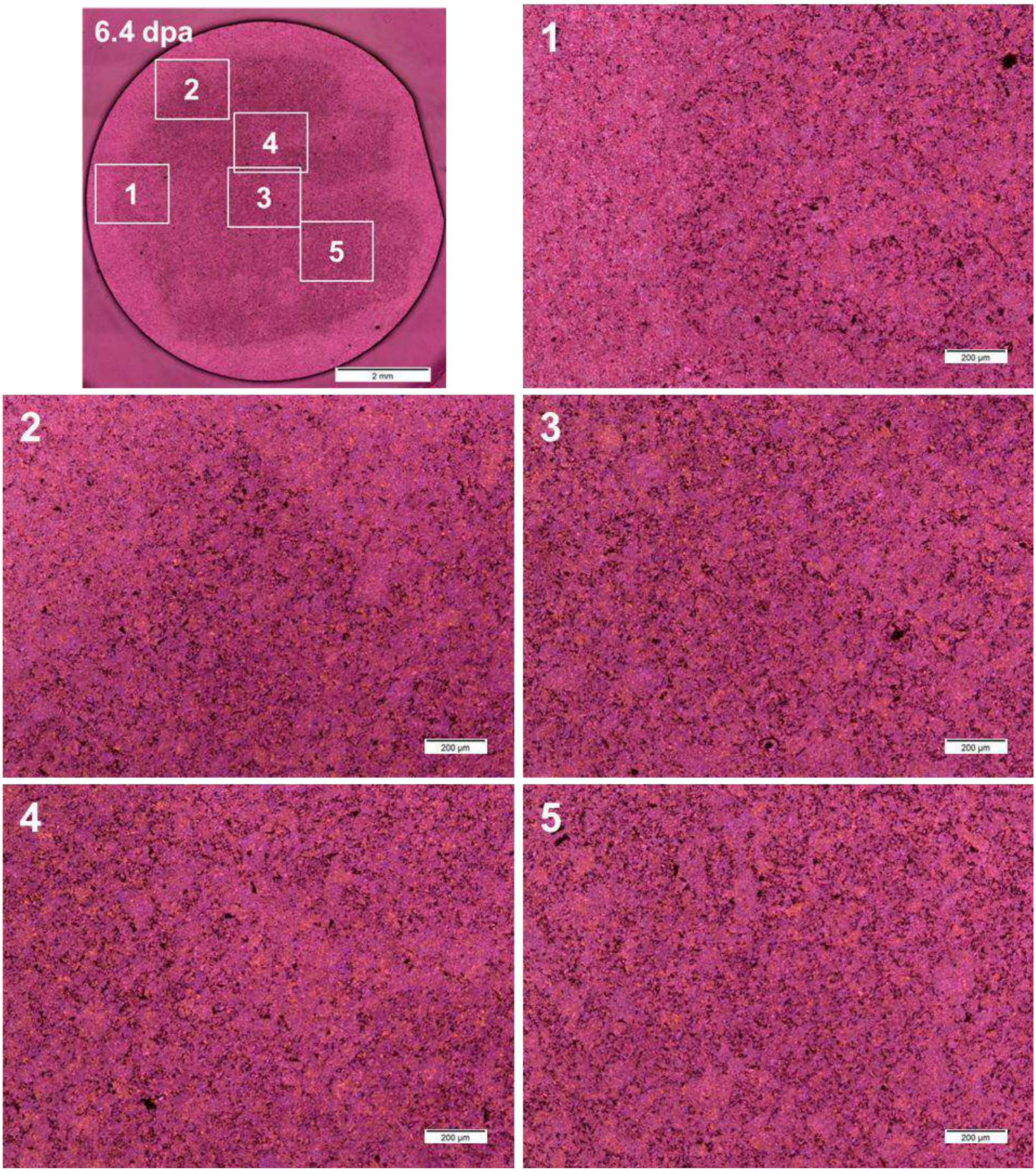

Figure 3-66 Polarisation microscopy images at 5x magnification of PCIB specimen U163 (6.4 dpa) and overview micrograph (top left) with indicated the locations of these micrographs on the sample

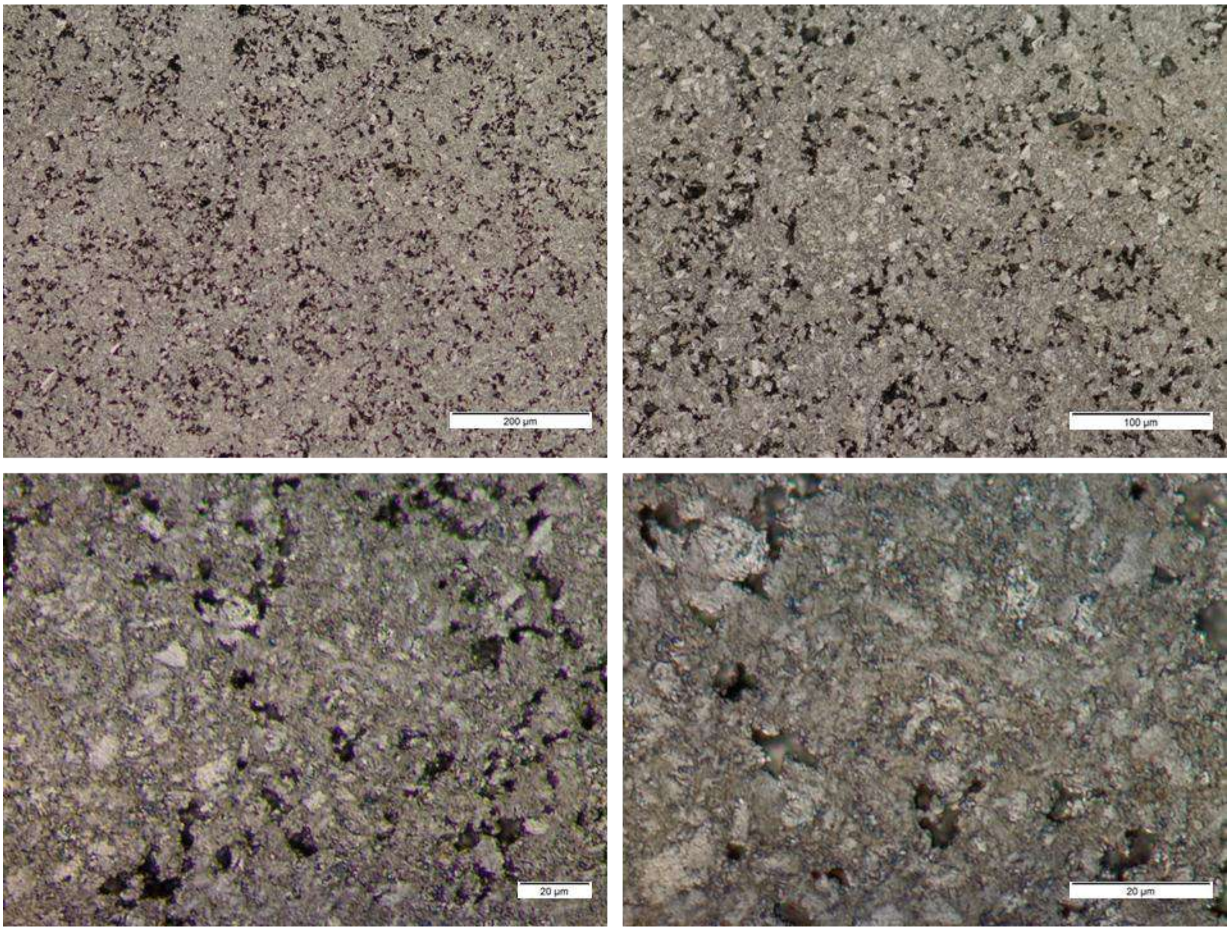

Figure 3-67 Bright field microscopy images of PCIB specimen U163 (6.4 dpa) at 10x to 100x magnification at detail location 5

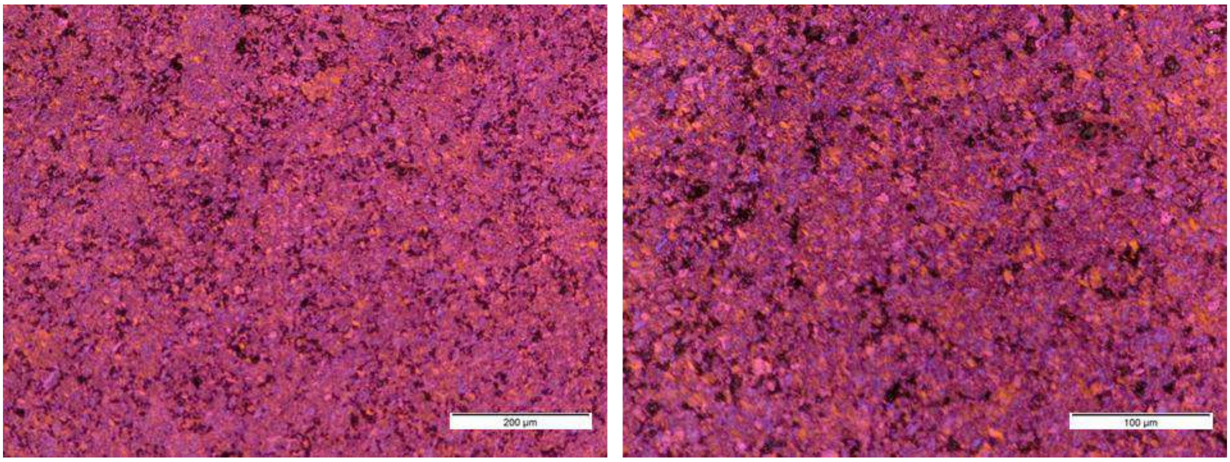

Figure 3-68 Polarisation microscopy images of PCIB specimen U163 (6.4 dpa) at 10x and 20x magnification at detail location 5

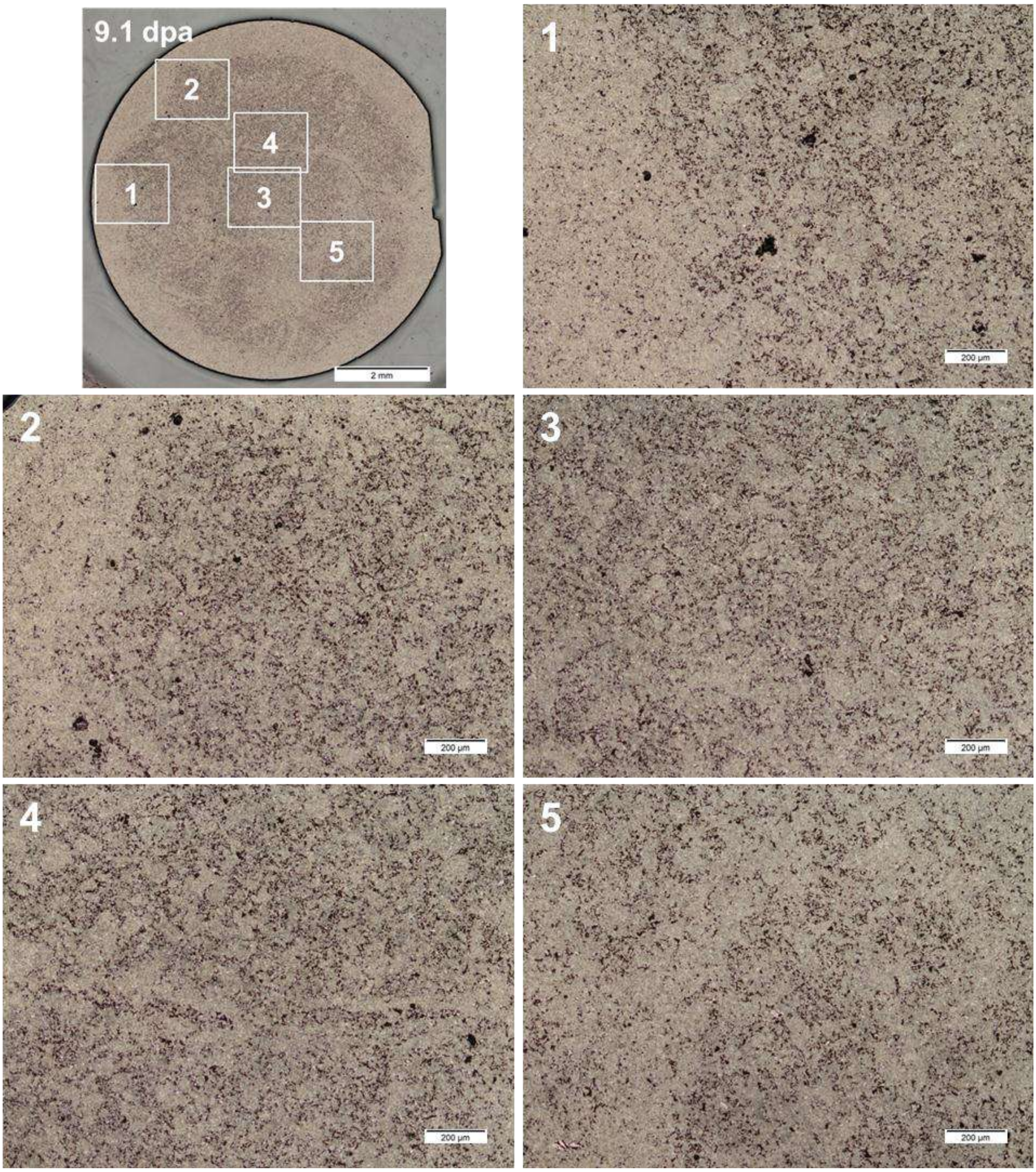

Figure 3-69 Bright field optical micrographs at 5x magnification of PCIB specimen U113 (9.1 dpa) and overview micrograph (top left) with indicated the locations of these micrographs on the sample

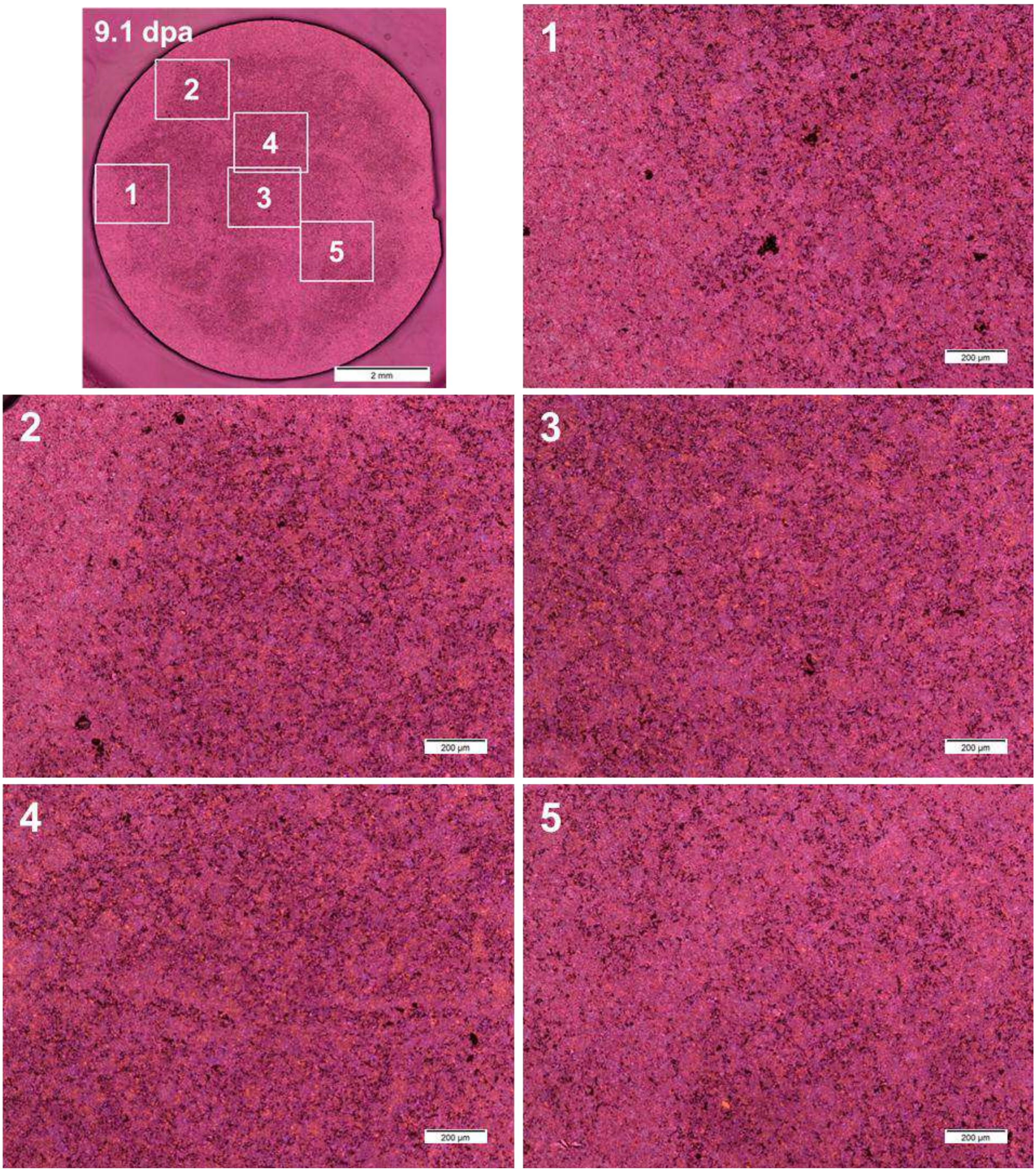

Figure 3-70 Polarisation microscopy images at 5x magnification of PCIB specimen U113 (9.1 dpa) and overview micrograph (top left) with indicated the locations of these micrographs on the sample

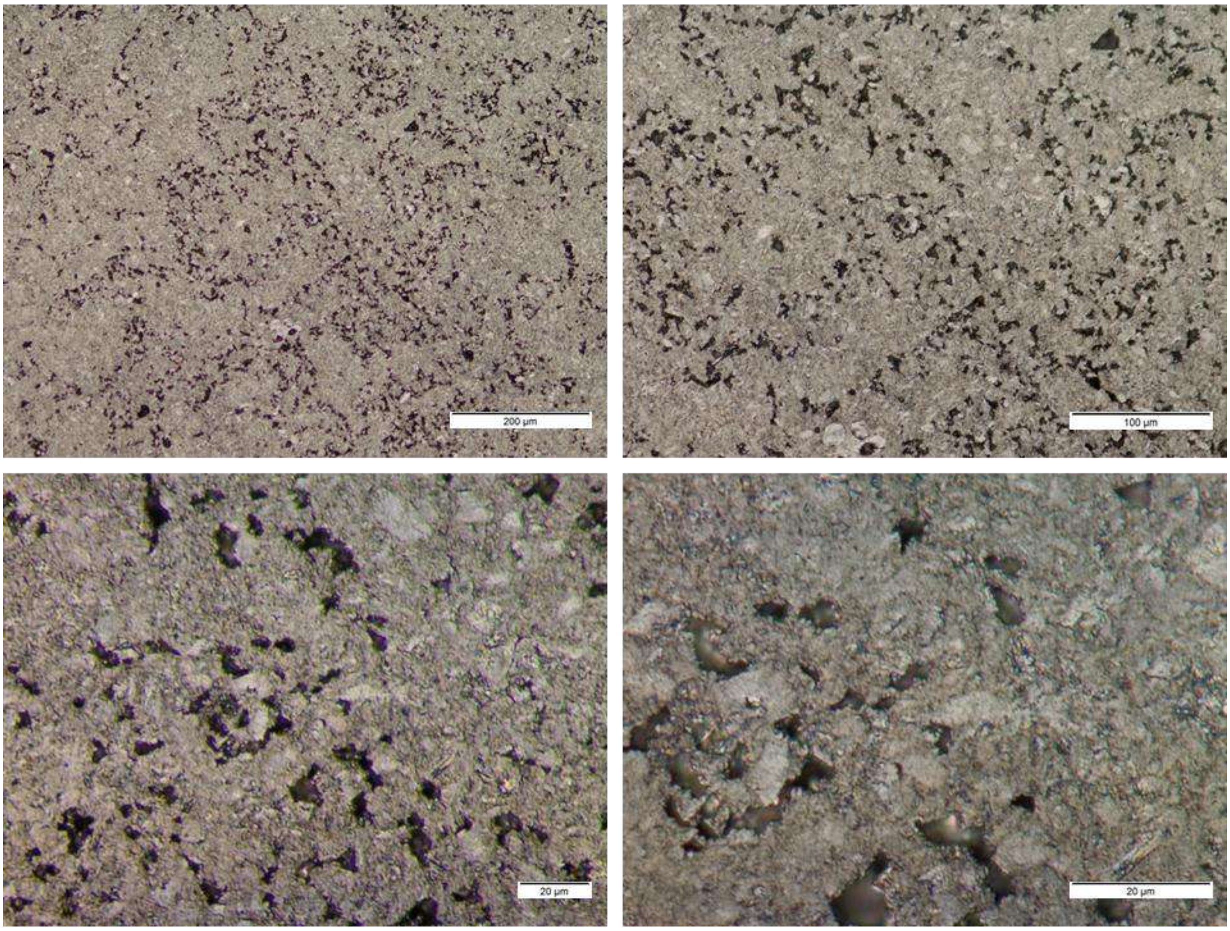

Figure 3-71 Bright field microscopy images of PCIB specimen U113 (9.1 dpa) at 10x to 100x magnification at detail location 5

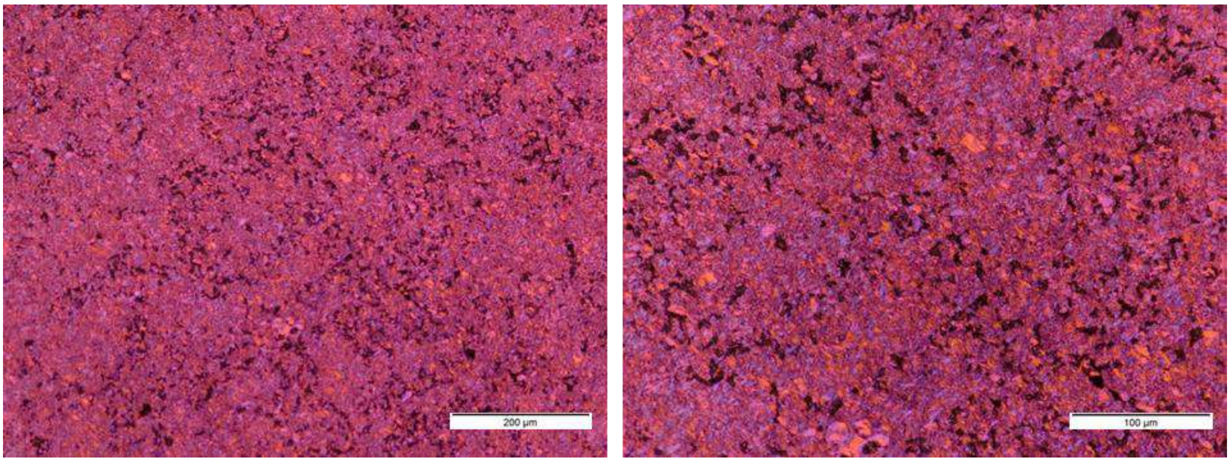

Figure 3-72 Polarisation microscopy images of PCIB specimen U113 (9.1 dpa) at 10x and 20x magnification at detail location 5

3.1.8 PPEA detail micrographs

Figure 3-73 to Figure 3-80 show the detail micrographs of the irradiated PPEA graphite specimens.

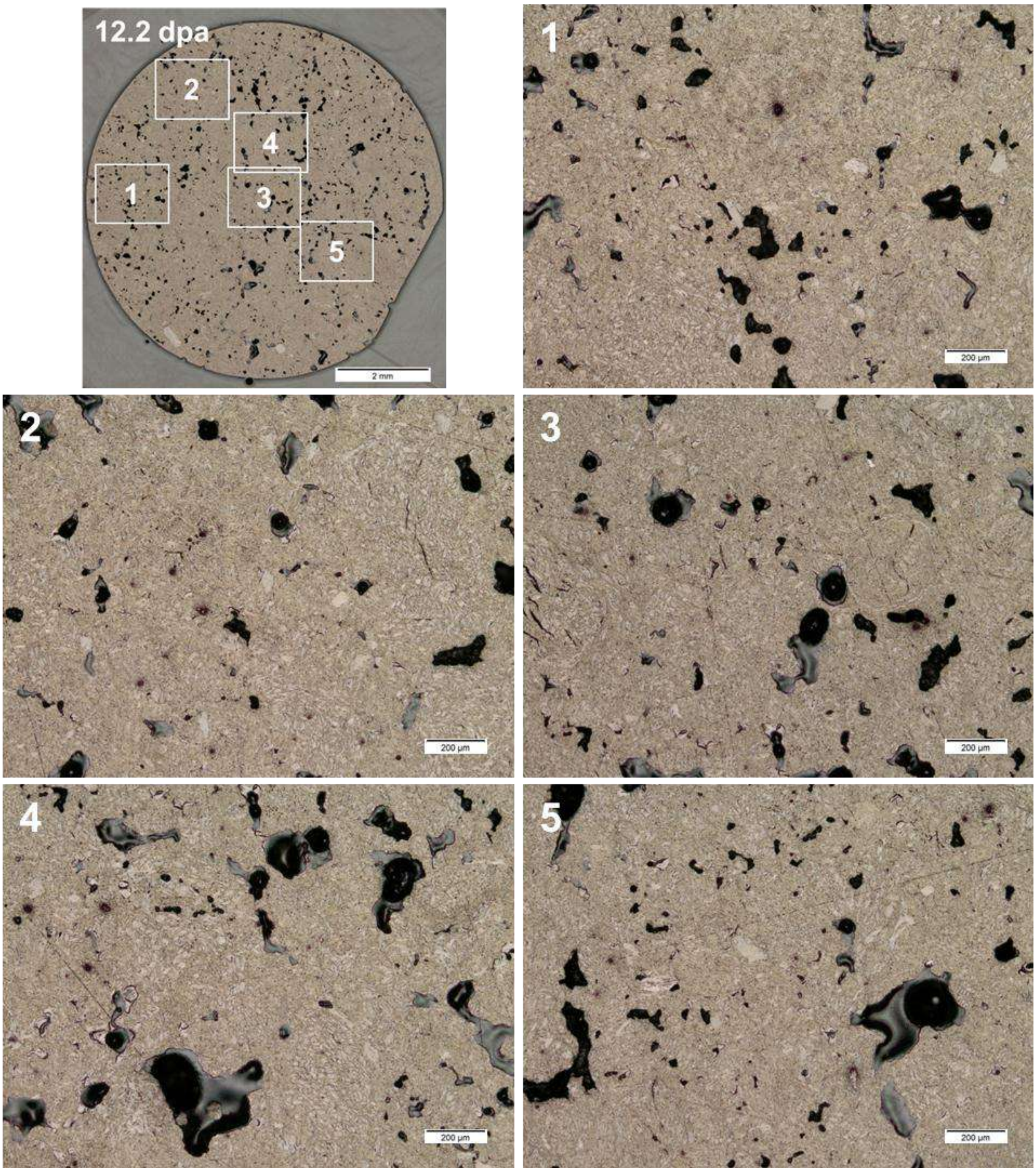

Figure 3-73 Bright field optical micrographs at 5x magnification of PPEA specimen U329 (12.2 dpa) and overview micrograph (top left) with indicated the locations of these micrographs on the sample

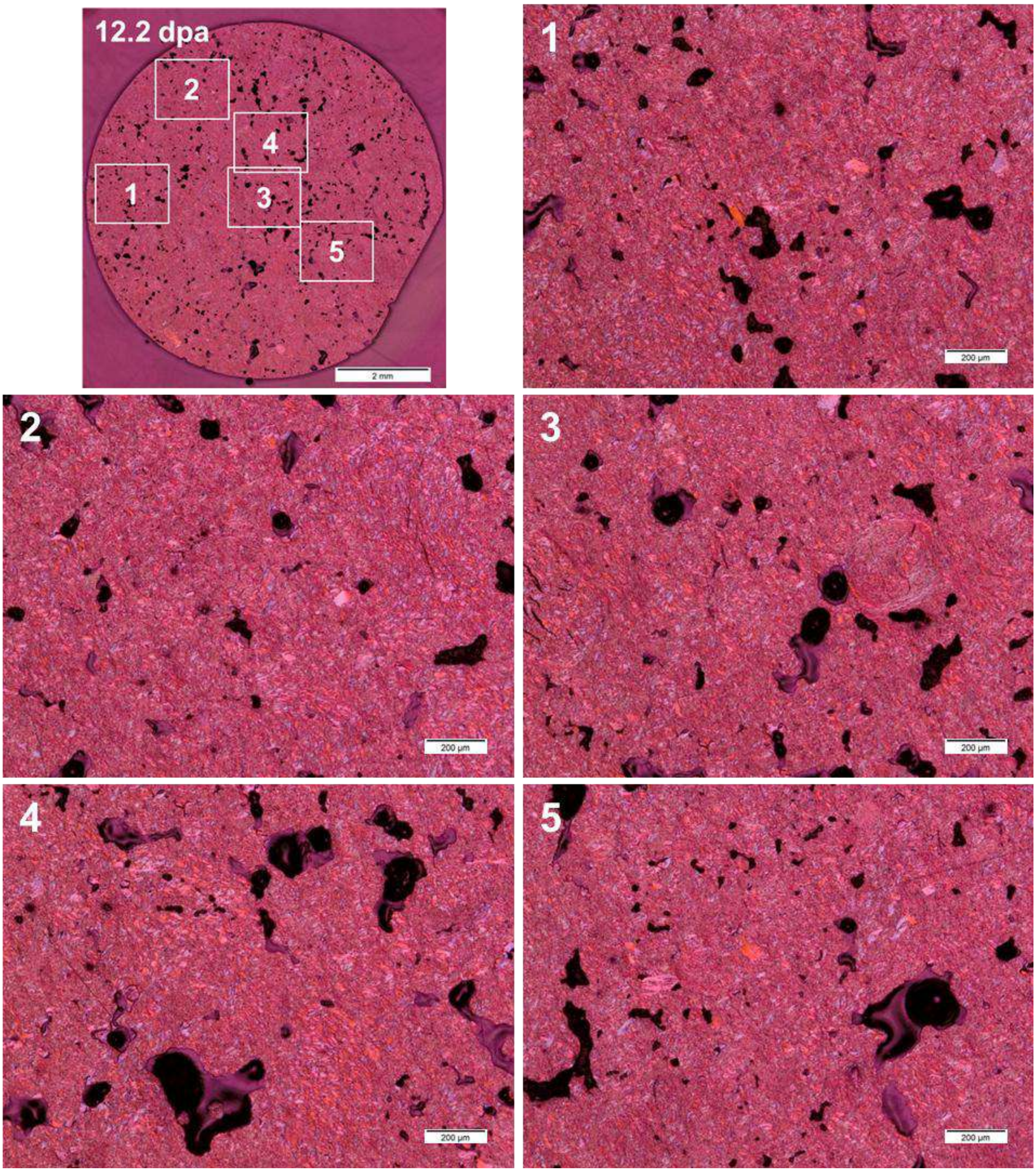

Figure 3-74 Polarisation microscopy images at 5x magnification of PPEA specimen U329 (12.2 dpa) and overview micrograph (top left) with indicated the locations of these micrographs on the sample

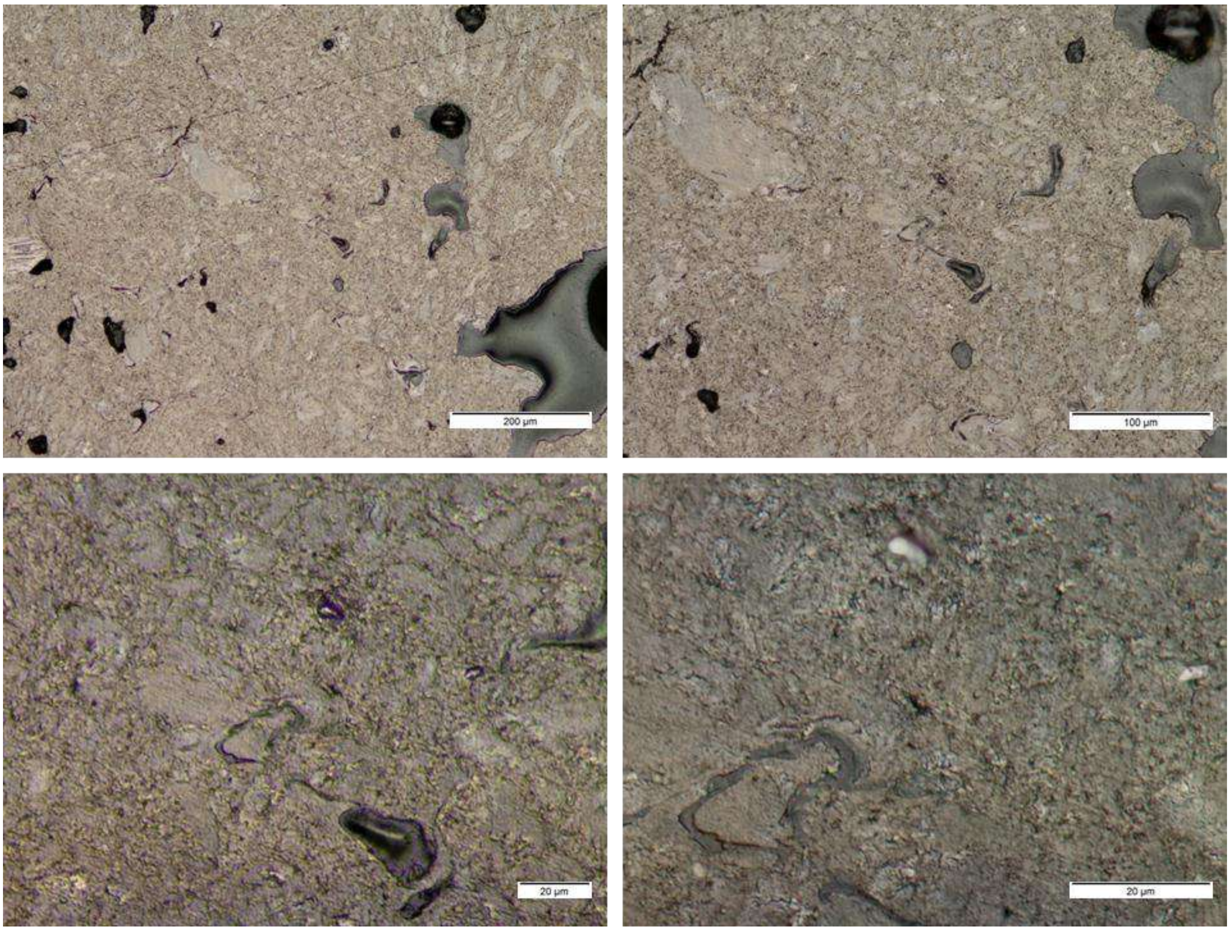

Figure 3-75 Bright field microscopy images of PPEA specimen U329 (12.2 dpa) at 10x to 100x magnification at detail location 5

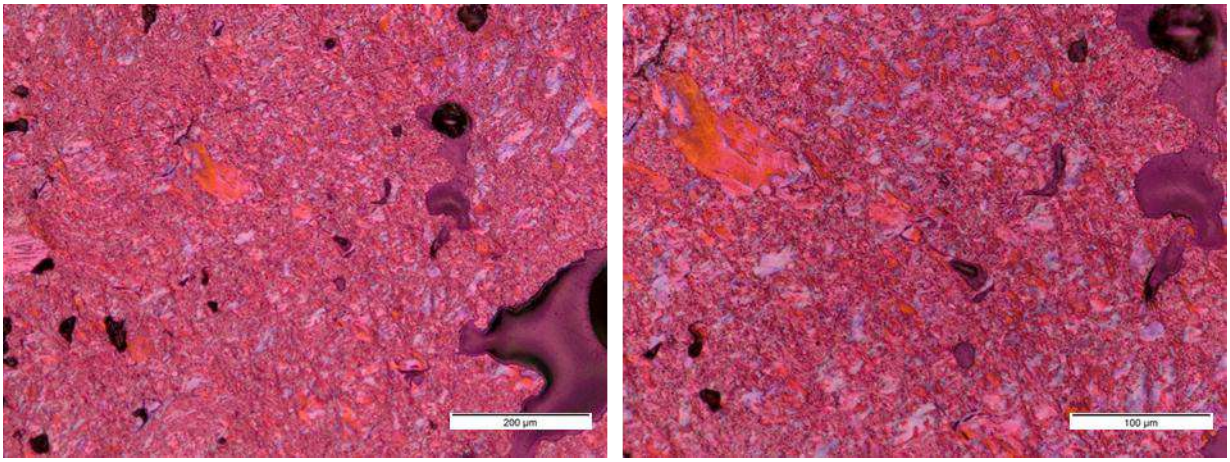

Figure 3-76 Polarisation microscopy images of PPEA specimen U329 (12.2 dpa) at 10x and 20x magnification at detail location 5

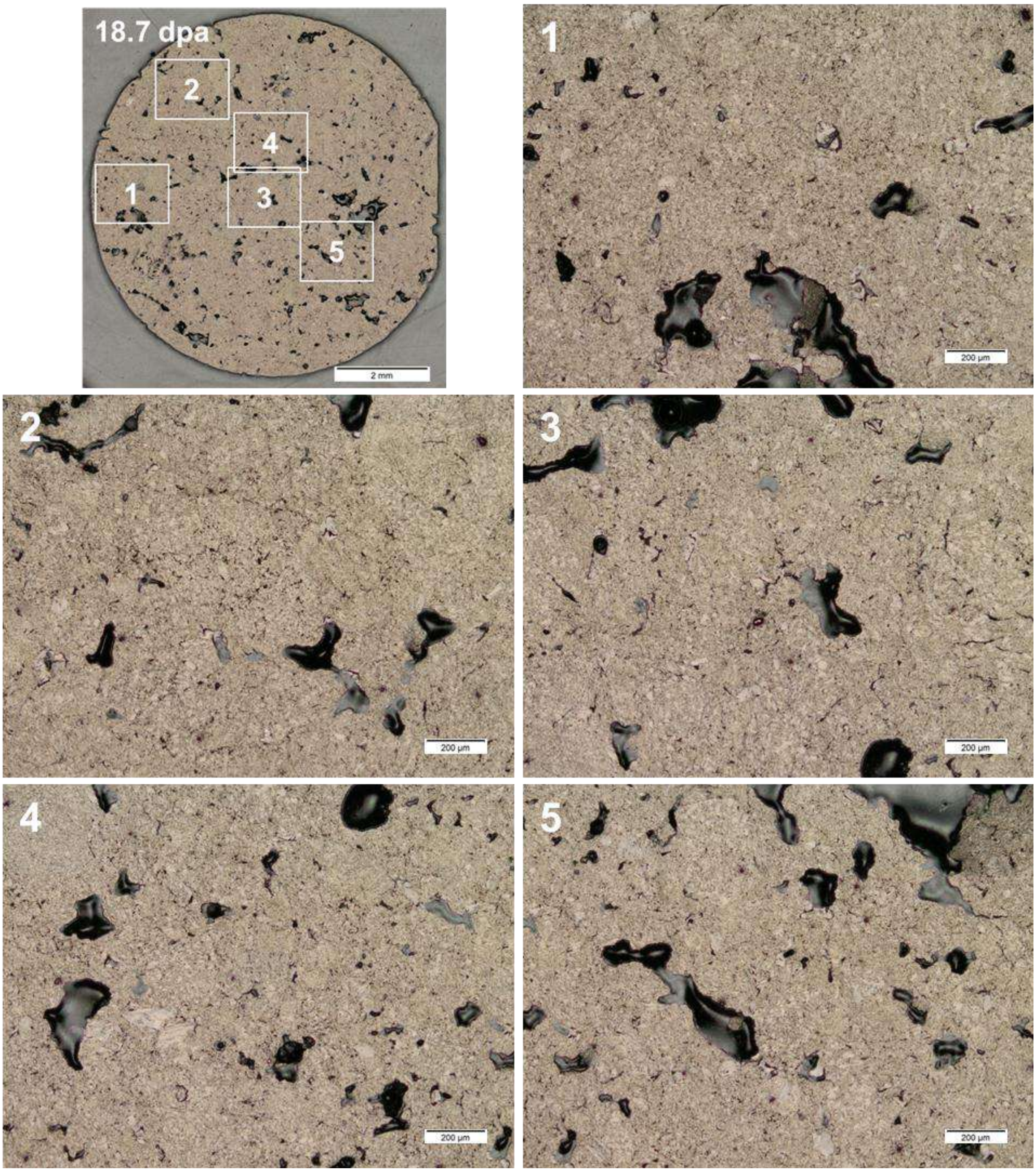

Figure 3-77 Bright field optical micrographs at 5x magnification of PPEA specimen U277 (18.7 dpa) and overview micrograph (top left) with indicated the locations of these micrographs on the sample

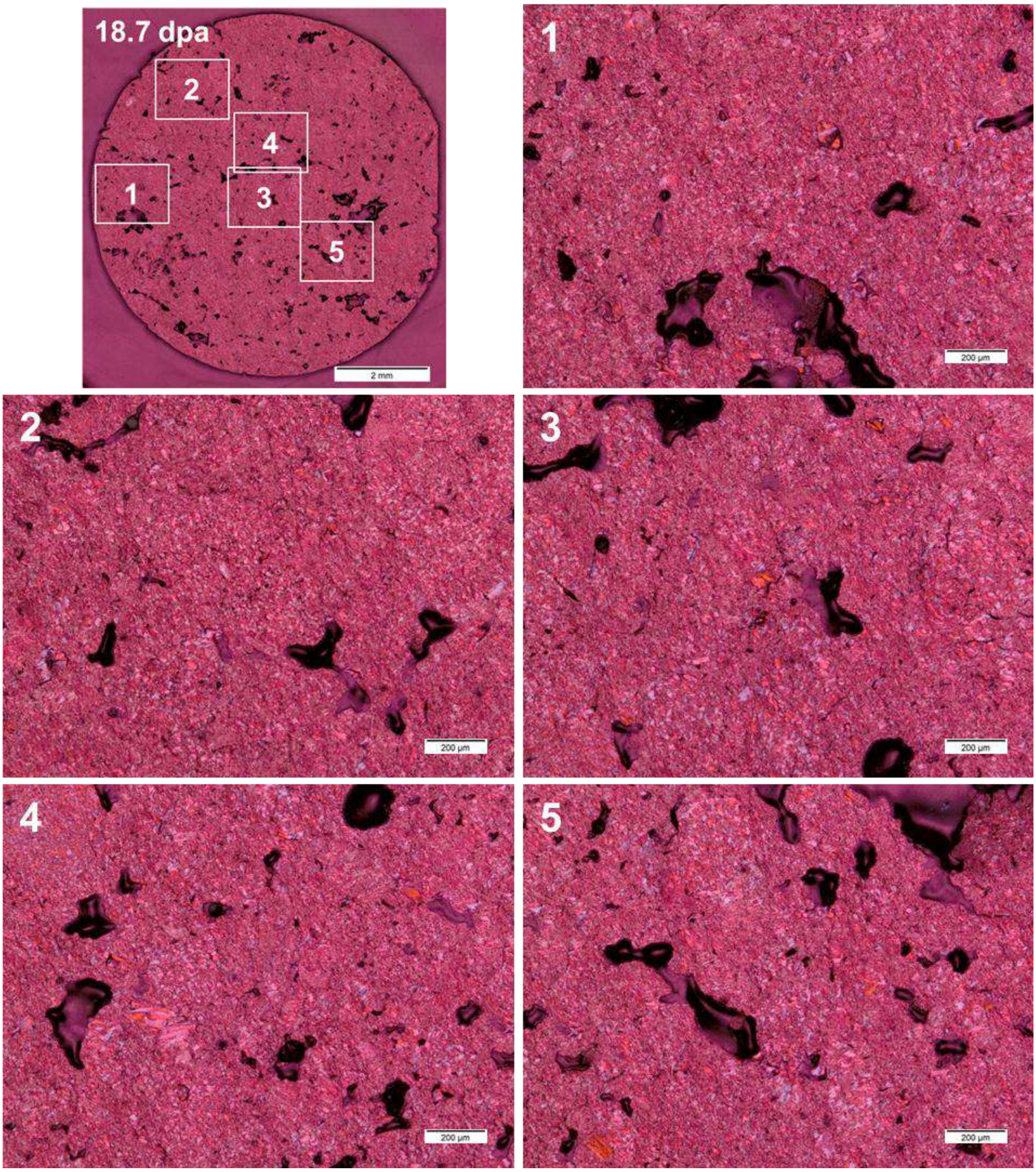

Figure 3-78 Polarisation microscopy images at 5x magnification of PPEA specimen U277 (18.7 dpa) and overview micrograph (top left) with indicated the locations of these micrographs on the sample

Figure 3-79 Bright field microscopy images of PPEA specimen U277 (18.7 dpa) at 10x to 100x magnification at detail location 3

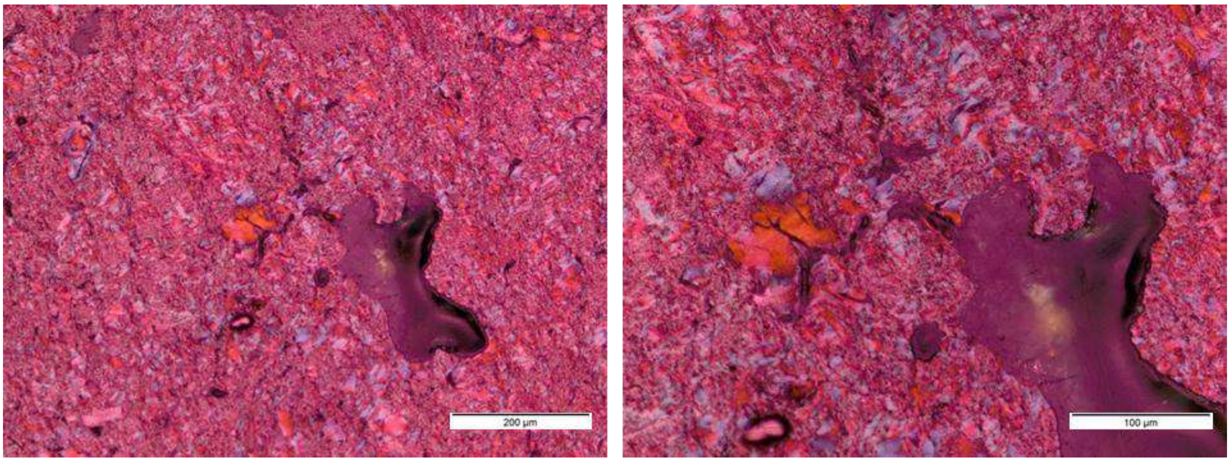

Figure 3-80 Polarisation microscopy images of PPEA specimen U277 (18.7 dpa) at 10x and 20x magnification at detail location 3

3.1.9 IG-110 detail micrographs

Figure 3-81 to Figure 3-88 show the detail micrographs of the irradiated IG-110 graphite specimens.

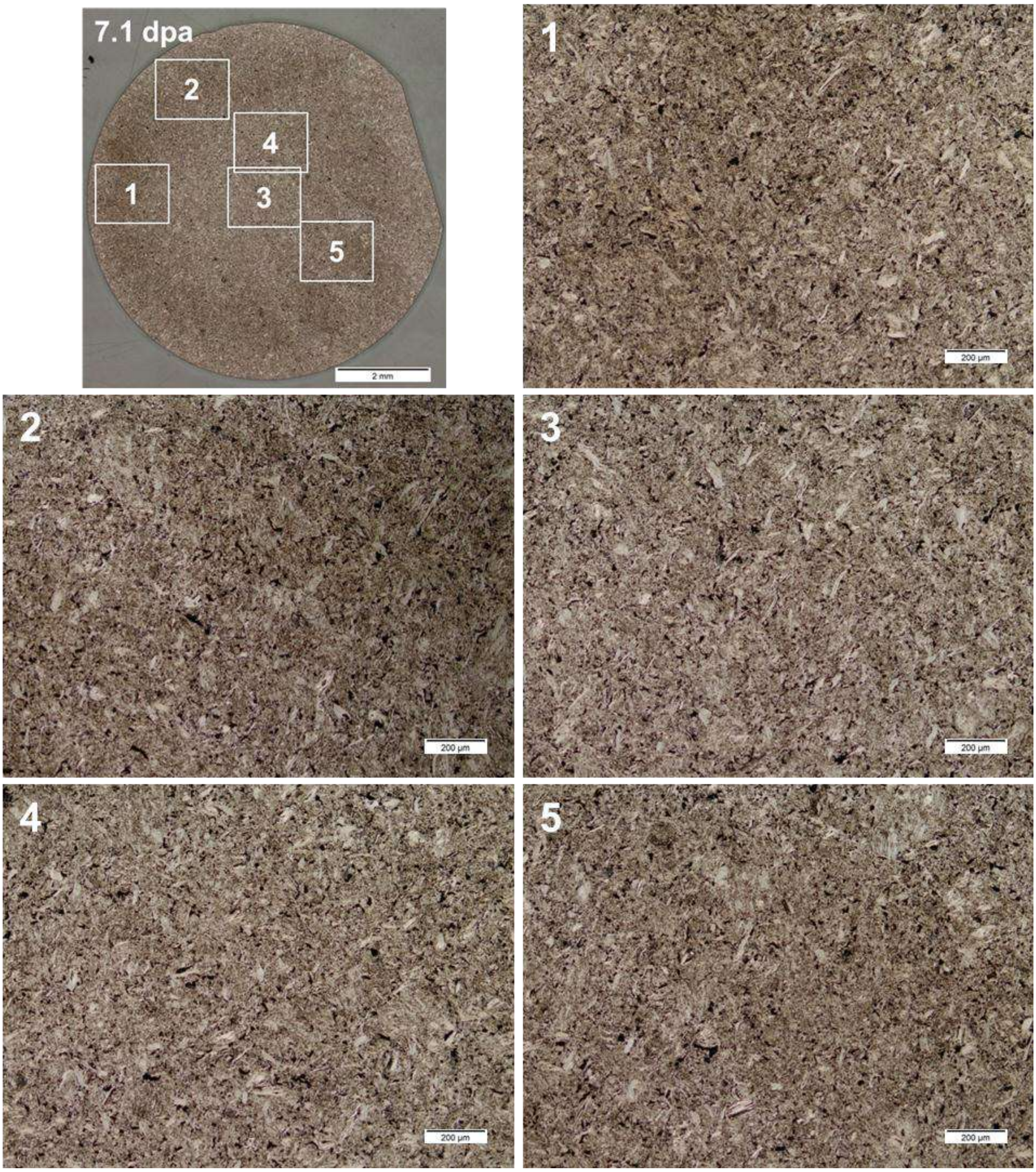

Figure 3-81 Bright field optical micrographs at 5x magnification of IG-110 specimen T024 (7.1 dpa) and overview micrograph (top left) with indicated the locations of these micrographs on the sample

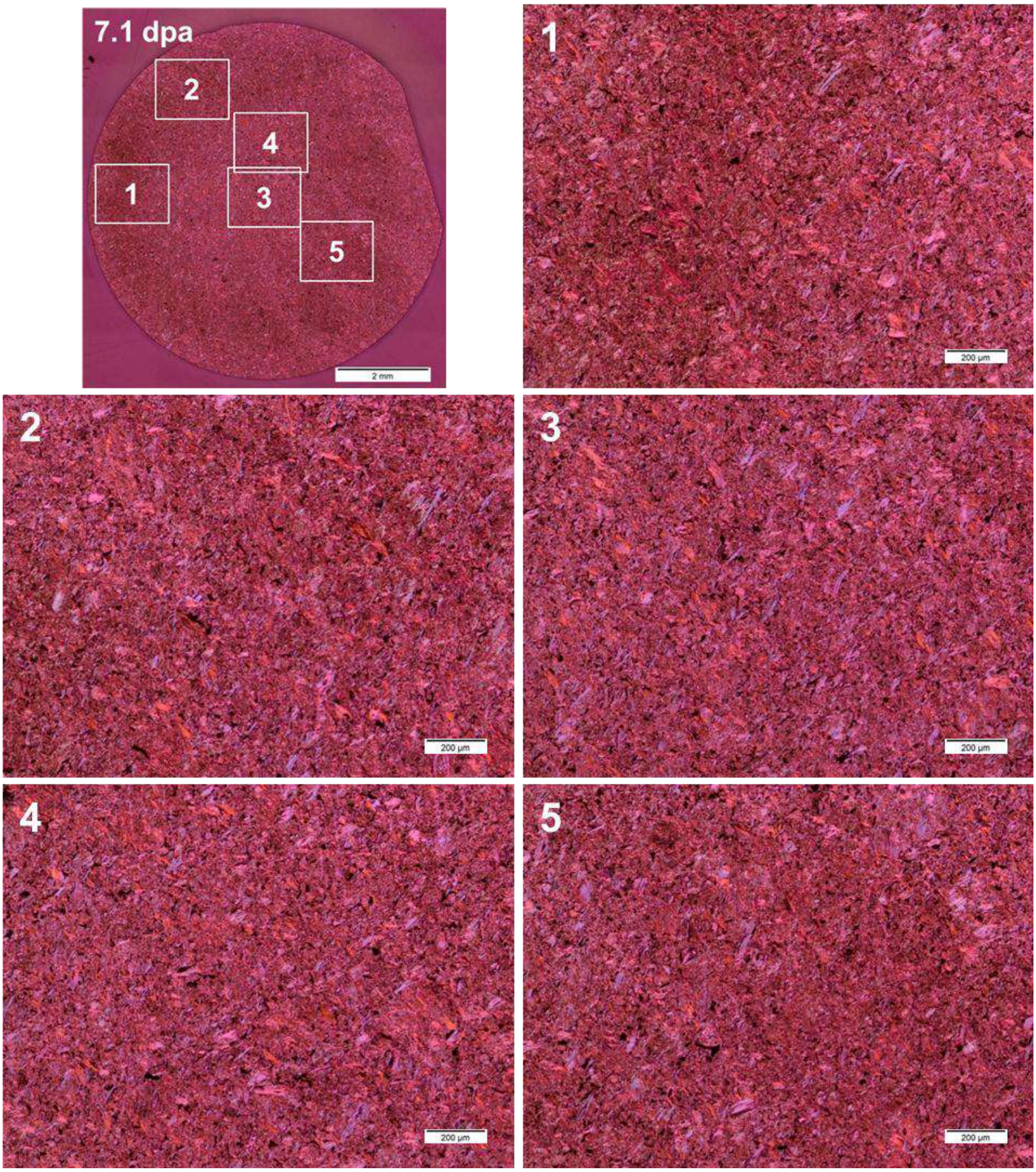

Figure 3-82 Polarisation microscopy images at 5x magnification of IG-110 specimen T024 (7.1 dpa) and overview micrograph (top left) with indicated the locations of these micrographs on the sample

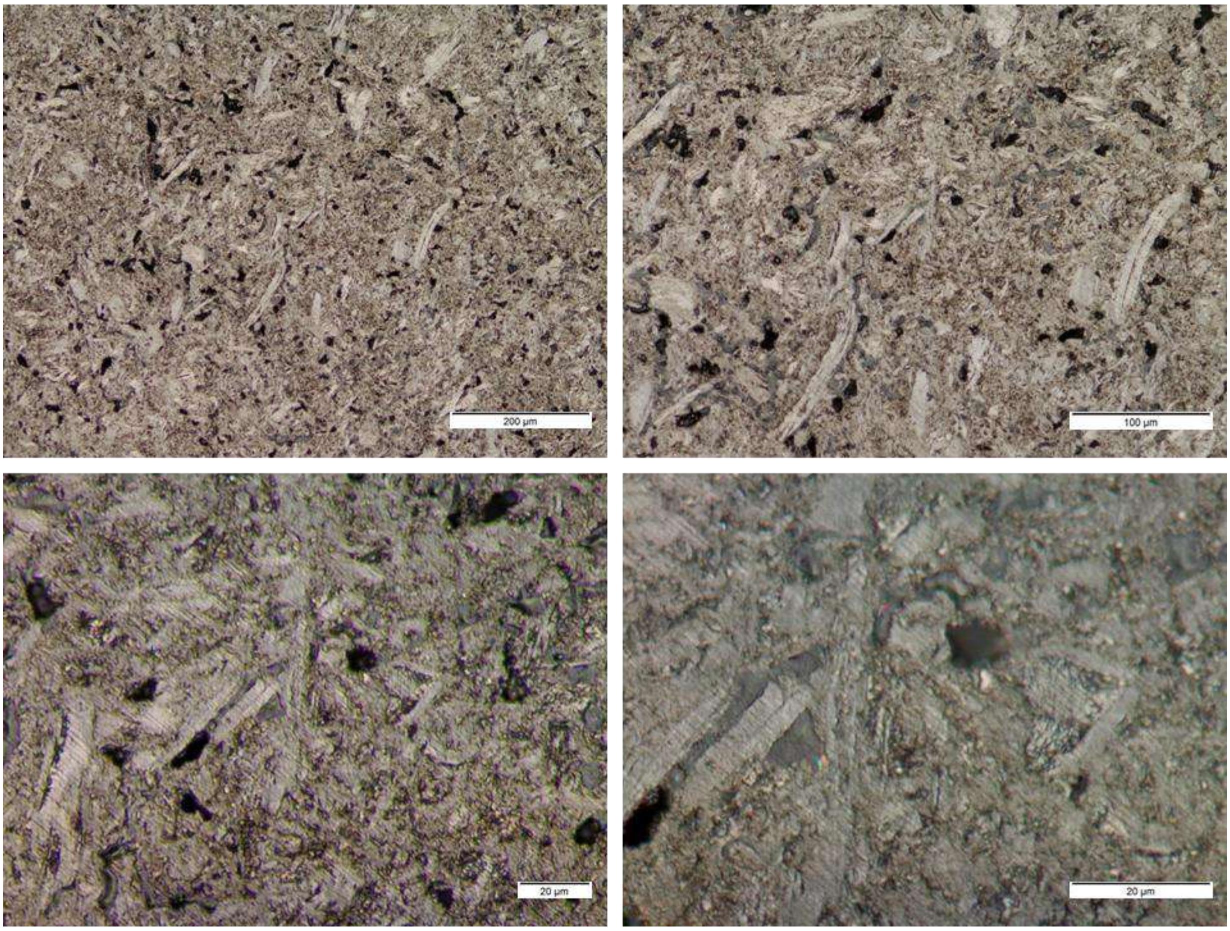

Figure 3-83 Bright field microscopy images of IG-110 specimen T024 (7.1 dpa) at 10x to 100x magnification at detail location 3

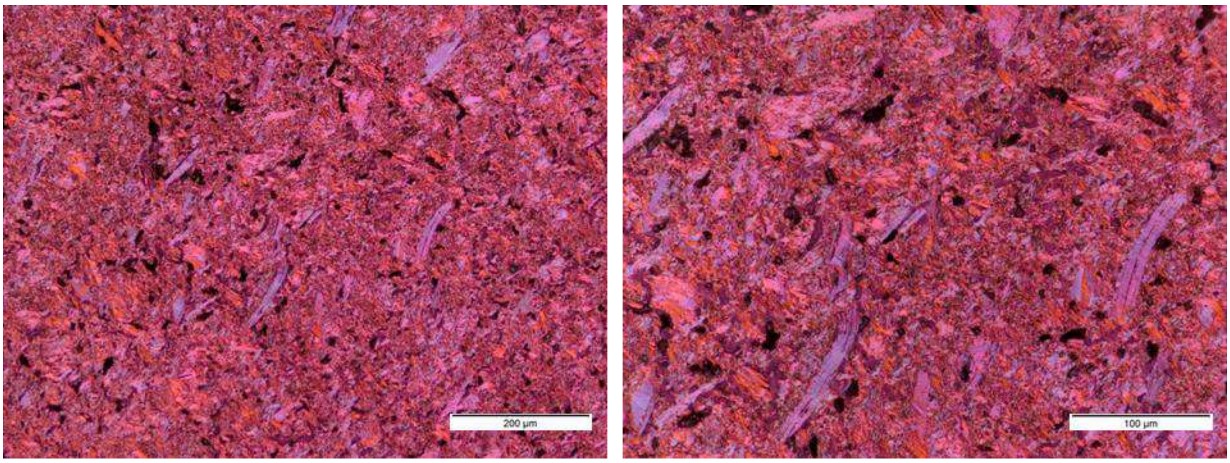

Figure 3-84 Polarisation microscopy images of IG-110 specimen T024 (7.1 dpa) at 10x and 20x magnification at detail location 3

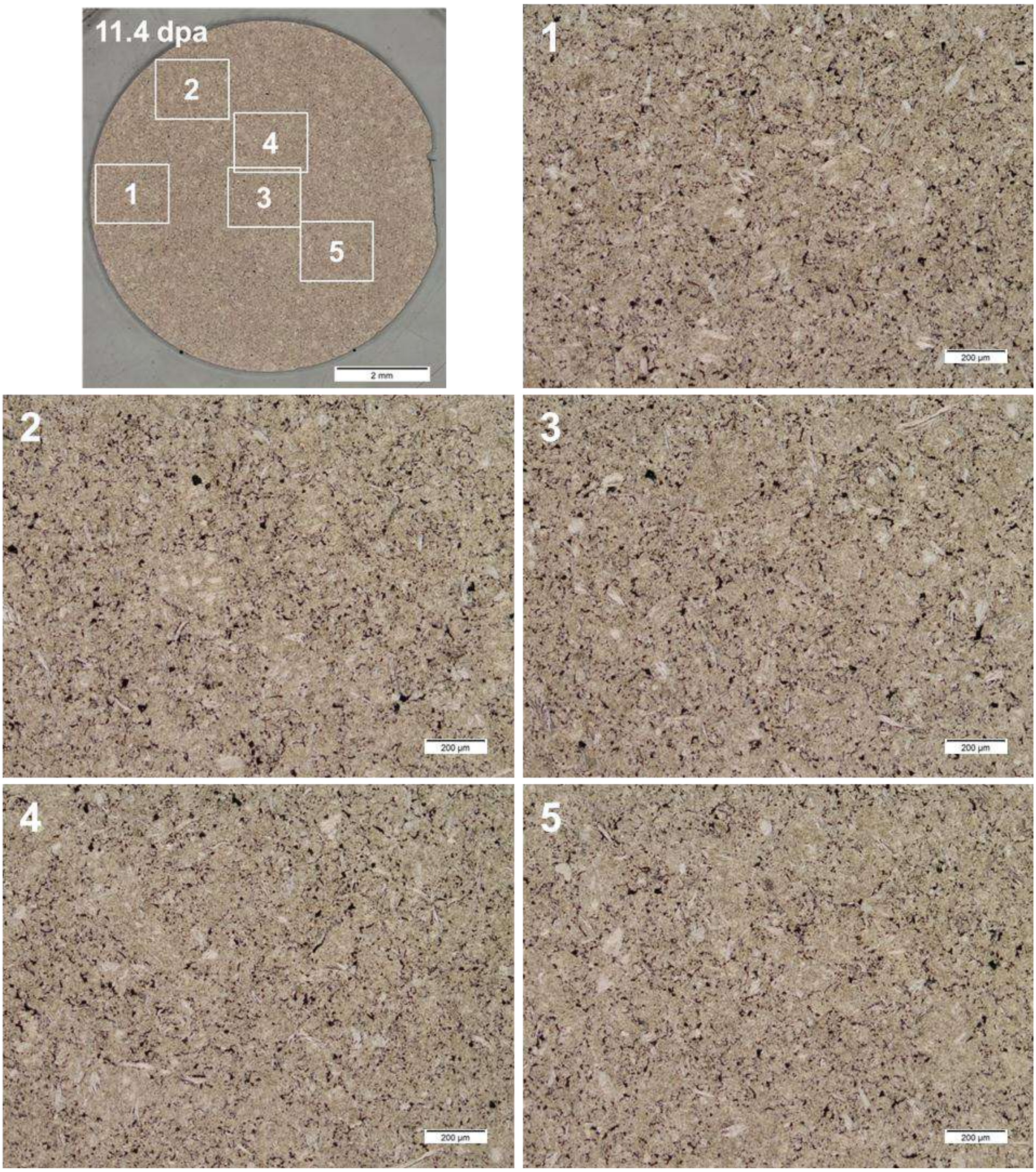

Figure 3-85 Bright field optical micrographs at 5x magnification of IG-110 specimen T040 (11.4 dpa) and overview micrograph (top left) with indicated the locations of these micrographs on the sample

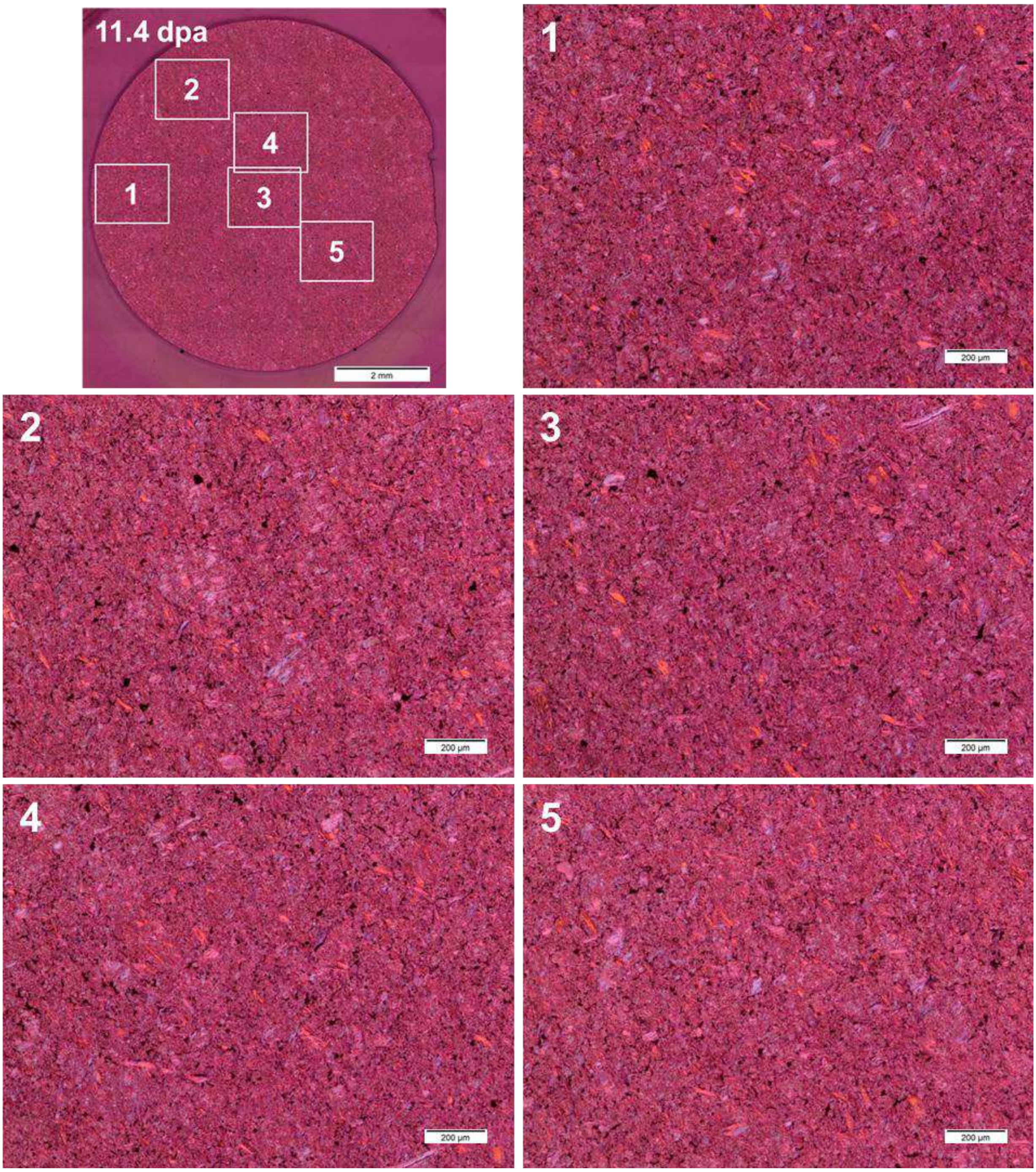

Figure 3-86 Polarisation microscopy images at 5x magnification of IG-110 specimen T040 (11.4 dpa) and overview micrograph (top left) with indicated the locations of these micrographs on the sample

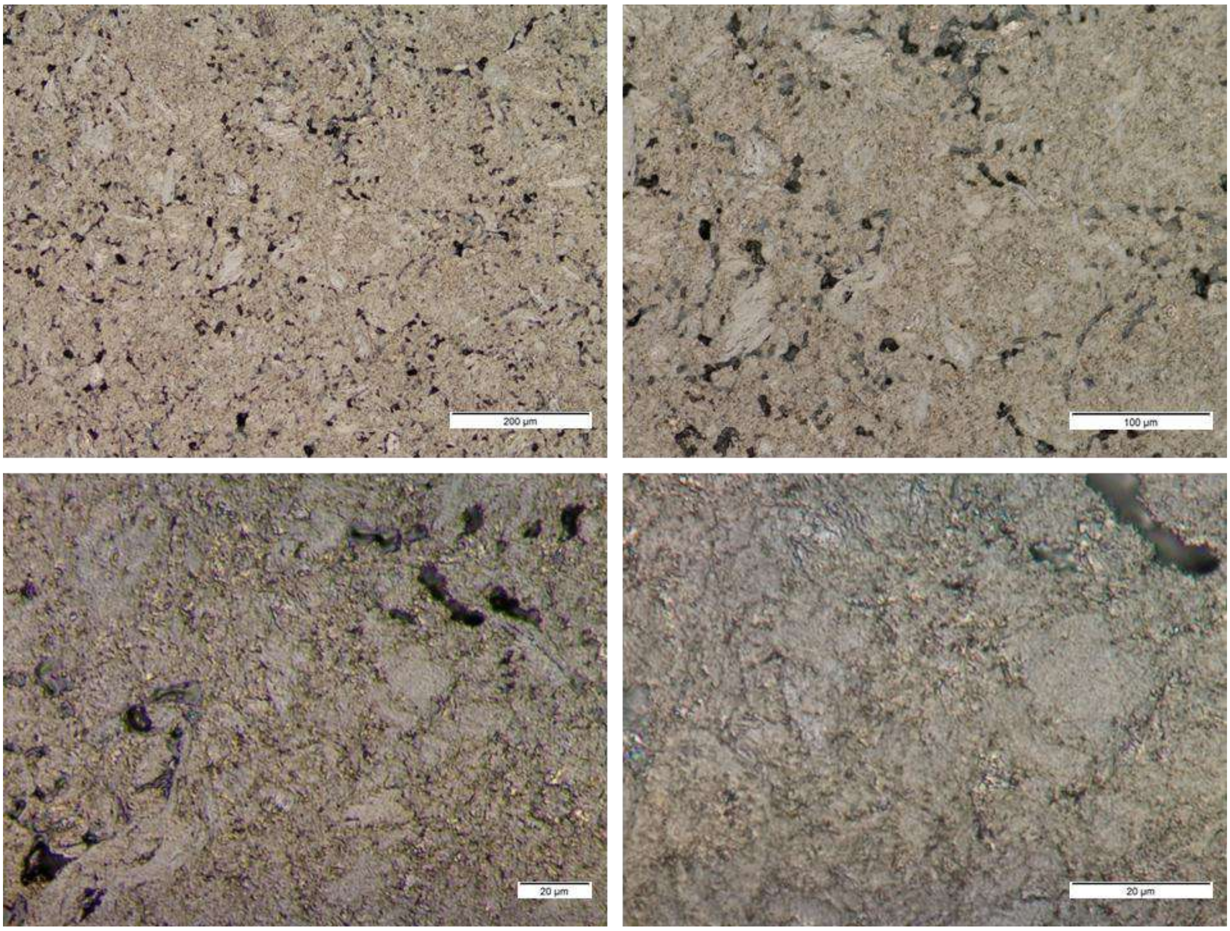

Figure 3-87 Bright field microscopy images of IG-110 specimen T040 (11.4 dpa) at 10x to 100x magnification at detail location 5

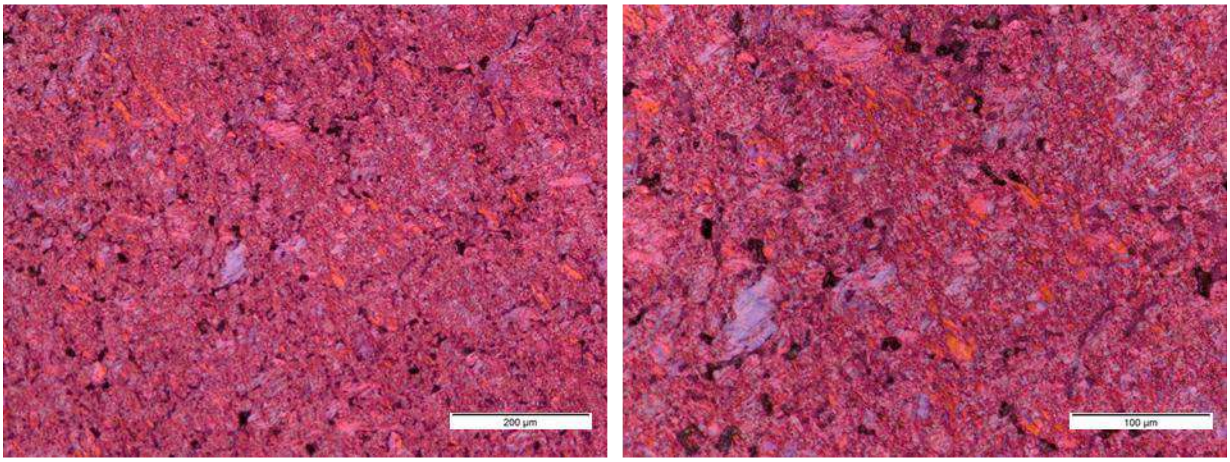

Figure 3-88 Polarisation microscopy images of IG-110 specimen T040 (11.4 dpa) at 10x and 20x magnification at detail location 5

3.2 Scanning Electron Microscopy

Nine of the irradiated samples from the INNOGRAPH-1A and -1B experiments that were prepared for optical microscopy were also used for scanning electron microscopy. In paragraphs 3.2.1 to 3.2.3, the SEM results these graphite specimens are presented. Images are taken at 3 kV and 20 kV, resulting in different appearances of the sample surface. At 3 kV, the impregnation resin is charged and lights up in the SEM images. At 20 kV, this charging seems to be reduced.

3.2.1 SGL graphites

NBG-10

Two irradiated NBG-10 samples were selected for SEM; S078 irradiated to 11.2 dpa, and S041 irradiated to 21.1 dpa. Both samples are "against grain" oriented samples.

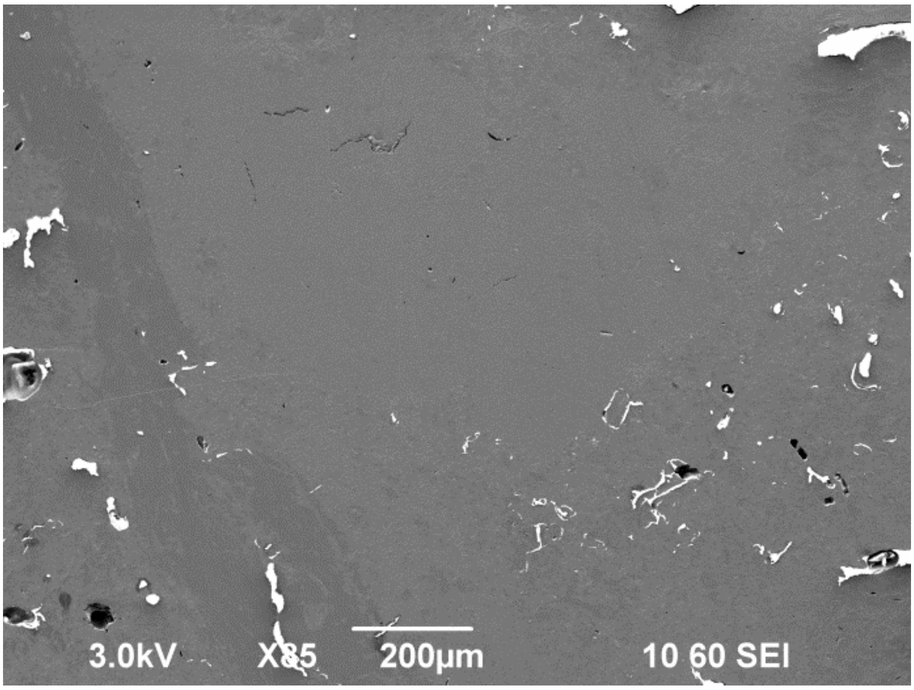

Figure 3-89 SEM image of irradiated NBG-10 sample S078 (11.2 dpa) at 85x magnification and 3 kV

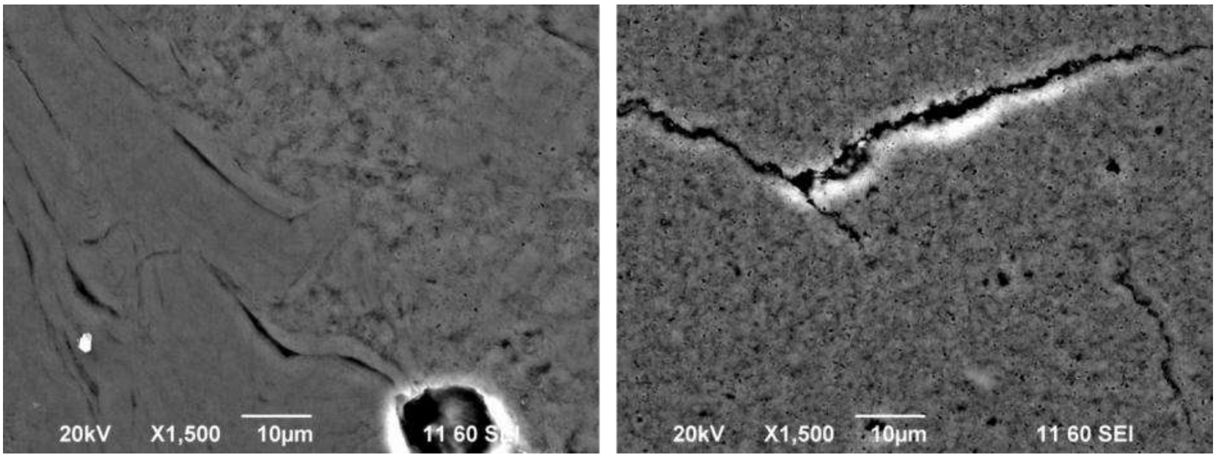

Figure 3-90 SEM images of irradiated NBG-10 sample S078 (11.2 dpa) at 1500x magnification and 20 kV

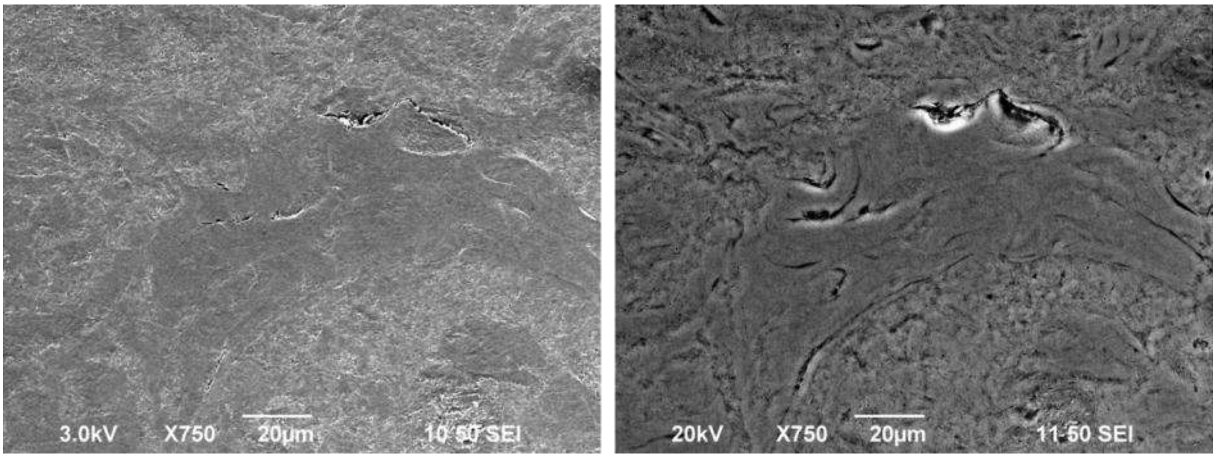

Figure 3-91 SEM image of irradiated NBG-10 sample S078 (11.2 dpa) at 750x magnification and 3 kV (left) and 20 kV (right)

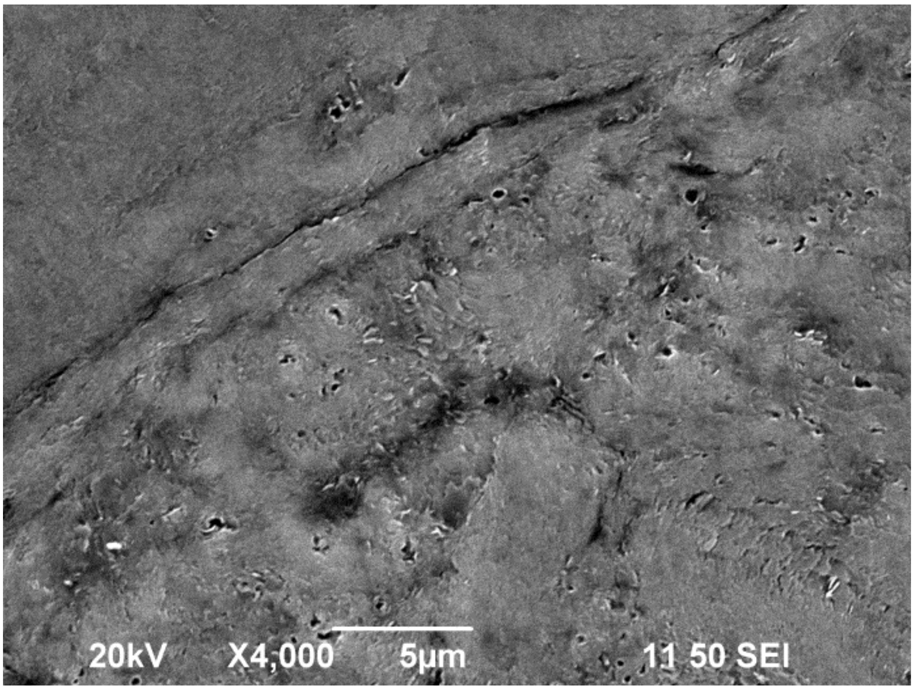

Figure 3-92 SEM image of irradiated NBG-10 sample S078 (11.2 dpa) at 4000x magnification and 20 kV

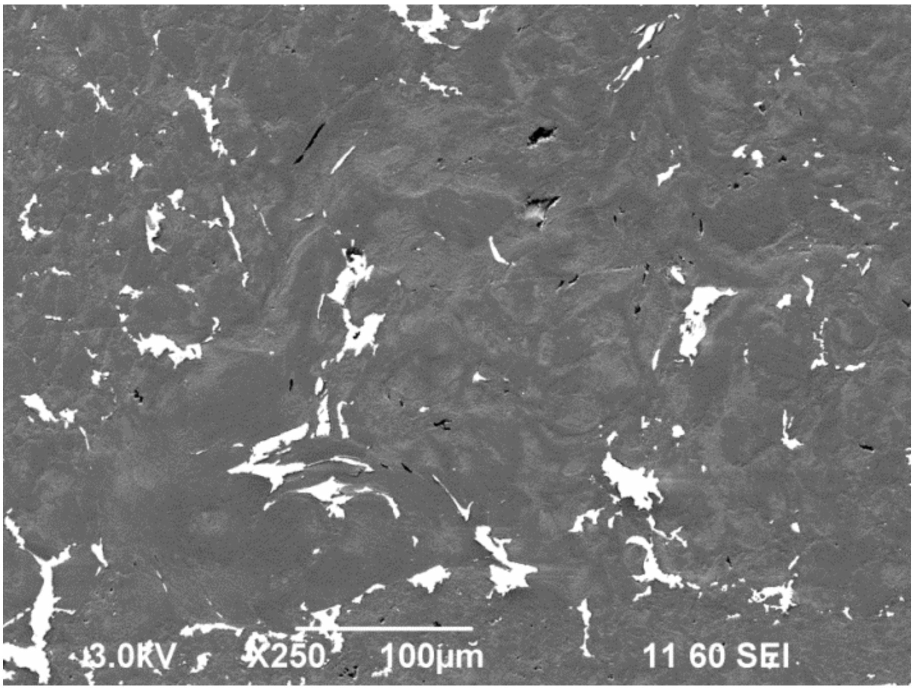

Figure 3-93 SEM image of irradiated NBG-10 sample S041 (21.1 dpa) at 250x magnification and 3 kV

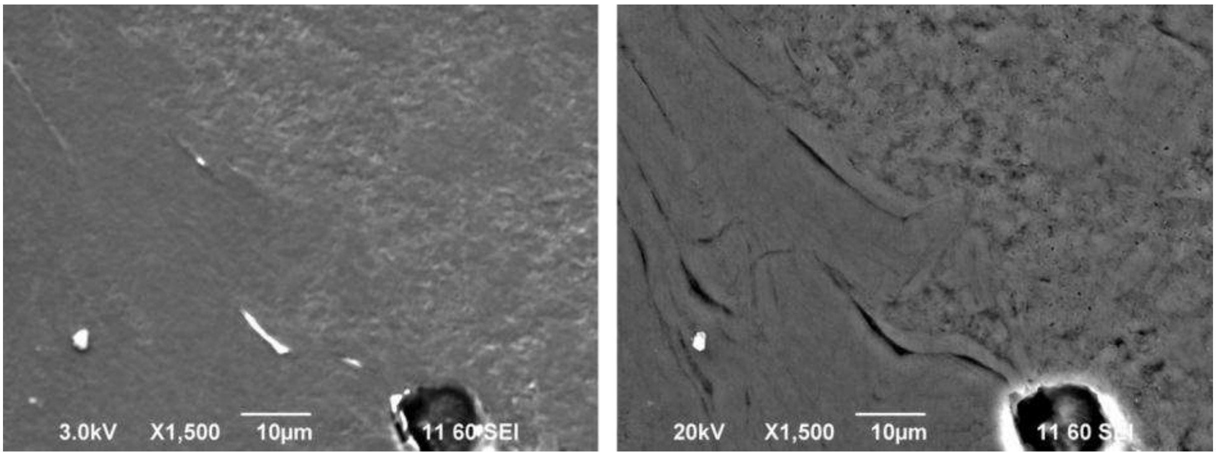

Figure 3-94 SEM image of irradiated NBG-10 sample S041 (21.1 dpa) at 2000x magnification and 3 kV (left) and 20 kV (right)

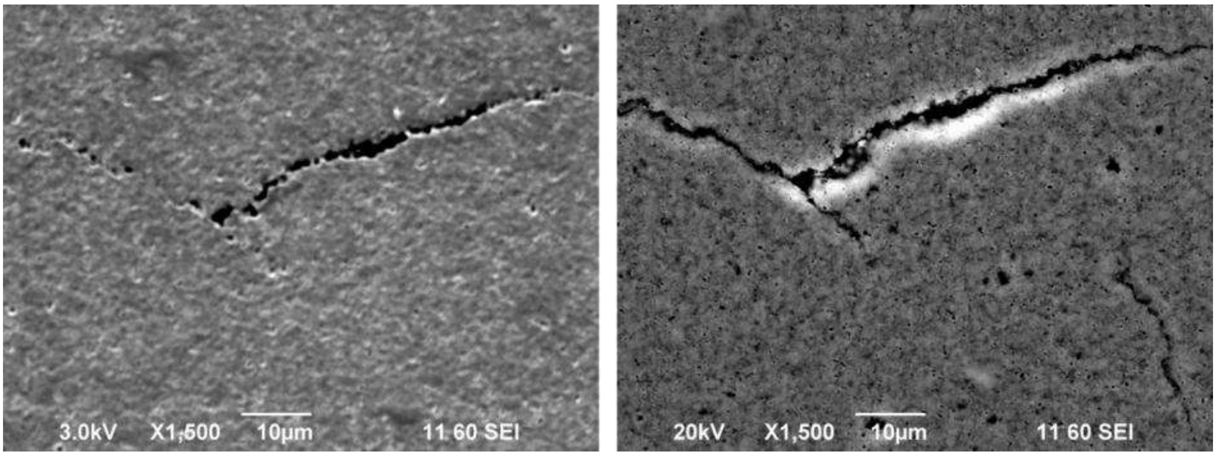

Figure 3-95 SEM image of irradiated NBG-10 sample S041 (21.1 dpa) at 500x magnification and 3 kV (left) and 20 kV (right)

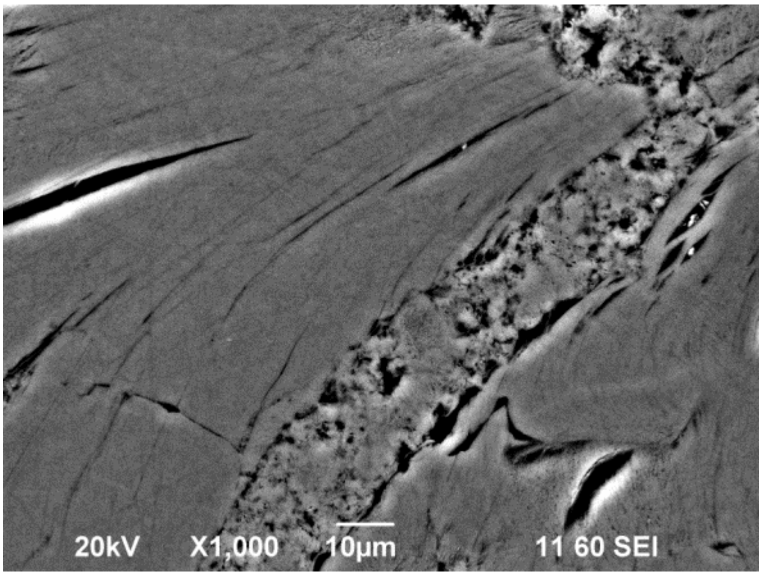

Figure 3-96 SEM image of irradiated NBG-10 sample S041 (21.1 dpa) at 1000x magnification and 20 kV

NBG-17

One irradiated NBG-17 sample was selected for SEM measurements; S579, irradiated to 13.2 dpa.

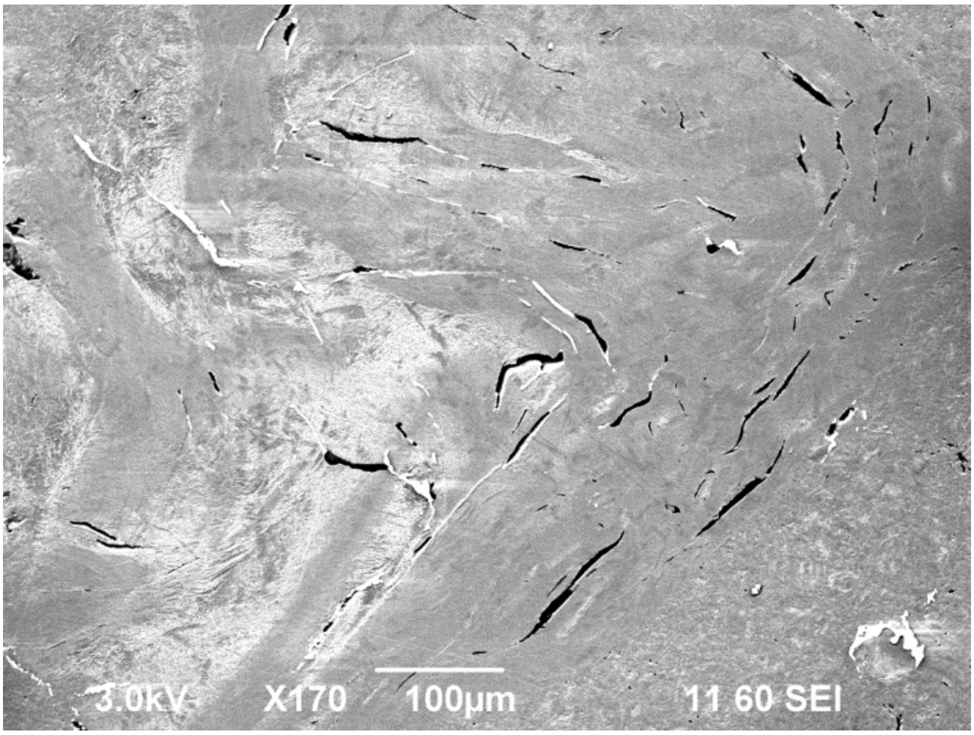

Figure 3-97 SEM image of irradiated NBG-17 sample S579 (13.2 dpa) at 170x magnification and 3 kV

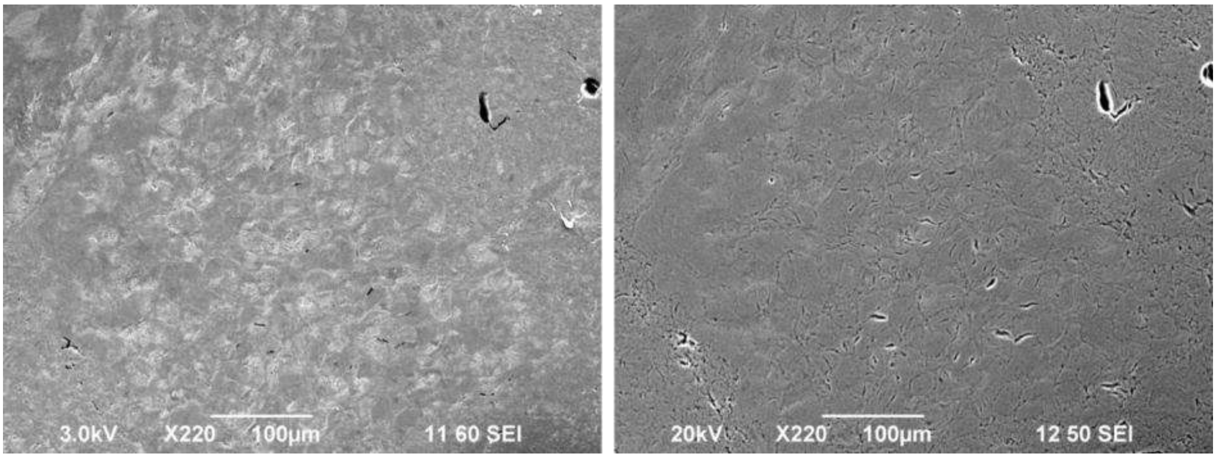

Figure 3-98 SEM image of irradiated NBG-17 sample S579 (13.2 dpa) at 220x magnification and 3 kV (left) and 20 kV (right)

NBG-18

One irradiated NBG-18 sample was selected for SEM measurements; S468, irradiated to 13.1 dpa.

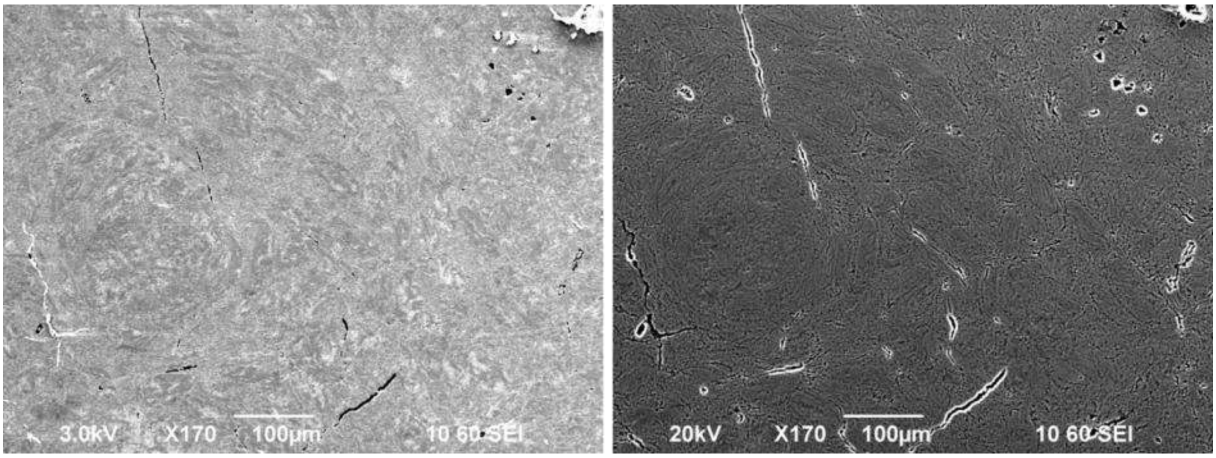

Figure 3-99 SEM image of irradiated NBG-18 sample S468 (13.1 dpa) at 170x magnification and 3 kV (left) and 20 kV (right)

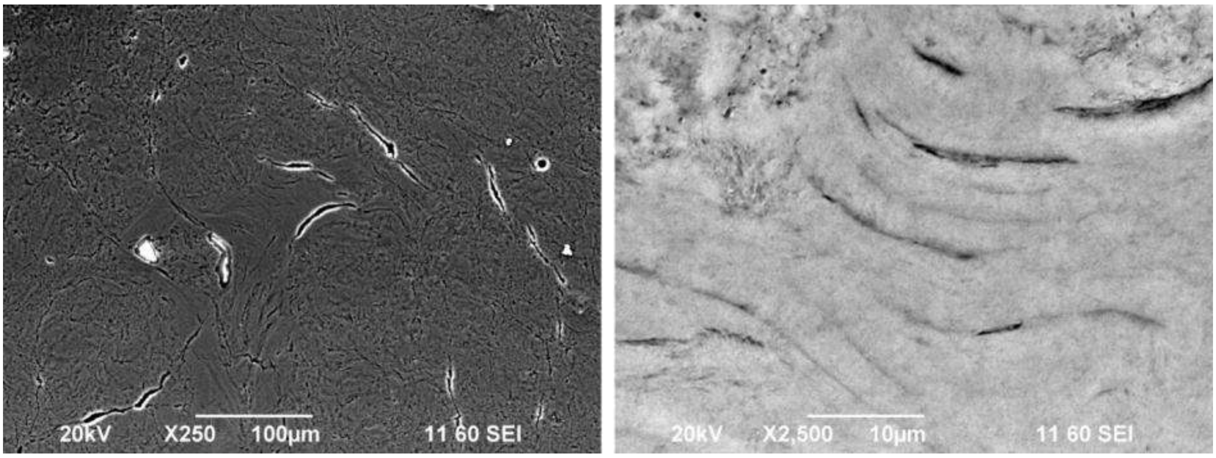

Figure 3-100 SEM image of irradiated NBG-18 sample S468 (13.1 dpa) at 20 kV and 250x magnification (left), and a detail at the same location at 2500x magnification (right)

3.2.2 GrafTech graphites

PCEA

One irradiated PCEA sample was selected for SEM; U021, irradiated to 17 dpa.

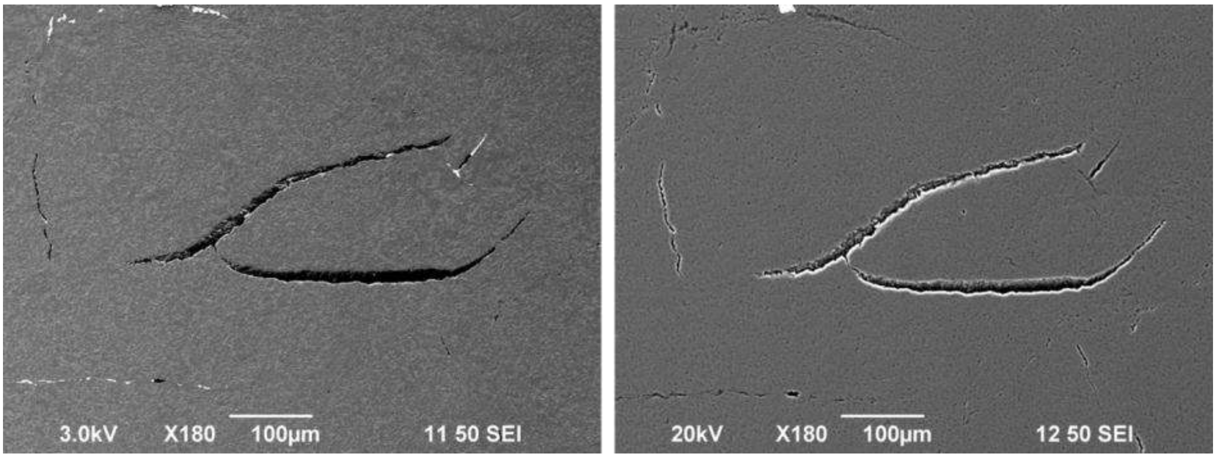

Figure 3-101 SEM image of irradiated PCEA sample U021 (17 dpa) at 180x magnification and 3 kV (left) and 20 kV (right)

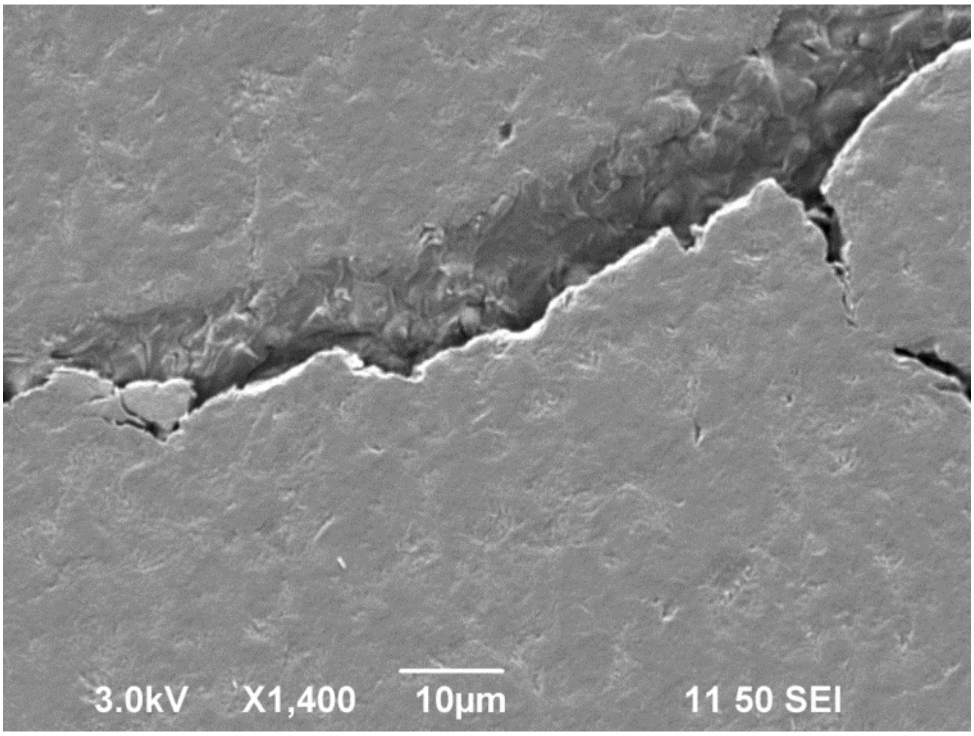

Figure 3-102 SEM image of irradiated PCEA sample U021 (17 dpa) at 1400x magnification and 3 kV

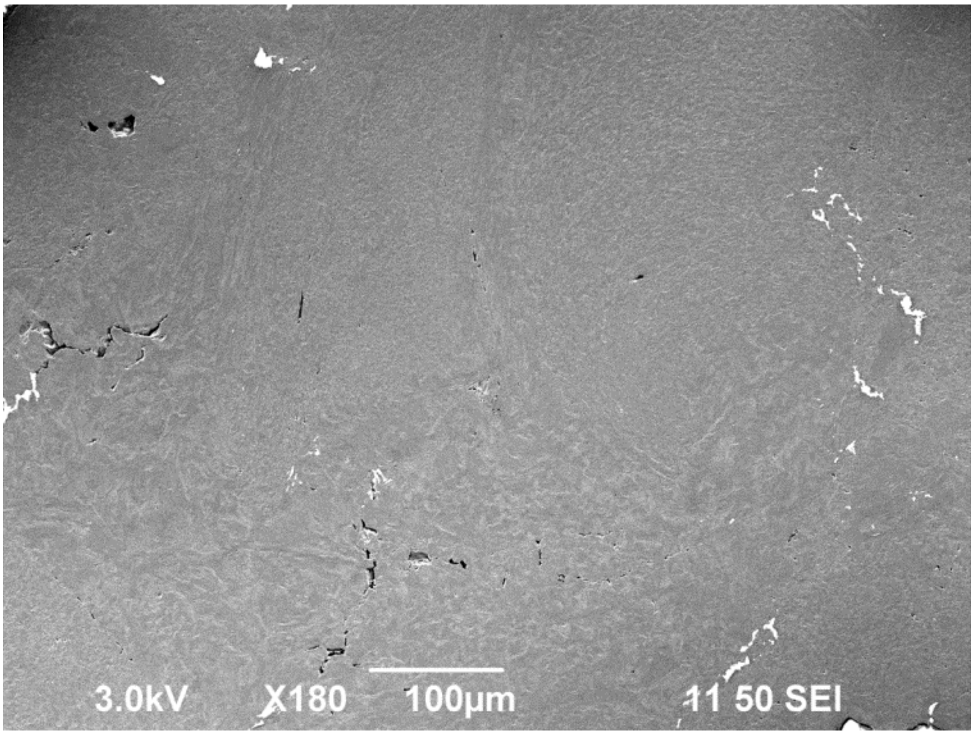

Figure 3-103 SEM image of irradiated PCEA sample U021 (17 dpa) at 120x magnification and 3 kV

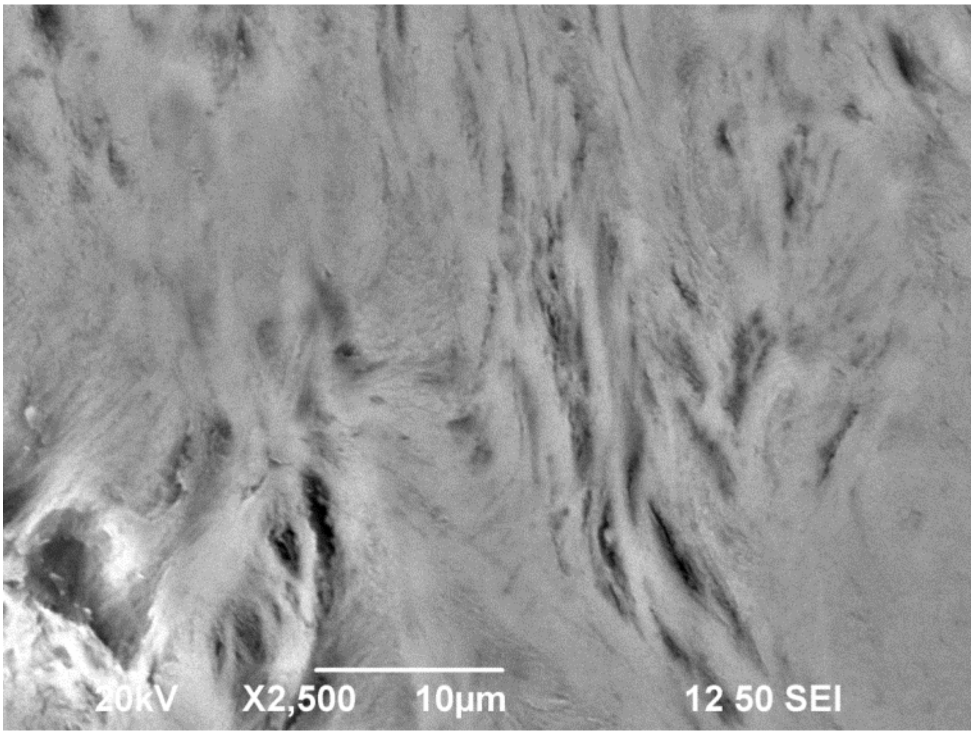

Figure 3-104 SEM image of irradiated PCEA sample U021 (17 dpa) at 2500x magnification and 20 kV

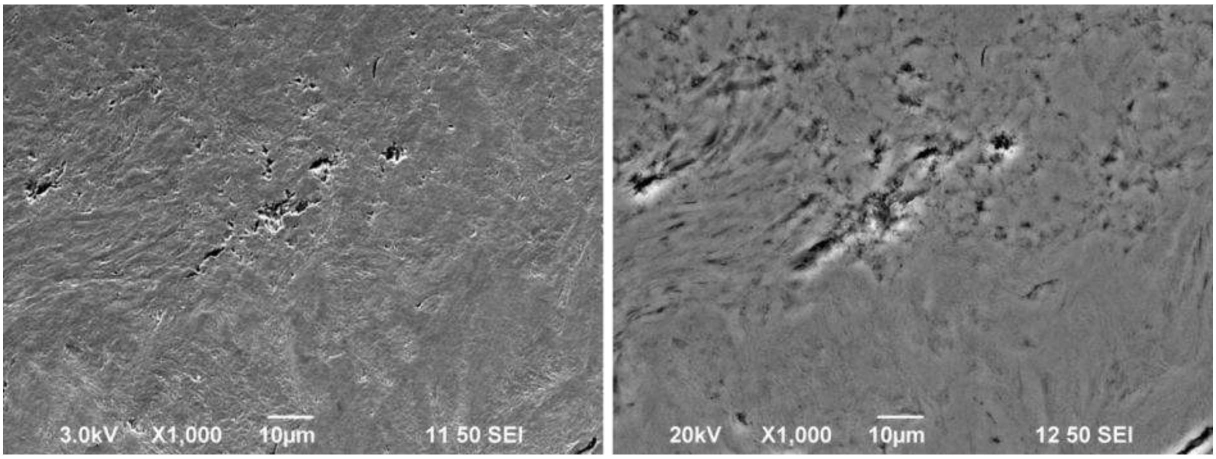

Figure 3-105 SEM image of irradiated PCEA sample U021 (17 dpa) at 1000x magnification and 3 kV (left) and 20 kV (right)

PCIB

Out of the available irradiated PCIB samples, sample U113 was selected for SEM. U113 was irradiated to 9.1 dpa. Figure 3-106 to Figure 3-108 show the SEM images of sample U113.

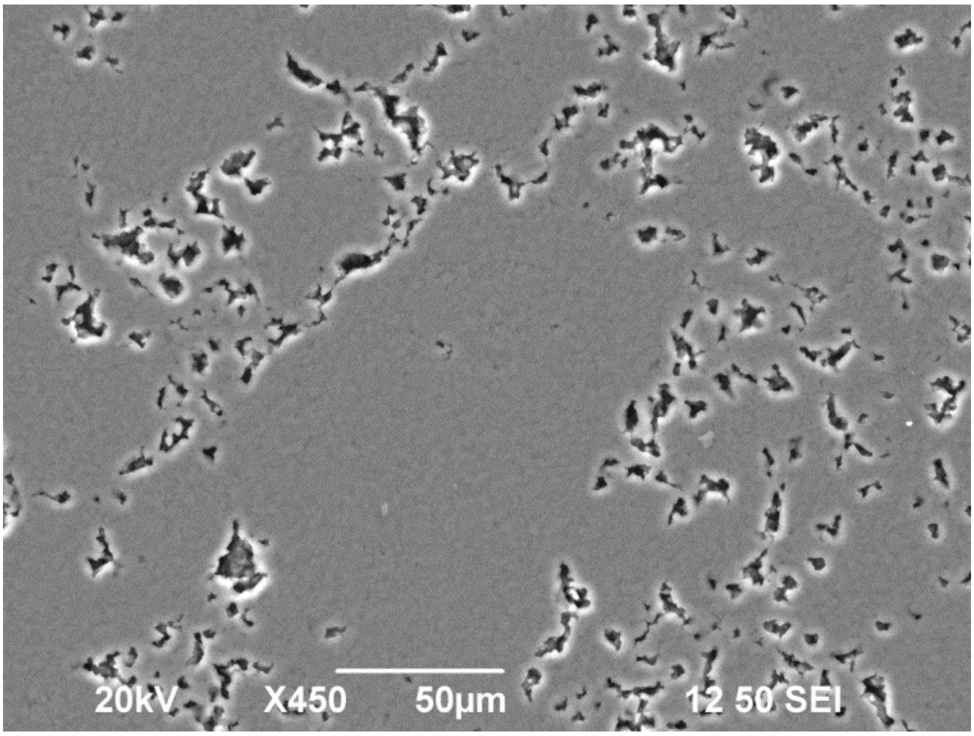

Figure 3-106 SEM image of irradiated PCIB sample U113 (9.1 dpa) at 20 kV and 450x magnification

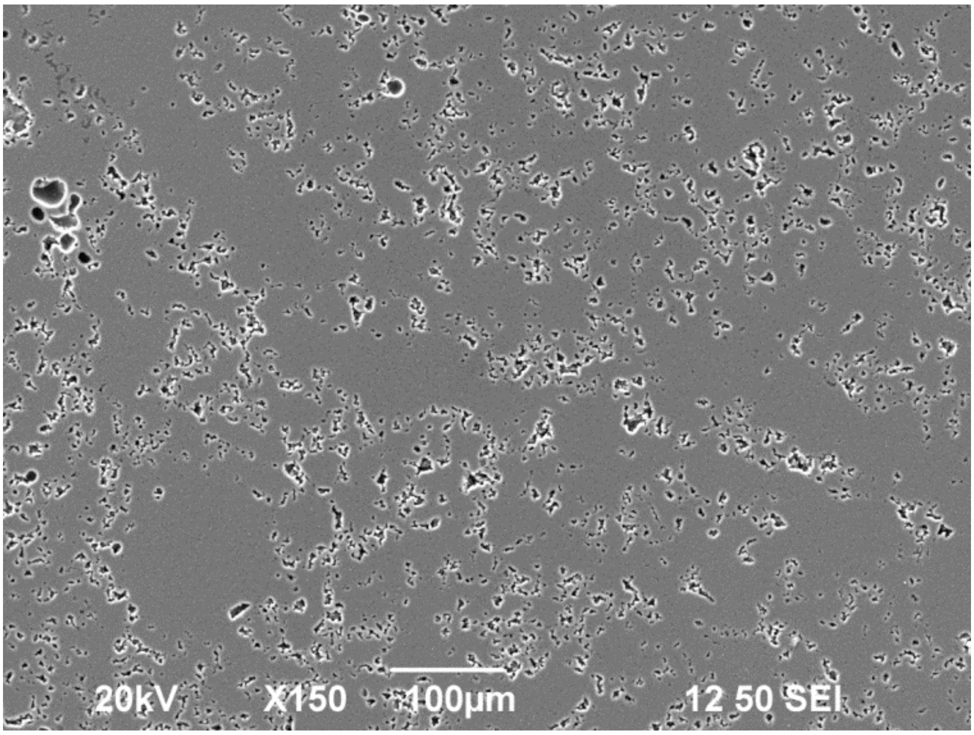

Figure 3-107 SEM image of irradiated PCIB sample U113 (9.1 dpa) at 20 kV and 150x magnification

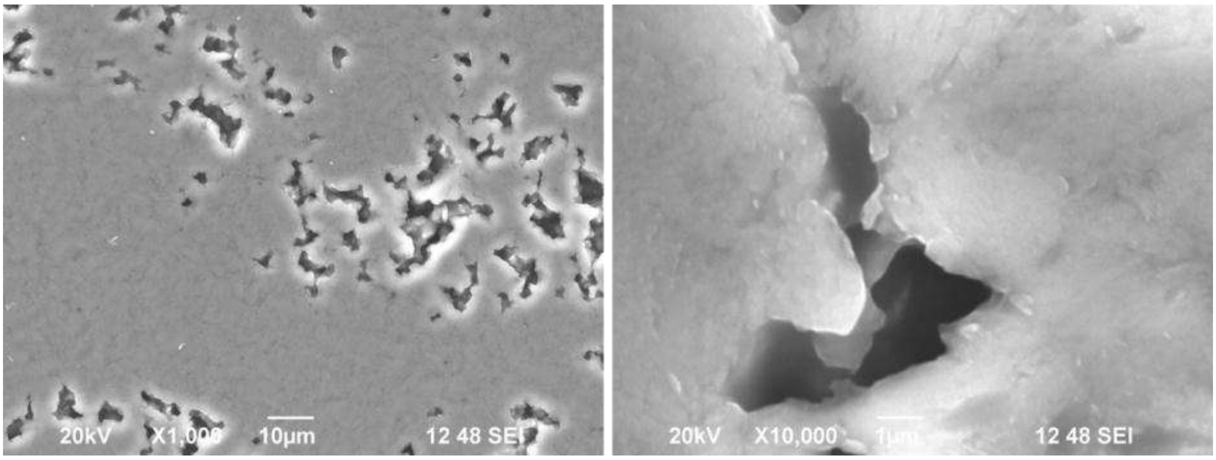

Figure 3-108 SEM image of irradiated PCIB sample U113 (9.1 dpa) at 20 kV, and 1000x and 10,000x magnification

PPEA

Two irradiated PPEA samples were selected for SEM; U329 irradiated to 12.2 dpa, and U277 irradiated to 18.7 dpa. Both samples are “with grain” oriented samples. Figure 3-109 to Figure 3-111 show the images of sample U329, Figure 3-112 and Figure 3-113 those of sample U277.

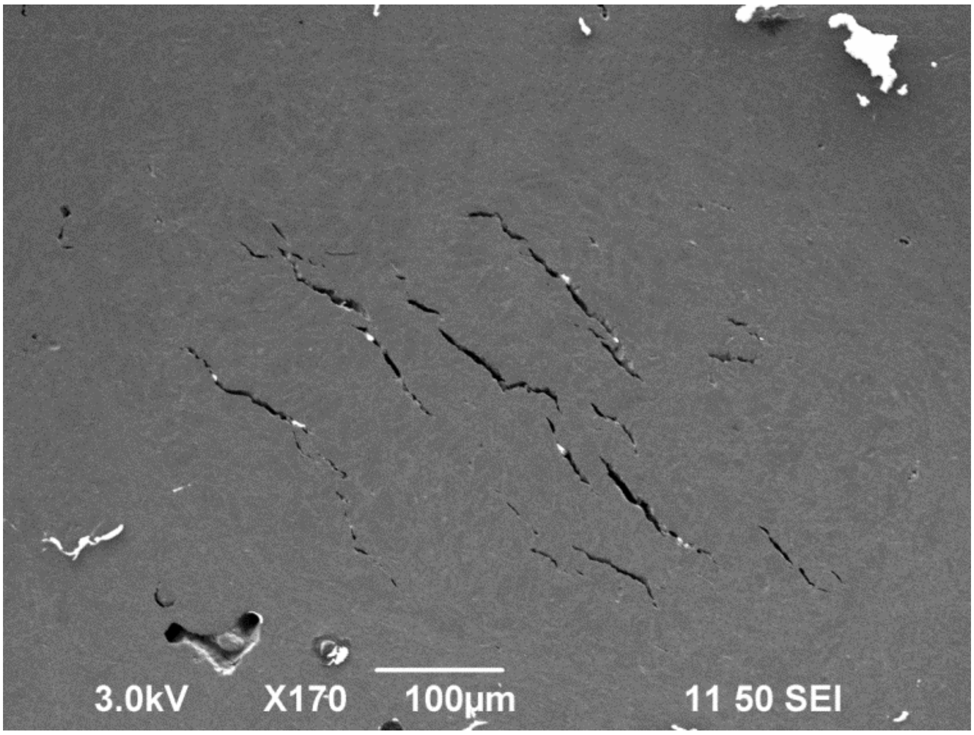

Figure 3-109 SEM image of irradiated PPEA sample U329 (12.2 dpa) at 3 kV and 170x magnification

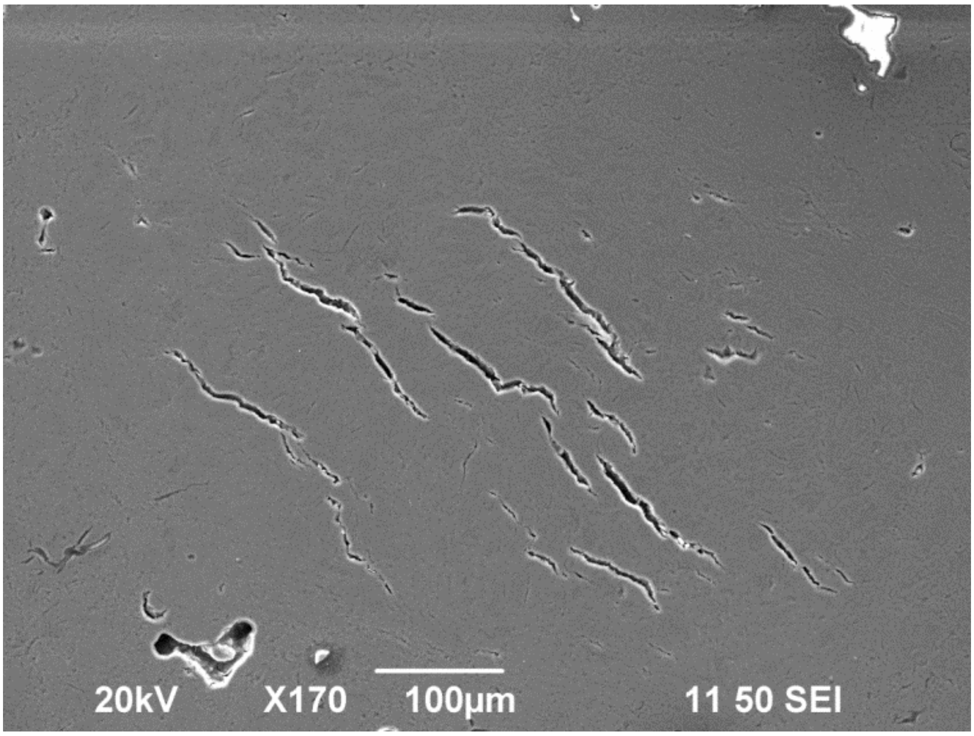

Figure 3-110 SEM image of irradiated PPEA sample U329 (12.2 dpa) at 20 kV and 170x magnification

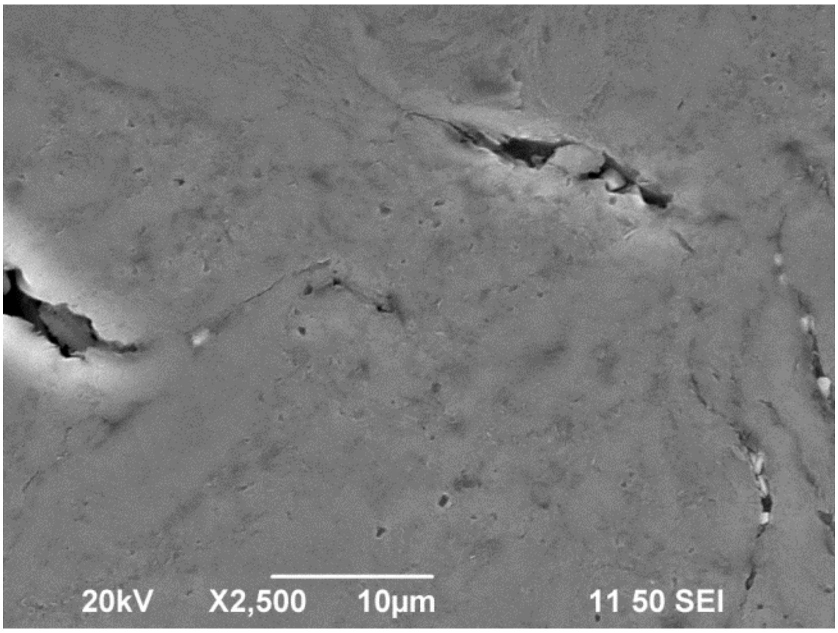

Figure 3-111 SEM image of irradiated PPEA sample U329 (12.2 dpa) at 20 kV and 2500x magnification

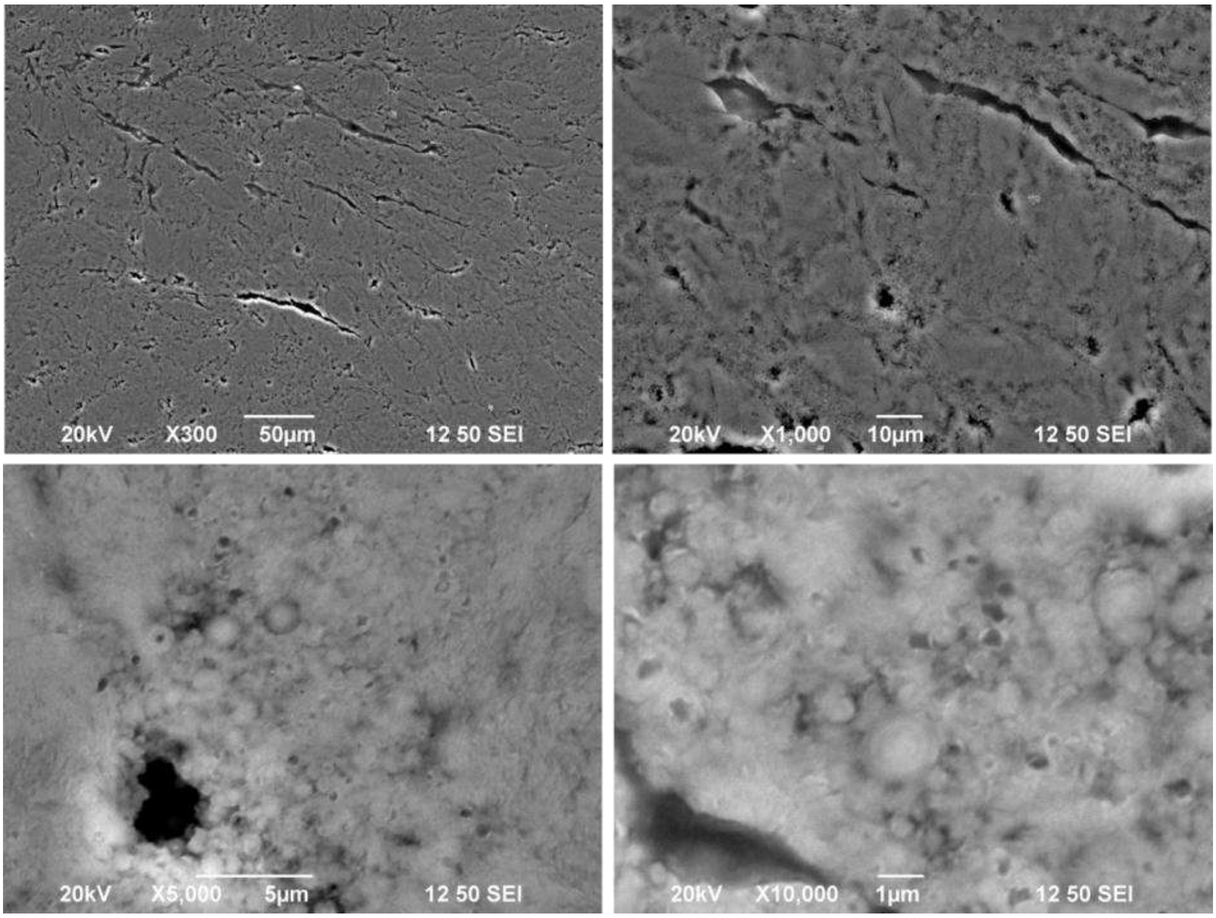

Figure 3-112 SEM image of irradiated PPEA sample U277 (18.7 dpa) at 20 kV and 300x, 1000x, 5000x and 10,000x magnification

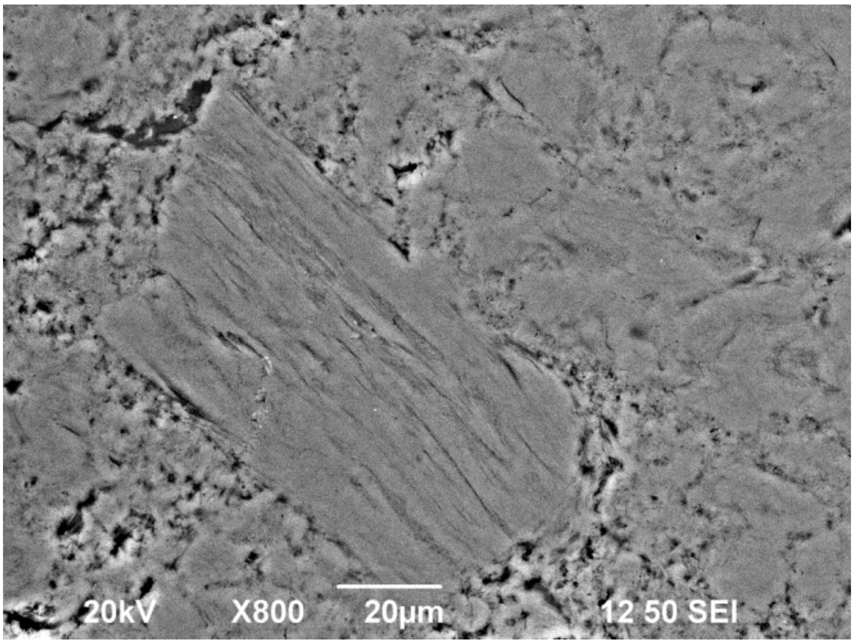

Figure 3-113 SEM image of irradiated PPEA sample U277 (18.7 dpa) at 20 kV and 800x magnification

3.2.3 IG-110

One irradiated IG-110 sample was selected for SEM; T040, irradiated to 11.4 dpa.

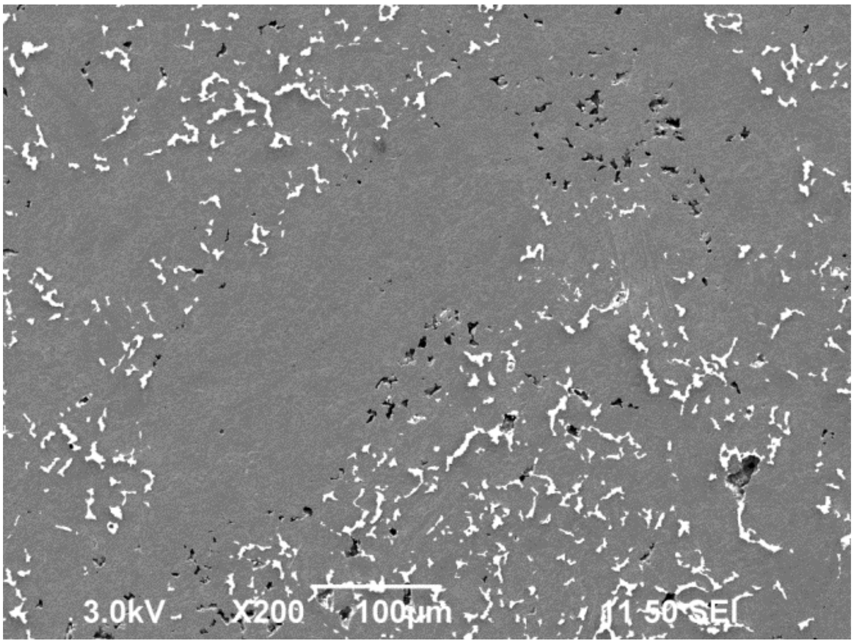

Figure 3-114 to Figure 3-116 show SEM images of T040 at 200x, 500x, and 1000x at different locations on the sample.

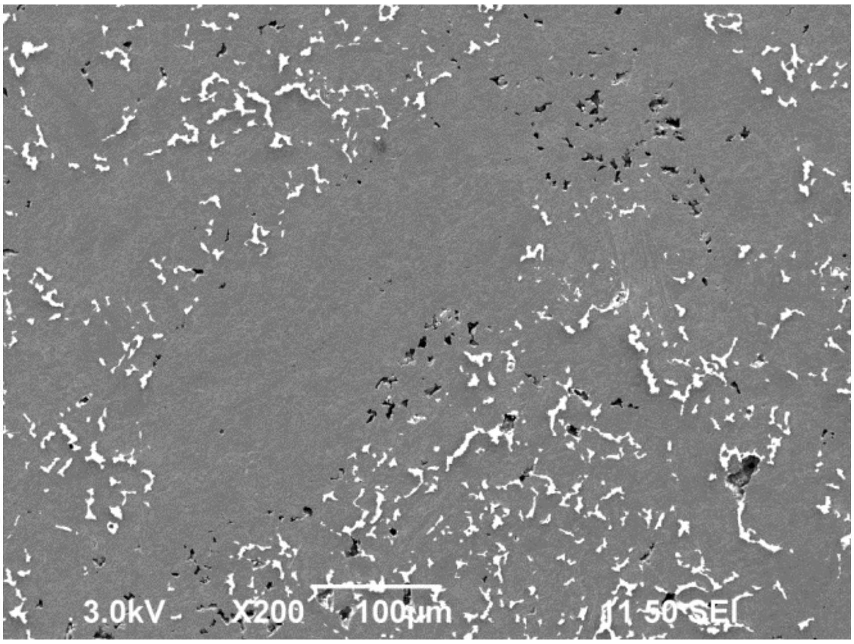

Figure 3-114 SEM image of irradiated IG-110 sample T040 (11.4 dpa) at 3 kV and 200x magnification

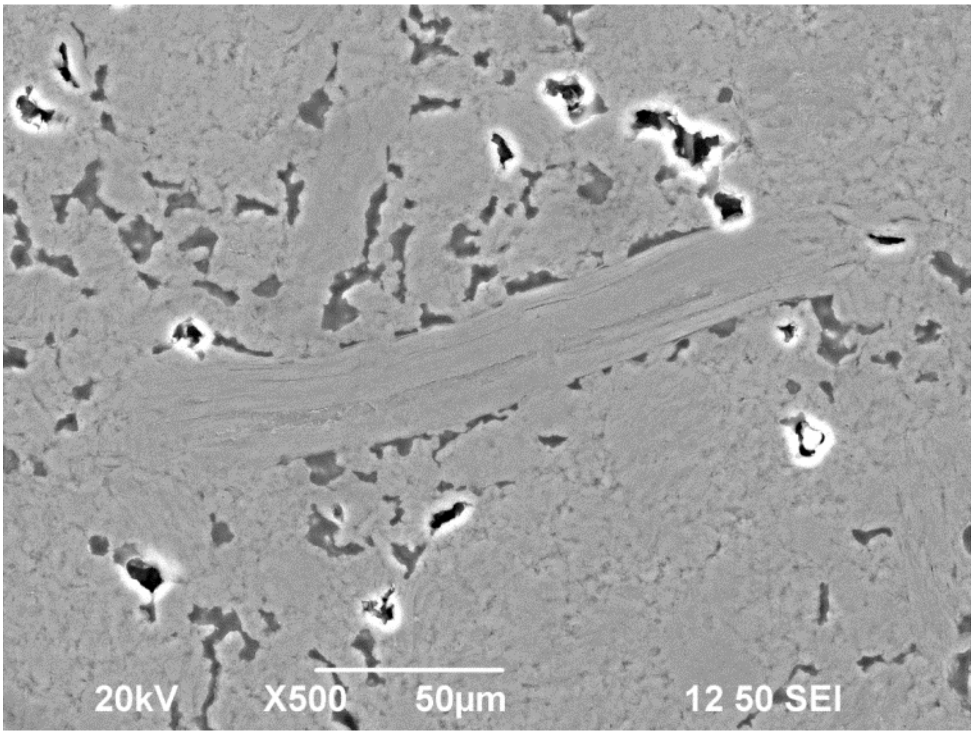

Figure 3-115 SEM image of irradiated IG-110 sample T040 (11.4 dpa) at 20 kV and 500x magnification

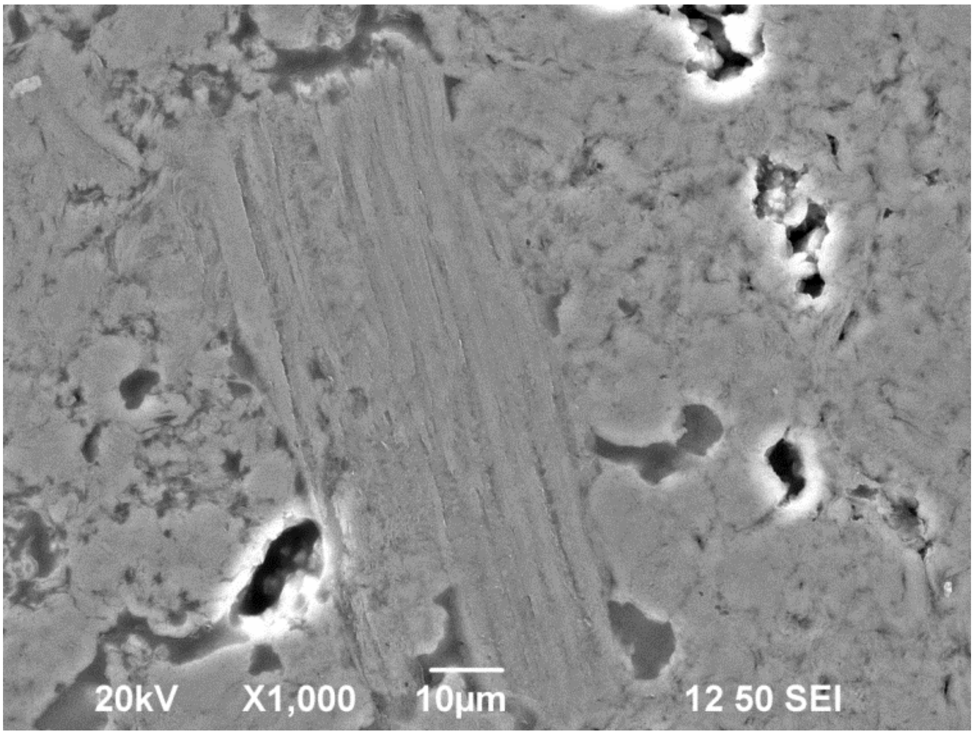

Figure 3-116 SEM image of irradiated IG-110 sample T040 (11.4 dpa) at 20 kV and 1000x magnification.

4 Conclusions

Twenty irradiated INNOGRAPH graphite samples were prepared for optical microscopy. On these samples optical microscopy was successfully performed. On nine of these prepared samples, scanning electron microscopy was successfully performed.

References

[1] F. Schmalz *et al.*, Preliminary irradiation testing of selected graphite grades for HTR, *Final report on HTR-M1 WP3*, 20787/05.71179/P, 19 December 2005

[2] J.A. Vreeling *et al.*, Designing loading and assembling an irradiation experiment with radioactive samples, *DLM 3.1: Progress on continuation of 750°C graphite irradiation test*, 21457/06.77295/P, 26 October 2006

[3] J.A. Vreeling, *DML3.8 Continuation of 950°C graphite irradiation, Status March* 2009, NRG-21457/09.94517, 18 March 2009

[4] J.A. Vreeling, B. Sakintuna, *DML3.13: Full PIE INNOGRAPH-1A and description INNOGRAPH-1B*, NRG-21457/10.101850, 14 April 2010.

[5] J.A. Vreeling, B. Sakintuna, Post Irradiation Examinations of experiment at 950°C, *DML 3.16 Full PIE of INNOGRAPH-2A*, NRG-21457/10.101644, 14 April 2010

[6] M.C.R. Heijna, D41.12: High dose experiments at 750°C and 950°C, *Full PIE of INNOGRAPH-1B and INNOGRAPH-2B*, NRG-22906/12.111097, 3 April 2012

[7] O. Wouters, J.A. Vreeling, INNOGRAPH-1B and INNOGRAPH-2A specimen manufacture and pre-characterisation, *DML3.3: Graphite material procurement & characterisation*, NRG-21457/06.77300/P, 23 October 2006

List of tables

List of figures